RHO EXCHANGE FACTORS IN THE REGULATION OF SQUAMOUS CELL STEMNESS AND CARCINOGENESIS

LUIS FRANCISCO LORENZO MARTÍN

Thesis for the degree of
Doctor of Philosophy

Centro de Investigación del Cáncer
Instituto de Biología Molecular y Celular del Cáncer
CSIC – Universidad de Salamanca
2019

CENTRO DE INVESTIGACIÓN
DEL CÁNCER

Universidad de Salamanca-CSIC
CSIC

Campus Miguel de Unamuno
37007 Salamanca, España
Tel. +34 923 29 47 20
Fax +34 923 29 47 43
www.cicancer.org

El **Dr. XOSÉ RAMÓN GARCÍA BUSTELO**, Profesor de Investigación del Consejo Superior de Investigaciones Científicas en el Centro de Investigación del Cáncer y el Instituto de Biología Molecular y Celular del Cáncer de Salamanca,

CERTIFICA

Que el trabajo de tesis titulado **"RHO Exchange Factors in the Regulation of Squamous Cell Stemness and Carcinogenesis"**, presentado por **D. LUIS FRANCISCO LORENZO MARTÍN** para optar al Grado de Doctor por la Universidad de Salamanca, ha sido realizado bajo mi dirección en el Centro de Investigación del Cáncer de Salamanca. Considerando que cumple con las condiciones necesarias, autorizo su presentación a fin de que pueda ser defendido ante el tribunal correspondiente.

Y para que conste a los efectos oportunos, expido y firmo el presente certificado en Salamanca, a 21 de mayo de 2019.

Fdo.: Dr. Xosé R. Bustelo

The research conducted in this Ph.D. thesis has been supported by:

i. Graduate student contracts from the Spanish Ministry of Education, Culture and Sports (FPU13/02923) and the ‘Programa de Fortalecimiento de Estructuras de Investigación de Castilla y León – Escalera de Excelencia’ (CLC–2017–01).

ii. Grants from the Castilla–León Government (CSI252P18, CLC–2017–01), the Spanish Ministry of Science, Innovation and Universities (MSIU) (SAF2015–64556–R), Worldwide Cancer Research (14–1248), the Ramón Areces Foundation, and the Spanish Association against Cancer (GC16173472GARC).

iii. The ‘Programa de Apoyo a Planes Estratégicos de Investigación de Estructuras de Investigación de Excelencia’ of the Castilla–León autonomous government (CLC–2017–01).

En ocasiones pienso que el premio de quienes escribimos duerme,

tímido y virginal, en el confuso corazón del lector más lejano.

Camilo José Cela

ABSTRACT

The squamous cell carcinoma (SCC) is a major cause of cancer mortality. The carcinogenesis of this tumor is linked to a series of molecular derangements that frequently features the deregulation of RHO GTPase signaling. However, the events and agents underpinning such deregulation are yet to be defined. RHO exchange factors (GEFs), the proteins that catalyze the activation of RHO GTPases, have been traditionally contemplated as potential protumorigenic players in this context, but their large numbers and the lack of appropriate models has precluded the elucidation of their true functions in cancer settings. To address this issue, in this thesis we have focused on VAV2 to spearhead the characterization of RHO GEFs as key mediators of tumorigenesis and, more importantly, as candidate targets for novel SCC-directed therapeutic approaches. Here we demonstrate that VAV2 becomes upregulated in cutaneous and head-and-neck SCCs, where it engages a transcriptional program involved in the induction of stem cell-like regenerative proliferation and undifferentiation. Significantly, we show that VAV2 activity predicts disease outcome and that its inhibition within specific catalytic thresholds provides antitumoral benefits without disturbing organismal homeostasis. This work also exposes non-oncogenic roles for this GEF in the physiological maintenance of the cutaneous squamous epithelium, where it regulates the abundance, activity and responsiveness of hair follicle stem cells through the control of their transcriptomic circuits. Lastly, by extending these studies to the whole family of RHO GEFs, our research shows that VAV2 belongs to a small collection of exchange factors with pivotal roles in either the promotion or impairment of SCC tumorigenesis-associated processes. Taken together, our findings unveil hitherto unknown regulators of SCC fitness whose activity can be harnessed to modulate tumor growth and malignancy.

TABLE OF CONTENT

LIST OF FIGURES 13

LIST OF ABBREVIATIONS 15

INTRODUCTION 17

1. PHYSIOLOGY OF THE STRATIFIED SQUAMOUS EPITHELIUM 19
1.1. Structure and function 19
1.2. Molecular regulation 21

2. EPIDERMAL STEM CELLS 24
2.1. Niches and populations 24
2.2. Molecular regulation of the bulge stem cell 26

3. THE SQUAMOUS CELL CARCINOMA 29
3.1. Epidemiology 29
3.2. Cell of origin 30
3.3. Molecular features 31

4. RHO SIGNALING IN SQUAMOUS EPITHELIA 35
4.1. Rho GTPases as molecular switches 35
4.2. Rho GTPases in epidermal stem cell homeostasis 37
4.3. Rho GTPases in squamous cell carcinoma 38
4.4. Rho GEFs in squamous cell carcinoma 41
4.5. Do Rho GEFs harbor therapeutic value? 43

OBJECTIVES 45

METHODS 49

EXPERIMENTAL MODEL AND SUBJECT DETAILS 51

METHOD DETAILS 54

QUANTIFICATION AND STATISTICAL ANALYSES 69

RESULTS 73

1. VAV2 SIGNALING PROMOTES REGENERATIVE PROLIFERATION AND POOR PROGNOSIS IN SQUAMOUS CELL CARCINOMA 75
1.1. Increased abundance of VAV2 is associated with poor prognosis in SCC 75
1.2. Upregulated Vav2 signaling creates a protumorigenic niche in the mouse epidermis 80
1.3. The Vav2 phenotype is keratinocyte-autonomous and catalysis-dependent 83
1.4. Vav2 controls a protumorigenic and stem cell-like program in keratinocytes 88
1.5. The Vav2^{Onc} transcriptome is regulated by c-Myc, Yap, E2F, and AP1 factors 93
1.6. The epithelial hyperplasia induced by Vav2 is c-MYC- and YAP-dependent 98
1.7. Endogenous VAV2 is required of oSCC maintenance 100

2. PRECLINICAL VALIDATION OF THE THERAPEUTIC VALUE OF Vav2 CATALYTIC ACTIVITY 107
2.1. The L332A mutation models the partial inhibition of Vav2 catalytic activity 107
2.2. There are therapeutic windows for the inhibition of Vav2 catalytic activity 109

3. Vav2 REGULATES EPIDERMAL STEMNESS IN THE HAIR FOLLICLE 115
3.1. Vav2 signaling induces the expansion of the epidermal stem cell reservoir 115
3.2. Vav2 promotes epidermal stem cell responsiveness 118
3.3. The Vav2-dependent epidermal stem cell phenotype is keratinocyte-autonomous 123
3.4. Vav2 drives key transcriptional programs for epidermal stem cell homeostasis 127
3.5. Vav2 controls the wiring of the epidermal stem cell transcriptome across time 129
3.6. Vav2 affects the time-dependent regulation of key EpSC signaling pathways 134
3.7. Vav2 signaling favors transcriptional coordination in epidermal stem cells 138
3.8. Vav2 governs the epidermal stem cell transcriptome through transcriptional hubs 140

4. BEYOND VAV2: THE LANDSCAPE OF RHO EXCHANGE FACTORS IN THE CARCINOGENESIS OF THE SQUAMOUS CELL EPITHELIUM 145
4.1. Two distinct sets of RHO GEFs are transcriptionally deregulated in SCC 145
4.2. RHO GEF transcriptional deregulation occurs coordinately 148
4.3. ECT2, FARP1, FGD6, TRIO and VAV2 play protumorigenic roles in vitro 152
4.4. ECT2, TRIO and VAV2 play protumorigenic roles in vivo 155
4.5. Downmodulation of VAV3 favors proliferation in transforming contexts in vitro 157
4.6. ITSN2, KALRN and VAV3 play antitumorigenic roles in vivo 160
4.7. Vav3 limits the development and aggressiveness of SCC tumors 161

DISCUSSION 165

Vav2 upregulation is a functionally relevant event in SCC carcinogenesis 167
Vav2 is a key mediator of stemness in epidermal and oral squamous cells 169
VAV2 is a potential therapeutic target in squamous cell carcinoma 170
Vav2 regulates stemness in the hair follicle 171
Vav2 signaling in the skin: stemness in two flavors 174
VAV2 belongs to a group of RHO GEFs with key roles in SCC carcinogenesis 175
The mechanisms underlying RHO GEF idiosynchrasy: a puzzle to be solved 179
Vav2 and Vav3: friends and foes 182

CONCLUSIONS 185

REFERENCES 189

PUBLICATIONS 209

ACKNOWLEDGEMENTS 215

APPENDIX: RESUMEN EN CASTELLANO 227

LIST OF FIGURES

Figure I: Structure of the epidermis 19

Figure II: Molecular determinants of epidermal development 22

Figure III: Stem cell populations within the epidermis 24

Figure IV: The hair follicle cycle 26

Figure V: Epidemiology of cSCC and hnSCC 29

Figure VI: Common genetic lesions in cSCC and hnSCC 32

Figure VII: Rho GTPases function as molecular switches 36

Figure VIII: Rho GEFs constitute a large and heterogeneous family 37

Figure IX: Implication of Rho GTPases in SCC 39

Figure X: Tiam1 and Vav GEFs play crucial roles in SCC development 42

Figure 1.1: Increased abundance of VAV2 is associated with poor prognosis in SCC (part I) 76

Figure 1.2: Increased abundance of VAV2 is associated with poor prognosis in SCC (part II) 78

Figure 1.3: Increased abundance of VAV2 is associated with poor prognosis in SCC (part III) 79

Figure 2.1: Upregulated VAV2 signaling creates a protumorigenic niche in the epidermis (part I) 80

Figure 2.2: Upregulated VAV2 signaling creates a protumorigenic niche in the epidermis (part II) 82

Figure 2.3: Upregulated VAV2 signaling creates a protumorigenic niche in the epidermis (part III) 83

Figure 3.1: The effect of Vav2 in keratinocytes is autonomous and catalysis–dependent (part I) 85

Figure 3.2: The effect of Vav2 in keratinocytes is autonomous and catalysis–dependent (part II) 85

Figure 3.3: The effect of Vav2 in keratinocytes is autonomous and catalysis–dependent (part III) 87

Figure 4.1: Vav2 controls a protumorigenic and stem cell–like program in keratinocytes (part I) 89

Figure 4.2: Vav2 controls a protumorigenic and stem cell–like program in keratinocytes (part II) 91

Figure 4.3: Vav2 controls a protumorigenic and stem cell–like program in keratinocytes (part III) 92

Figure 5.1: The *Vav2*$^{\mathrm{Onc}}$ transcriptome is regulated by c–Myc, Yap, E2F, and AP1 factors (part I) 94

Figure 5.2: The *Vav2*$^{\mathrm{Onc}}$ transcriptome is regulated by c–Myc, Yap, E2F, and AP1 factors (part II) 96

Figure 5.3: The *Vav2*$^{\mathrm{Onc}}$ transcriptome is regulated by c–Myc, Yap, E2F, and AP1 factors (part III) 97

Figure 6.1: The hyperplasia induced by Vav2 signaling is c–MYC– and YAP–dependent (part I) 99

Figure 6.2: The hyperplasia induced by Vav2 signaling is c–MYC– and YAP–dependent (part II) 99

Figure 7.1: Endogenous VAV2 is required for oSCC maintenance (part I) 101

Figure 7.2: Endogenous VAV2 is required for oSCC maintenance (part II) 102

Figure 7.3: Endogenous VAV2 is required for oSCC maintenance (part III) 104

Figure 7.4: Endogenous VAV2 is required for oSCC maintenance (part IV) 105

Figure 8.1: Preclinical evaluation of the therapeutic value of Vav2 catalytic activity (part I) 108

Figure 8.2: Preclinical evaluation of the therapeutic value of Vav2 catalytic activity (part II) 109

Figure 8.3: Preclinical evaluation of the therapeutic value of Vav2 catalytic activity (part III) 110

Figure 8.4: Preclinical evaluation of the therapeutic value of Vav2 catalytic activity (part IV) 111

Figure 8.5: Preclinical evaluation of the therapeutic value of Vav2 catalytic activity (part V) 112

Figure 9.1: Upregulated Vav2 signaling induces the expansion of the EpSC reservoir (part I) 116

Figure 9.2: Upregulated Vav2 signaling induces the expansion of the EpSC reservoir (part II) 117

Figure 10.1: Vav2 promotes epidermal stem cell responsiveness (part I) 118
Figure 10.2: Vav2 promotes epidermal stem cell responsiveness (part II) 119
Figure 10.3: Vav2 promotes epidermal stem cell responsiveness (part III) 121
Figure 10.4: Vav2 promotes epidermal stem cell responsiveness (part IV) 122
Figure 11.1: The Vav2-dependent EpSC phenotype is keratinocyte autonomous (part I) 124
Figure 11.2: The Vav2-dependent EpSC phenotype is keratinocyte autonomous (part II) 125
Figure 11.3: The Vav2-dependent EpSC phenotype is keratinocyte autonomous (part III) 126
Figure 12.1: Vav2 drives key transcriptional programs for EpSC homeostasis 128
Figure 13.1: Vav2 controls the wiring of the EpSC transcriptome across time (part I) 129
Figure 13.2: Vav2 controls the wiring of the EpSC transcriptome across time (part II) 131
Figure 13.3: Vav2 controls the wiring of the EpSC transcriptome across time (part III) 132
Figure 13.4: Vav2 controls the wiring of the EpSC transcriptome across time (part IV) 133
Figure 14.1: Vav2 affects the time-dependent regulation of key EpSC signaling pathways (part I) 136
Figure 14.2: Vav2 affects the time-dependent regulation of key EpSC signaling pathways (part II) 137
Figure 15.1: Upregulated Vav2 signaling favors transcriptional coordination in EpSC 139
Figure 16.1: Vav2 governs the EpSC transcriptome through transcriptional hubs (part I) 141
Figure 16.2: Vav2 governs the EpSC transcriptome through transcriptional hubs (part II) 143
Figure 16.3: Vav2 governs the EpSC transcriptome through transcriptional hubs (part III) 144
Figure 17.1: Two distinct sets of RHO GEFs are transcriptionally deregulated in SCC (part I) 145
Figure 17.2: Two distinct sets of RHO GEFs are transcriptionally deregulated in SCC (part II) 147
Figure 17.3: Two distinct sets of RHO GEFs are transcriptionally deregulated in SCC (part III) 148
Figure 18.1: RHO GEF transcriptional deregulation occurs coordinately (part I) 150
Figure 18.2: RHO GEF transcriptional deregulation occurs coordinately (part II) 151
Figure 19.1: ECT2, FARP1, FGD6, TRIO and VAV2 play protumorigenic roles in vitro (part I) 153
Figure 19.2: ECT2, FARP1, FGD6, TRIO and VAV2 play protumorigenic roles in vitro (part II) 154
Figure 19.3: ECT2, FARP1, FGD6, TRIO and VAV2 play protumorigenic roles in vitro (part III) 155
Figure 20.1: ECT2, TRIO and VAV2 play key protumorigenic roles in vivo 156
Figure 21.1: VAV3 hampers keratinocyte proliferation in transforming contexts in vitro (part I) 158
Figure 21.2: VAV3 hampers keratinocyte proliferation in transforming contexts in vitro (part II) 159
Figure 22.1: ITSN2, KALRN and VAV3 play antitumorigenic roles in vivo 160
Figure 23.1: Vav3 limits the development and aggresiveness of SCC tumors 161
Figure XI: Vav2 signaling in the skin: stemness in two flavors 175
Figure XII: RHO GEF catalytic specificity, subcellular localization and interactome 180

LIST OF ABBREVIATIONS

AK	Actinic keratosis
BrdU	Bromodeoxyuridine
ceSCC	Cervix squamous cell carcinoma
cSCC	Cutaneous squamous cell carcinoma
DAPI	4’,6-diamino-2-phenylindole
DMBA	7,12-dimethylbenz[a]anthracene
DMEM	Dulbecco’s modified Eagle’s medium
DMSO	Dimethyl sulfoxide
DNA	Deoxyribonucleic acid
DKO	$Vav2^{-/-}$;$Vav3^{-/-}$ mice
ECM	Extracellular matrix
EDTA	Ethylenediaminetetraacetic acid
EdU	5-ethynyl-2’-deoxyuridine
EGFP	Enhanced green fluorescent protein
EMEM	Eagle’s minimum essential medium
EpSC	Epidermal stem cell
eSCC	Esophageal squamous cell carcinoma
FACS	Fluorescence-activated cell sorting
FDR	False discovery rate
GAP	GTPase activating protein
GDI	Guanine nucleotide dissociation inhibitor
GDP	Guanosine diphosphate
GEF	Guanine nucleotide exchange factor
GEO	Gene expression omnibus
GPCR	G-protein coupled receptor
GSEA	Gene set enrichment analysis
GTP	Guanosine triphosphate
HPV	Human papillomavirus
HRP	Horseradish peroxidase
hnSCC	Head and neck squamous cell carcinoma
IFE	Interfollicular epidermis
IP	Immunoprecipitation
iPS	Induced pluripotent stem cell
KSFM	Keratinocyte serum-free medium
LIF	Leukemia inhibitory factor
LRC	Label retaining cell
lSCC	Lung squamous cell carcinoma
MAPK	Mitogen-activated protein kinase
mRNA	Messenger ribonucleic acid
MVGS	Minimal Vav2^{Onc} gene signature
n	Number of experimental replicates
NES	Normalized enrichment score
NSCLC	Non-small cell lung cancer
oSCC	Oral squamous cell carcinoma
PBS	Phosphate-buffered saline
PCR	Polymerase chain reaction
PWM	Position weight matrix
RMA	Robust multi-array average
RNA	Ribonucleic acid
rRNA	Ribosomic ribonucleic acid
RNP	Ribonucleoprotein
ROS	Reactive oxygen species
rpm	Revolutions per minute
RT–PCR	Reverse-transcription polymerase chain reaction
SC	Stem cell
SCC	Squamous cell carcinoma
shRNA	Short hairpin ribonucleic acid
ssGSEA	Single-sample gene set enrichment analysis
TAC	Transit amplifying cell
T–ALL	T-cell acute lymphoblastic leukemia
TBS–T	Tris-buffered saline and Tween 20
TCGA	The cancer genome atlas
TPA	12-O-tetradecanoylphorbol-13-acetate
TKR	Tyrosine-kinase receptor
UCSC	University of California, Santa Cruz
$\textbf{Vav2}^{\textbf{Onc}}$	Hyperactive Vav2 (Δ1–186)
WGCNA	Weighted correlation network analysis
WT	Wild type

INTRODUCTION

1. PHYSIOLOGY OF THE STRATIFIED SQUAMOUS EPITHELIUM

1.1. STRUCTURE AND FUNCTION

The stratified squamous epithelium is one of the most abundant epithelia of the human body. It is fundamentally composed of several layers of stacked cells arranged along an apical-basal axis resting on a basement membrane. Suited to endure constant abrasion, this epithelium covers the outermost layers of different organs, including the skin, the inner lining of the mouth, the esophagus and the vagina. Among these, the skin contains arguably the most illustrative representative of this kind of epithelium: the epidermis (**Figure I**).

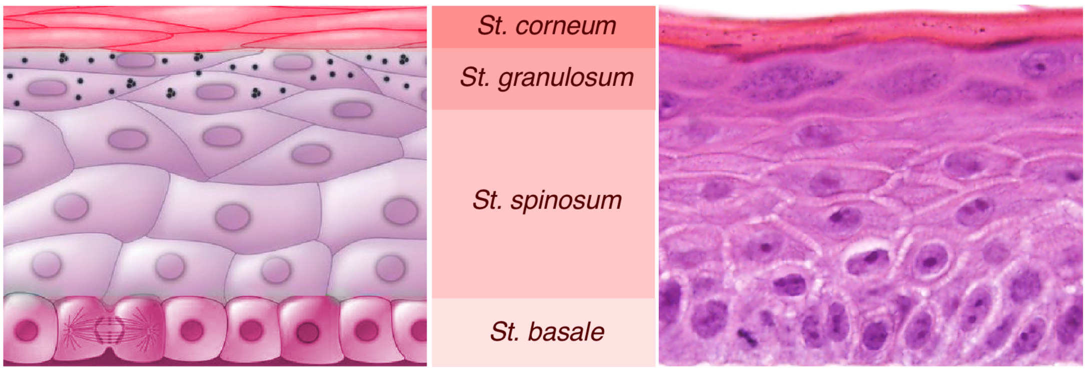

FIGURE I. Structure of the epidermis. Schematic representation (left) and example of a histological section stained with hematoxylin and eosin (right) of the epidermis. The span of the different strata (St.) that compose the epidermal tissue is indicated. Adapted from [1].

The epidermis is primarily made up of keratinocytes, epithelial cells that constitute different strata from the bottom to the top of the epithelium: the stratum basale, the stratum spinosum, the stratum granulosum and the stratum corneum (**Figure I**). Mature keratinocytes are continuously sloughed from the epidermal surface and replaced by younger cells emerging from deeper layers, making the epidermis one of the tissues with the highest self-renewal rates [1]. The maintenance of such balance requires a tightly regulated cell proliferation activity, a process that takes place in the deepest epidermal layer, the stratum basale (**Figure I**). Here, cuboidal-shaped keratinocytes directly attached to the basement membrane alternate between proliferating and quiescent states [2]. When these cells divide, daughter cells detach from the basement membrane and embark on a journey towards the epidermal surface as they follow a terminal differentiation program known as keratinization.

The cells that leave the stratum basale firstly give rise to the stratum spinosum (**Figure I**). These polyhedral keratinocytes are tightly bound to one another through the establishment of abundant desmosomes, which gives them their ‘spiny’ appearance. It is at this stratum where the synthesis of certain groups of cytokeratins, lipids and enzymes involved in the keratinization process starts [3, 4].

On top of this layer flattened keratinocytes accumulate keratohyalin and lamellar granules, forming the stratum granulosum (**Figure I**). Keratohyalin granules contain mainly filaggrin and loricrin, which work in concert with other proteins involved in keratinocyte differentiation such as involucrin and transglutaminases. Lamellar bodies, on the other hand, contain primarily ceramides and cholesterol esters, which are required to regulate the permeability of the epidermal epithelium [3, 4].

In their last differentiation stage, keratinocytes go through a number of processes that dramatically change their cellular identity: **i)** they lose their nucleus and cytoplasm, **ii)** their keratin filaments aggregate into microfibrils, **iii)** their lipids are released into the intercellular space and **iv)** their plasma membrane is replaced by a cross-linked protein envelope. The resulting fully mature keratinocytes, also termed corneocytes, are the ones that compose the outermost epidermal layer, the stratum corneum (**Figure I**). The conjunction of the densely packed keratin and the cross-linked cell envelope makes this stratum a highly resistant barrier, which is impermeabilized by the lipidic component found in the intercellular space. This structure is held together by desmosomes, whose eventual proteolytic cleavage leads to the desquamation of the corneocyte, drawing the life cycle of the epidermal cell to an end [3, 4].

The epidermis is not the only stratified squamous epithelium with this architecture. Despite appearances, the oral mucosa has more in common with the epidermis than with the epithelial lining of rest of the gastrointestinal tract [5]. In fact, in the buccal regions involved in mastication, such as the masticatory (hard palate and gingiva) and specialized (dorsal surface of the tongue) mucosae, the epithelium is keratinized and histologically very similar to the epidermis [6].

Both the epidermis and the oral mucosa are also populated by non-epithelial cells, such as melanocytes, Merkel cells and Langerhans cells. Melanocytes are neural crest-derived melanin-producing cells that reside in the stratum basale and protect keratinocytes from ultraviolet radiation [7]. Also located in the basal layer and in close proximity to nerve tissue, Merkel cells participate in the mechanoreception responsible for touch sensing [8]. Lastly, lodged in the stratum spinosum, the bone marrow-derived Langerhans cells perform antigen presentation to T-cells, thus providing immunological protection to the epithelium [9].

The conjunction of all these cell types and structures makes the squamous epithelium a physically-, chemically-, and biologically-competent barrier with key roles in thermoregulation, water loss prevention and sensorial perception.

1.2. MOLECULAR REGULATION

1.2.1. Undifferentiation and proliferation

The homeostatic maintenance of the squamous epithelium is regulated by a vast signaling network that orchestrates keratinocyte division and maturation in a stratum-specific manner [10] (**Figure II**). In the basal layer, the undifferentiated and proliferative states are maintained by the transcription factor p63 [11]. This protein is an essential regulator of all squamous specification, since its loss prevents the development of every stratified epithelia of the body [12]. Basal keratinocyte homeostasis also requires other key regulators such as: **i)** c-Myc, which stimulates proliferation and regulates differentiation in a dosage-dependent manner [13], **ii)** the yes-associated protein (YAP), involved in the maintenance of the progenitor-like undifferentiated state [14], and **iii)** AP1, which regulates proliferation and differentiation at different maturation stages [15, 16].

The basal balance between differentiation and proliferation is further controlled by the mitogen-activated protein kinase (MAPK) cascade (**Figure II**). Loss of Mek1/2 [17] or Erk1/2 [18] signaling results in epidermal hypoplasia, while the activation of Ras, Raf or Mek1 leads to hyperplasia and reduced differentiation [19, 20]. The physiological activation of this cascade relies on basal integrins and tyrosine kinase receptors, such as the epidermal growth factor receptor (EGFR). On the other hand, adhesion molecules such as cadherins and catenins are responsible for its downmodulation [10].

Epidermal layer	Process	Marker	Signaling
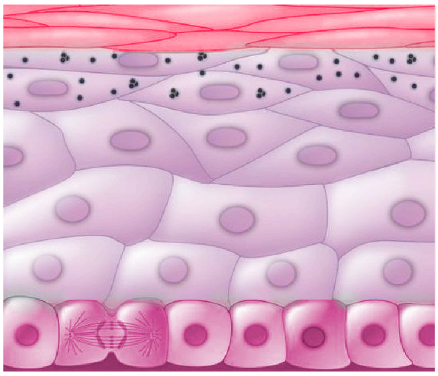	Late Differentiation	Lor, Flg, Ivl, Tgm	CaR, PKC, Klf4, Grhl3, Notch, AP1
	Early & Middle Differentiation	K1, K10, Ivl, Tgm	p63, Notch, Irf6, Ovol1, Kdf1, AP1
	Proliferation	K5, K14	p63, EGFR, Ras, Myc, YAP, AP1

FIGURE II. **Molecular determinants of the epidermal development**. Schematic representation of the epidermal tissue along with the differentiation markers and signaling elements that characterize each maturation stage. Adapted from [1].

1.2.2. Early differentiation

Keratinocytes undergo a profound signaling rewiring when they detach from the basement membrane and begin to differentiate. In this process they lose the expression of the basal markers K5 and K14, which are replaced by K1, K10 and, later on, by involucrin and transglutaminases [4, 11] (**Figure II**).

The canonical Notch pathway is one of the major drivers of keratinocyte differentiation (**Figure II**) [21]. This pathway is mainly active in suprabasal cells and its upregulation leads to an expansion of the spinous layer. Conversely, the inactivation of Notch signaling causes impaired differentiation and aberrant formation of the skin barrier [10, 21].

These stages of early keratinocyte differentiation also require p63 activity, showing that this transcription factor plays bivalent roles in epidermal stratification [22]. Additionally, other proteins such as Irf6, Ovol1, Kdf1 and AP1 also have been implicated in the spinous differentiation process (**Figure II**) [10, 11, 15, 16].

1.2.3. Late differentiation

Late keratinocyte differentiation in the granular layer is accompanied by the expression of specific markers such as filagrin, loricrin and some transglutaminases [4] (**Figure II**). Along with Notch and AP1, calcium signaling is one of the most prominent pathways at this stage. Such signaling is mediated by the extracellular calcium-sensing receptor (CaR) and the serine/threonine kinase PKCα, whose respective overexpression leads to expanded layers of highly differentiated keratinocytes [23, 24]. In addition, the transcription factors Klf4 and Grhl3 have also been shown to play crucial roles in keratinocyte terminal differentiation [10, 11].

2. EPIDERMAL STEM CELLS

2.1. NICHES AND POPULATIONS

2.1.1. Interfollicular epidermis stem cells

The homeostatic maintenance of the squamous epithelium relies on cells capable of ensuring the turnover of the tissue throughout the whole life of the organism. This demand requires a fine-tuned balance between quiescence and proliferation that allows the generation of differentiated lineages while preserving an undifferentiated progenitor pool. That is the function of the stem cells of the squamous epithelium, which reside in specific niches. As previously mentioned, the basal layer of the interfollicular epidermis contains cells with those properties; however, it is in the hair follicle where the majority of stem niches are found (**Figure III**).

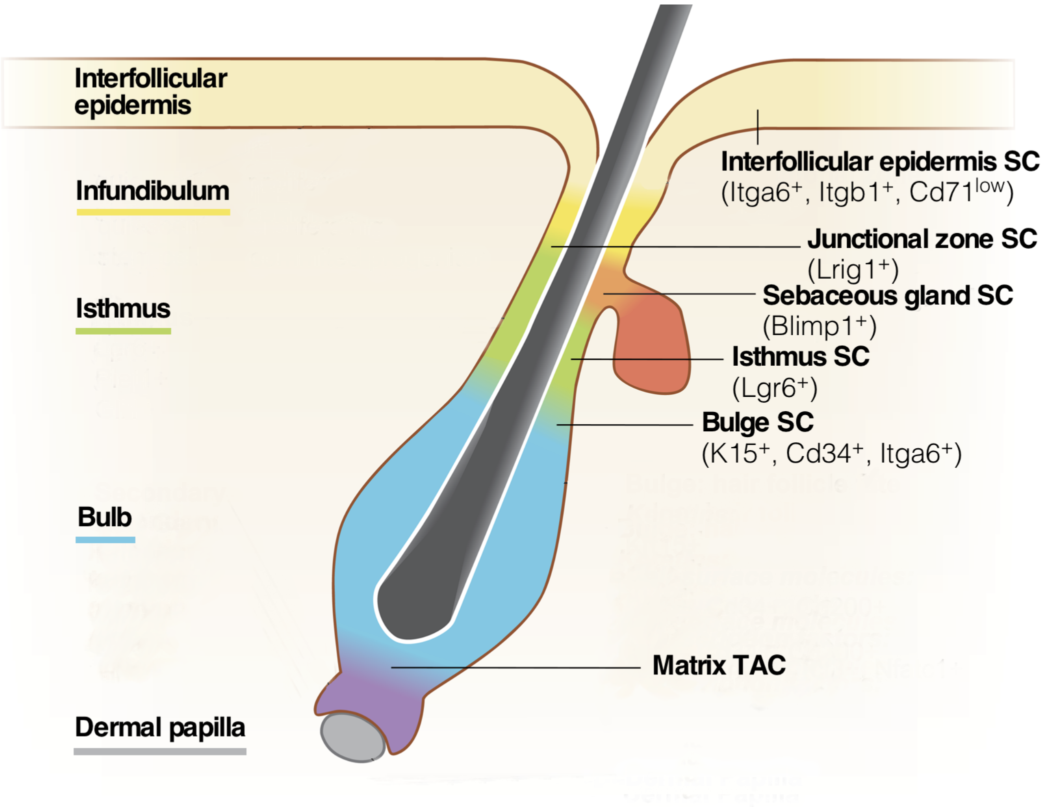
Interfollicular epidermis
Infundibulum
Isthmus
Bulb
Dermal papilla
Interfollicular epidermis SC
(Itga6$^+$, Itgb1$^+$, Cd71^{low})
Junctional zone SC
(Lrig1$^+$)
Sebaceous gland SC
(Blimp1$^+$)
Isthmus SC
(Lgr6$^+$)
Bulge SC
(K15$^+$, Cd34$^+$, Itga6$^+$)
Matrix TAC

FIGURE III. **Stem cell populations within the epidermis**. Schematic representation of the hair follicle and the interfollicular epidermis with the different epidermal stem cell (SC) niches, populations and expression markers. The structural parts of the hair follicle are also indicated. Adapted from [25].

The basal layer of the epidermis contains fast cycling unipotent progenitors characterized by the expression of high levels of β1 and α6 integrins and low levels of the transferrin receptor (CD71) (**Figure III**) [26, 27]. These cells maintain a constant cell number within the interfollicular epidermis (IFE) by compensating the cells lost by desquamation. To that end, upon division they generate a daughter stem cell and a poised progenitor that leaves the basal layer towards the terminal differentiation pathway [28]. Although under physiological conditions these cells take care of the IFE independently of other stem populations [29, 30], it has been shown that upon challenges, such as wounding, stem cells from the hair follicle also intervene [26].

2.1.2. Hair follicle stem cells

The hair follicle is a dynamic cylindrical structure composed of epidermal cells arranged in several concentric layers of sheath and hair-producing keratinocytes. This body is usually associated with accessory structures such as the sebaceous gland and the arector pili muscle (for a review, see [31]). In terms of structure, the hair follicle is divided in infundibulum, isthmus and bulb (**Figure III**). The infundibulum connects the opening of the hair canal with the isthmus through the junctional zone, where the insertion point of the arector pili muscle is found. The isthmus connects with the bulb at the bulge, the lower end of the non-cycling fraction of the hair follicle. The bulb contains the matrix keratinocytes, the pigmentary unit and the mesoderm-derived dermal papilla, all of which participate in the generation of the hair shaft and the surrounding epidermal layers.

The upper part of the hair follicle is known to contain various kinds of unipotent stem cells that take care of homeostatic demands in an independent fashion [10] (**Figure III**). Under physiological conditions their contributions are restricted to the areas where they are found, i.e., Lrig1- and MTS24-positive cells at the junctional zone, Blimp1-positive cells at the sebaceous gland, and Lgr6-positive cells at the isthmus. However, these cells have the potential to give rise to all epidermal lineages, proving their plasticity as stem cells [32-36]. Despite this, when looking for quiescence as one of the key features of true stem cells, one region in the hair follicle stands out: the bulge (**Figure III**).

Label-retention studies in the early 1990s showed that the bulge contains the slowest cycling stem cell population of the whole epidermis, characterized by the expression of CD34, K15 and high levels of integrin α6 (**Figure III**) [37-39]. These cells fuel and replenish the hair follicle matrix in order to produce the hair shaft and its surrounding layers [10]. In addition, they also **i)** participate actively in the epidermis repair following wounding, **ii)** have a long-lived clonogenic nature when cultured in vitro and **iii)** are able to fully regenerate the epidermal tissue upon transplantation, including all its structures and lineages [40-42]. For these characteristics, such pool of bulge-residing multipotent cells has been traditionally viewed as the main epidermal stem cell (EpSC) population.

2.2. MOLECULAR REGULATION OF THE BULGE STEM CELL

Unlike the case of the progenitors of the upper hair follicle, the activity of the EpSC is intimately linked to the hair follicle cycle. Hair follicles transition through rest (telogen), growth (anagen) and regression (catagen) phases in order to produce new hair, a process that is orchestrated by a highly-regulated balance between activation and quiescence cues within the EpSC niche (for a review see [31]) (**Figure IV**).

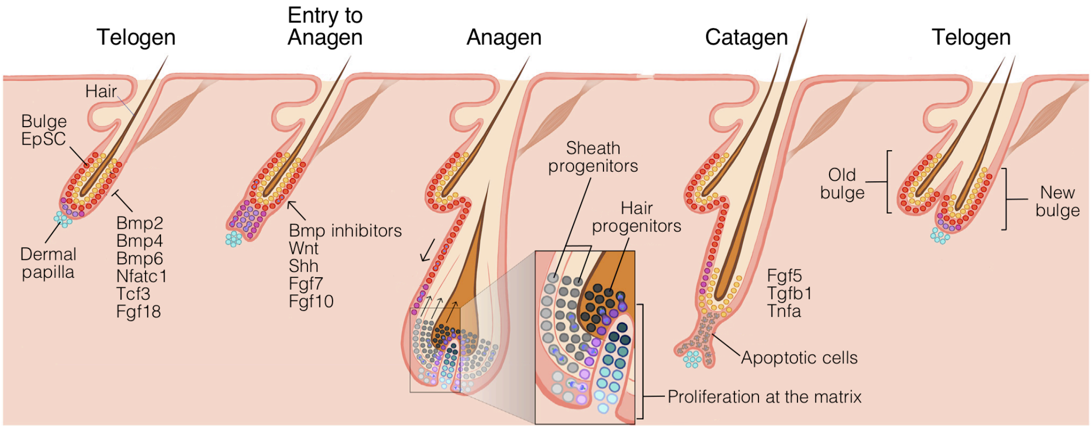
Telogen
Entry to Anagen
Anagen
Catagen
Telogen
Hair
Bulge EpSC
Dermal papilla
Bmp2
Bmp4
Bmp6
Nfatc1
Tcf3
Fgf18
Bmp inhibitors
Wnt
Shh
Fgf7
Fgf10
Sheath progenitors
Hair progenitors
Proliferation at the matrix
Fgf5
Tgfb1
Tnfa
Apoptotic cells
Old bulge
New bulge

FIGURE IV. **The hair follicle cycle**. Schematic representation of the different phases of the hair follicle cycle. The main signaling elements involved in each phase are also indicated. Adapted from [28].

2.2.1. Quiescence

During telogen, quiescence is maintained in the bulge through the presence of extrinsic inhibitory signals. Among these, BMP signaling is essential as it regulates the expression of the key CDK4-repressor Nfatc1, and the absence of Bmpr1a results in a continuously activated follicle [43-45]. Hence, equilibrium between BMP ligands (Bmp2/4/6) and antagonists (Noggin) is required for proper hair follicle cycling (**Figure IV**) [46]. Quiescence within the EpSC niche is also regulated by Tcf3, which represses the Wnt/β-catenin signaling pathway, and the multipotency-associated the transcription factors Lhx2, Sox9 and c-Myc [31].

2.2.2. Proliferation

EpSC quiescence is maintained as long as Bmp levels are elevated, as these factors make the EpSC insensitive to anagen-inducing agents [47]. However, when BMP signaling decreases and activating cues from the dermal papilla reach certain levels, EpSC begin to proliferate and telogen gives way to anagen (**Figure IV**) [31]. One of the key elements regulating this transition is the Wnt/β-catenin signaling pathway, which also plays many other crucial roles in hair follicle morphogenesis, the maintenance of the EpSC identity and the promotion of terminal differentiation [48]. Consistent with this, the deletion of β-catenin results in either absent or aberrant hair follicle formation and the generation of epidermal cysts [49]. Conversely, its overexpression induces EpSC proliferation and anagen reentry [49].

Downstream of Wnt/β-catenin, Shh signaling is another crucial component in EpSC activation. The blockade of this pathway prevents the expansion of hair follicle progenitors and impairs anagen progression, while its activation leads to a rise in the number of hair follicles in anagen [50, 51]. Other transcription factors such as c-Myc and Runx1 also become upregulated upon EpSC activation [31].

Once activated, the proliferation of EpSC induces the growth of the lower fraction of the hair follicle, thus moving the bulge away from the dermal papilla and eventually making the EpSC go back to quiescence. At the same time, the EpSC-derived transient-amplifying cells at the hair matrix in the bulb continue dividing until they differentiate towards the various epithelial lineages [31] (**Figure IV**).

2.2.3. Regression

Along with a series of catagen-inducing soluble factors that include Fgf5, Tgfb1, Il-1β, Bmp2/4 and Tnf-α, the receptors for the vitamin D and the retinoic acid seem to have a relevant role in the control of the anagen-catagen transition [31, 52, 53].

When catagen is established, the destructive phase starts and apoptosis of matrix and sheath keratinocytes leads to the regression of the lower two-thirds of the hair follicle. As a result, the bulge and the dermal papilla are brought close together once again, giving way to a new telogen and closing the homeostatic cycle (**Figure IV**).

3. THE SQUAMOUS CELL CARCINOMA

3.1. EPIDEMIOLOGY

The squamous cell carcinoma (SCC) results from the accumulation of oncogenic events in any squamous epithelium of the human body, which as a whole makes it the most common cancer worldwide [54, 55]. The majority of the cases belong to one of the four main subgroups: cutaneous SCC (cSCC), head and neck SCC (hnSCC), esophageal SCC (eSCC) and lung SCC (lSCC). Among these, two arise from keratinized epithelia: the cSCC and hnSCC (**Figure V**).

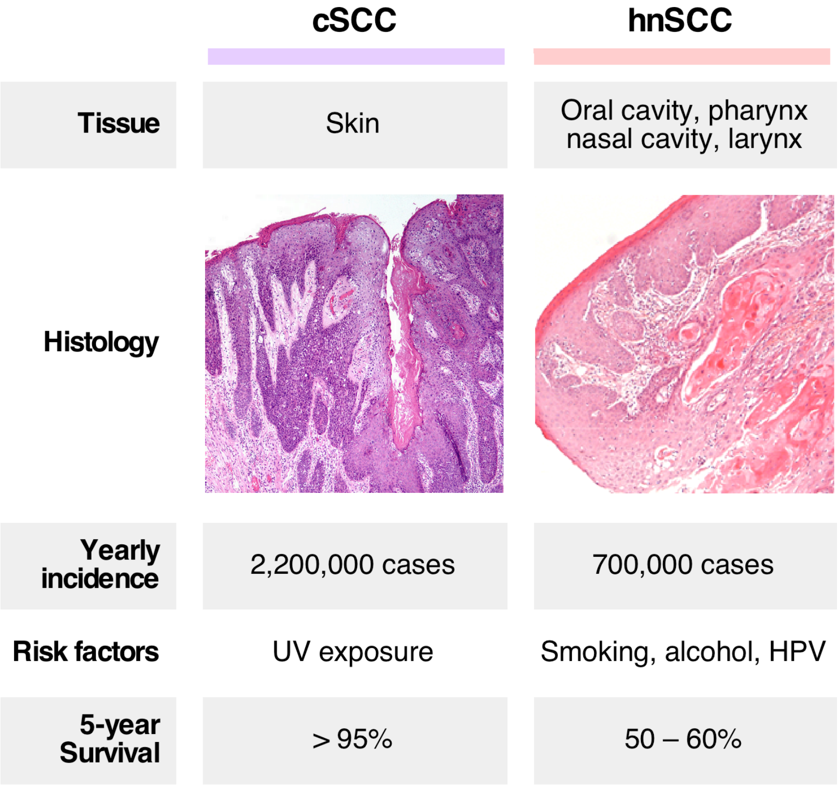

	cSCC	**hnSCC**
Tissue	Skin	Oral cavity, pharynx nasal cavity, larynx
Histology		
Yearly incidence	2,200,000 cases	700,000 cases
Risk factors	UV exposure	Smoking, alcohol, HPV
5-year Survival	> 95%	50 – 60%

FIGURE V. Epidemiology of cSCC and hnSCC. Scheme indicating the most relevant epidemiological parameters associated with cSCC and hnSCC. Histological images where obtained from the HSP atlas.

3.1.1. Cutaneous squamous cell carcinoma

The cSCC is the second most common nonmelanoma skin cancer, representing from 20% to 50% of all cases [56], an incidence rate that is currently climbing [57]. The most common risk factor accounting for such high incidence is the ultraviolet solar radiation exposure, which along with other non-behavioral factors such as age and skin color is the key contributor to cSCC development (**Figure V**) [56, 57]. Fortunately, the majority of these tumors can be successfully eradicated by surgery, which translates to 5-year mortality rates below 5% [56, 57]. Nevertheless, this cancer still accounts for 20% of all skin cancer-related deaths and constitutes a serious burden for our health systems given its extremely high incidence [54]. Furthermore, around 5% of cSCC cases display very aggressive features, with high recurrence, elevated metastatic potential, and poor response to the available therapeutic options [55, 57].

3.1.2. Head and neck squamous cell carcinoma

The hnSCC can arise from the nasal and oral cavities, the pharynx and the larynx. It is the sixth most common type of cancer worldwide, and makes up more than 90% of all head and neck tumors (**Figure V**) [55, 58]. Over the past decade there has been a notorious change in the incidence of the different hnSCC subtypes, with a decline in larynx and hypopharynx cases and a concomitant increase in oral SCC tumors [55, 59]. For these cancers, the main risk factors are alcohol and tobacco consumption, both separately and in a synergistic manner. In addition, human papillomavirus (HPV) infection is associated with 25-45% of all hnSCC tumors, which tend to be less aggressive than the HPV-negative counterparts [55]. Given its body location the hnSCC is usually detected in advanced stages, which leads to a 5-year mortality rate of 40-50% [60].

The oral SCC (oSCC) is a subtype of hnSCC that arises from the tongue, the floor of mouth, the buccal and alveolar surfaces and the hard palate. This is the hnSCC subtype that constitutes the greatest threat, as its incidence is currently climbing in young individuals who are not exposed to the traditional risk factors [61]. The most common oSCC subtype is the tongue SCC, which also has one of worst prognosis [58, 61].

3.2. CELL OF ORIGIN

Given the high cell turnover rate that characterizes squamous epithelia, it would seem prima facie that the only oncogenic events that can give rise to the development of SCC are those that occur in the long-term residing cells. This is easily demonstrated by the classic chemically-induced SCC mouse carcinogenesis model, which is based on a single topical treatment with the carcinogen DMBA (7,12-dimethylbenz[a]anthracene) followed by periodic applications of the proliferation-inducing agent TPA (12-O-tetradecanoylphorbol-13-acetate) [62]. Since TPA can induce the formation of papillomas even one year after DMBA treatment, the DMBA-induced mutations necessarily need to occur in long-lived epidermal cells [63, 64].

These long-lived cells include both the progenitors at the basal layers of the epithelium and, in the case of the epidermis, the hair follicle stem cells. This is corroborated by the fact that mice with either of those two cell compartments disrupted develop a reduced number of tumors upon chemical carcinogenesis [65]. Furthermore, it has been proved that the expression of oncogenic KRas along with p53 deletion in the interfollicular epidermis, the hair follicle lineages, or the oral basal cells, results in the development of SCC [66-68].

Interestingly, although the aforementioned studies demonstrate that the stem cell compartment is the primary niche where carcinogenesis occurs, several studies have revealed that transit-amplifying cells and post-mitotic keratinocytes can also give rise to tumors, although of reduced malignancy. For example, differentiated suprabasal cells from the interfollicular epidermis can also lead to neoplastic changes and tumor formation when the expression of an oncogene, such as HRas or c-Myc, is induced [65, 69-71].

3.3. MOLECULAR FEATURES

In order to elucidate the molecular players that drive SCC carcinogenesis, extensive molecular profiling of tumors collected from a large number of patients has been performed in the last years. Such analyses have revealed that despite their separate body location and their diverse risk factors, the different SCC subtypes share a remarkably conserved molecular signature in terms of mutation, copy-number variation, methylation, mRNA expression, microRNA expression and, in some cases, protein expression [72, 73]. This conserved SCC signature is dominated by genes associated with cell cycle control, response to growth factors, Ras/MAPK signaling, Wnt/Hippo signaling and squamous specification and differentiation (**Figure VI**).

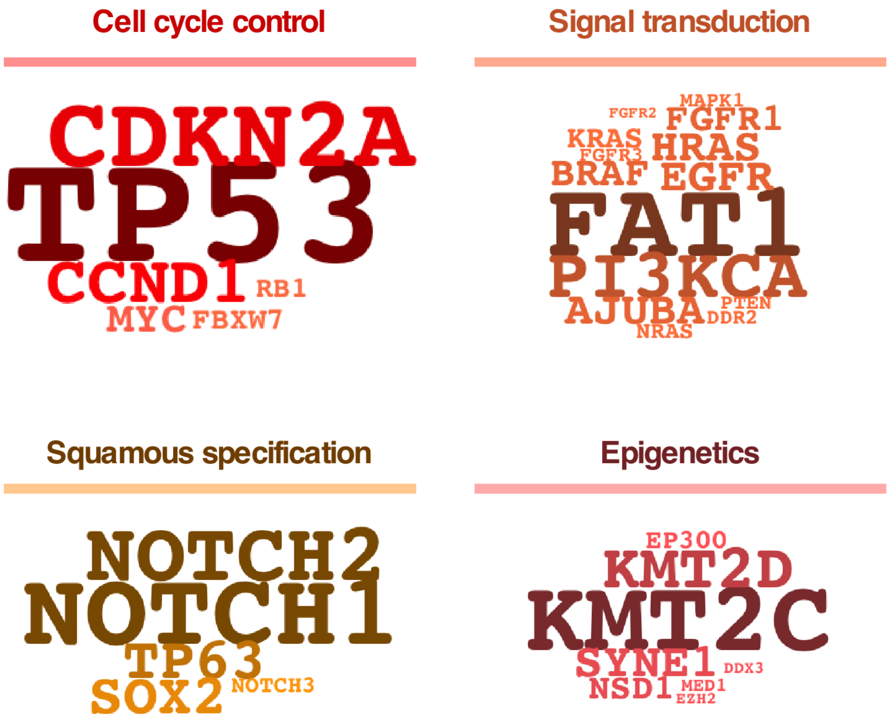

FIGURE VI. **Common genetic lesions in cSCC and hnSCC**. Functionally-arranged wordclouds representing the targets of the most frequent mutations and copy number variations found in cSCC and hnSCC. The size of the gene name is proportional to the genetic lesion frequency [54].

3.3.1. Cell cycle control

In terms of cell cycle control, the tumor suppressors *TP53* and *CDKN2A* are the most frequently mutated genes in every HPV-negative SCC subtype (**Figure VI**) [54, 60]. Alternatively, in HPV-positive tumors the viral proteins E6 and E7 inhibit P53 and RB proteins directly [54, 60]. This loss of key players in cell cycle arrest is frequently accompanied by amplifications of proliferation-driving genes, especially *CCND1* and *MYC* [54, 60]. Along with them, the ubiquitin ligase FBXW7, which is involved in the degradation of cell-cycle regulatory molecules such as cyclin E and c-MYC, is also highly mutated in SCC [54, 60]. The conjunction of these genomic lesions promotes an accelerated cell cycle deprived of checkpoint mechanisms, leading to the appearance of further oncogenic lesions.

3.3.2. Signal transduction

Mutations in some tyrosine kinase receptors (TKR) involved in growth factor signaling are also frequently found in SCC (**Figure VI**). Among them, *EGFR* is the most prominent case, as it is commonly amplified [54, 60]. To a lesser extent, the genes encoding C-MET, FGFR1, FGFR2 and FGFR3 are also recurrently amplified [54, 60]. The signals from these tyrosine kinases are integrated by the downstream RAS/MAPK and PI3K signaling pathways. At this level, *HRAS* mutations are frequently found in cSCC and HPV-negative hnSCC, whereas *KRAS* and *NRAS* mutations are detected at lower frequencies [54, 74]. The PI3K/AKT pathway is frequently altered through the amplification or mutation of *PIK3CA* or, alternatively, through the loss of *PTEN* [54, 72]. The deregulation of the TKR-RAS/MAPK/PI3K signaling axes leads to an increase in both the proliferation and survival potential of the SCC cell.

The Wnt signaling pathway is another preferred target in SCC tumors (**Figure VI**). This is probably owing to the role of Wnt in stem cell maintenance and carcinogenesis [60]. Such role is mainly mediated by β-catenin, which explains why the cadherin-related FAT1 protein, that sequesters β-catenin at the plasma membrane, is so frequently mutated in SCC [75]. Another member of the pathway recurrently mutated, the LIM domain-containing protein AJUBA, is also involved in the control of β-catenin, in this case through the activation of GSK3β-mediated degradation [76]. Interestingly, these two proteins are also connected to the Hippo signaling pathway [77], whose downstream regulators YAP and TAZ are known players in SCC development [78].

3.3.3. Squamous differentiation and specificaction

Among the genes involved in squamous specification, the transcription factor *TP63* is frequently overexpressed, but rarely mutated, in SCC (**Figure VI**) [54]. Also recurrently amplified is *SOX2*, a key mediator of pluripotency and squamous epithelium embryogenesis which is known to physically interact with P63 [79, 80]. On the other hand, and in keeping with its role in the promotion of keratinocyte differentiation, NOTCH1 is commonly found either downmodulated or with loss-of-function mutations in virtually every SCC subtype [54]. To a lesser extent, this also occurs in the cases of NOTCH2 and NOTCH3 [54].

3.3.4. Epigenetics

Some epigenetic regulators involved in the control of processes such as proliferation and squamous differentiation are also commonly altered in SCC (**Figure VI**). This includes the mutation of the N-methyltransferases NSD1, KMT2C, KMT2D, EZH2 and the acetyltransferase EP300 [54, 60]. In addition, some microRNAs have been described to be consistently downmodulated in SCC, such as miR-let-7c-5p and miR-100-5p [60].

3.3.5. RHO signaling

Functional analyses of these molecular features indicate that SCC cells are highly dependent on signaling pathways involved in proliferation, differentiation, MAPK signal transduction, hypoxia-related responses, and motility processes [72, 73]. Recently, pan-cancer multiomic analyses revealed that such molecular signature is linked to a SCC-specific enrichment of RAC and RHO signaling output [72]. This drew our interest, as although the roles of RHO GTPases in cell biology have been extensively characterized in vitro, their true relevance in vivo remains obscure, both in physiological and pathological scenarios. For this reason, we made RHO signaling the focus of our work.

4. RHO SIGNALING IN SQUAMOUS EPITHELIA

4.1. RHO GTPASES AS MOLECULAR SWITCHES

4.1.1. The family of Rho GTPases

Rho GTPases are small G proteins that respond to extracellular cues to regulate a variety of cellular processes including cytoskeletal dynamics, polarity, migration, proliferation, differentiation and survival [81, 82]. These proteins make up a large family which is classified into the Rho (RhoA, RhoB, RhoC), Rac (Rac1, Rac2, Rac3, RhoG), Cdc42 (Cdc42, RhoQ, RhoJ), RhoD (RhoD, RhoF), RhoH, RhoU (RhoU, RhoV) and Rnd (Rnd1, Rnd2, Rnd3) subfamilies [83]. Among these, RhoA, Rac1 and Cdc42 are the best-characterized GTPases in terms of biochemical properties, molecular regulation and biological roles.

Most Rho GTPases cycle between two conformations according to the guanosine molecule residing at their nucleotide-binding pocket: an inactive one in the presence of GDP and an active counterpart in presence of GTP. Hence, the activation of these proteins takes place when the GDP molecule is exchanged for GTP, a process that requires the catalytic activity of a family of proteins known as guanine nucleotide exchange factors (GEFs). On the other hand, the GTP-to-GDP hydrolysis abrogates the activity of the GTPases and is catalyzed by GTPase activating proteins (GAPs). In this inactive state, guanine nucleotide dissociation inhibitors (GDIs) can bind to and sequester Rho GTPases in order to prevent their activation [81, 82]. All together, GEFs, GAPs and GDIs are the key players that make Rho GTPases function as molecular switches, thus enabling them to dynamically integrate and transduce the different extracellular signals into the appropriate cellular responses (**Figure VII**). Such signal transduction is mediated by a set of proximal effectors that interact with the GTP-bound form of the GTPases. Over 60 Rho GTPase proximal effectors have been characterized so far, which include: **i)** regulators of the cytoskeleton, **ii)** transcription factors, **iii)** serine/threonine kinases, **iv)** tyrosine kinases, and **v)** phospholipid kinases, among others [83]. Each GTPase binds to a particular collection of effectors, which is one of the key determinants of the functional idiosyncrasy of each member of the Rho family [84].

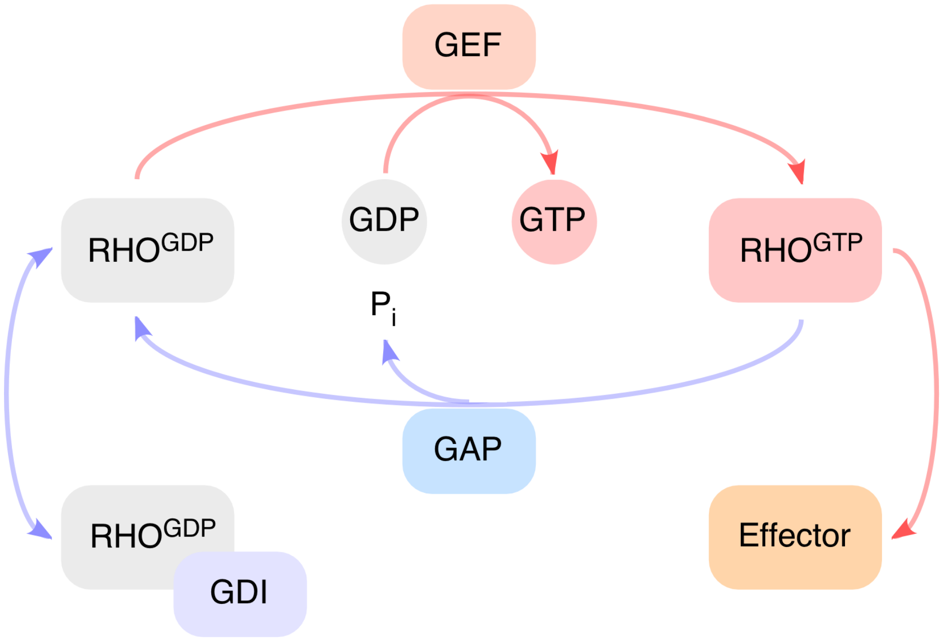

FIGURE VII. Rho GTPases function as molecular switches. Scheme depicting the main agents and mechanisms that regulate the activity of Rho GTPases.

4.1.2. The family of Rho exchange factors

The Rho GEFs constitute a large and heterogeneous family of more than 70 members that differ in expression patterns, subcellular locations, regulatory mechanisms, Rho GTPase specificity, scaffolding of downstream effectors and other non-catalytical functions (**Figure VIII**). Such diversity is linked to their structure: a GEF-specific set of domains that accompanies a conserved Dbl or Dock catalytic core (for a review, see [85]).

In the activation of Rho GTPases, Rho GEFs play a doubly-essential role as they catalyze the GDP-for-GTP exchange and also function as scaffolds that bring GTPase and effector into close proximity. Consequently, one of the best-characterized mechanisms of Rho GTPase hyperactivation is through the upregulation of GEF activity, either by mutation or increased expression [83, 85, 86]. This shows that GEFs can be very relevant in the pathobiological programs mediated by Rho GTPases, and even have potential therapeutic value for some Rho-signaling-addicted diseases. Nevertheless, as happens with Rho GTPases, the actual in vivo role of these proteins in physiologically- and pathologically-relevant contexts still remains poorly characterized.

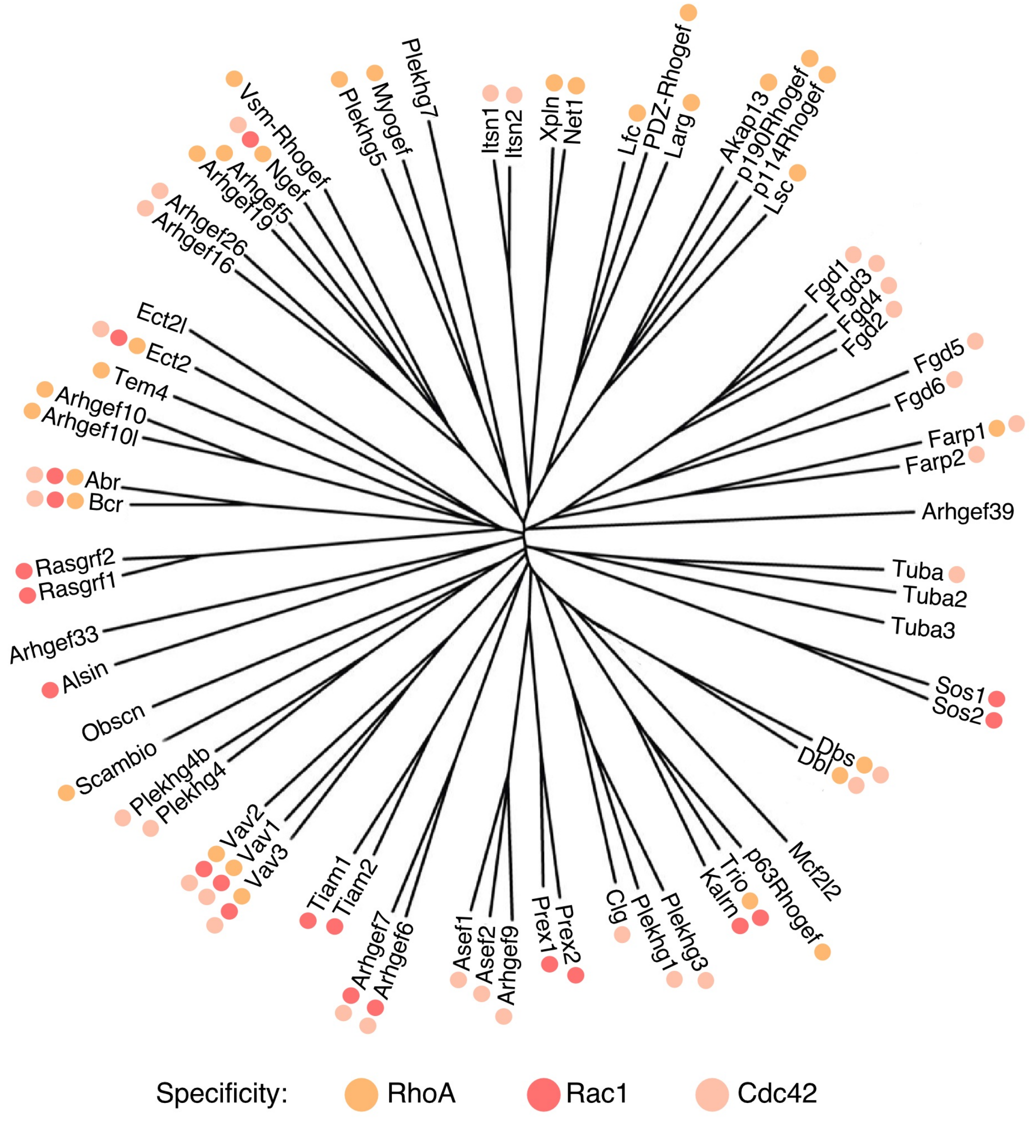
Vsm-Rhogef
Ngef
Arhgef5
Arhgef19
Arhgef26
Arhgef16
Plekhg5
Myogef
Plekhg7
Itsn1
Itsn2
Xpln
Net1
Lfc
PDZ-Rhogef
Larg
Akap13
p190Rhogef
p114Rhogef
Lsc
Fgd1
Fgd3
Fgd4
Fgd2
Fgd5
Fgd6
Farp1
Farp2
Arhgef39
Tuba
Tuba2
Tuba3
Sos1
Sos2
Dbs
Dbl
Mcf2l2
p63Rhogef
Trio
Kalrn
Plekhg3
Plekhg1
Clg
Prex2
Prex1
Arhgef9
Asef2
Asef1
Arhgef6
Arhgef7
Tiam2
Tiam1
Vav3
Vav1
Vav2
Plekhg4
Plekhg4b
Scambio
Obscn
Alsin
Arhgef33
Rasgrf1
Rasgrf2
Bcr
Abr
Arhgef10l
Arhgef10
Tem4
Ect2
Ect2l
Specificity:
RhoA
Rac1
Cdc42

FIGURE VIII. **Rho GEFs constitute a large and heterogeneous family**. Dendrogram showing the phylogenetic classification and the catalytic specificity of every Rho GEF. Adapted from [85].

4.2. RHO GTPASES IN EPIDERMAL STEM CELL HOMEOSTASIS

Discovered on the basis of their homology to Ras GTPases, most studies on Rho GTPases have been primarily directed towards tumorigenesis-related processes. This bias has led to a gap in our understanding of the function of these proteins in the maintenance of tissue homeostasis in purely physiological settings. However, their well-documented roles in adhesion, proliferation and differentiation suggest that Rho GTPases play crucial roles in the maintenance of many tissues, including the epidermis. Supporting this hypothesis, some mouse models have shown that epidermal stem cells are strongly dependent on Rho signaling.

Rac1 has been found by several studies to be unequivocally essential for the maintenance of the EpSC population [87-89]. Different knockout mice for this GTPase display a dramatic differentiation and exhaustion of the EpSC reservoir at the hair follicle bulge, which translates to defective hair follicle formation [87-89]. Furthermore, depletion of epidermal Rac1 also leads to loss of clonogenic potential [87, 90] and impaired wound healing, both in vivo and in vitro [89, 91]. Whether the deletion of Rac1 also affects the integrity of the interfollicular epidermis, however, has been the subject of conflicting reports. Although it was initially proposed that this GTPase would be essential for the maintenance of the epidermis, later studies found that Rac1 is dispensable in such context [87-89].

Much less is known of the role of RhoA in epidermal stem cell homeostasis, as its depletion does not lead to overt epidermal defects [92]. Nevertheless, in vitro studies have shown that this GTPase regulates EpSC proliferation, migration and differentiation [93-95]. There are also evidences associating Cdc42 signaling with the fitness of epidermal stem cells, as it has been shown in vivo that this GTPase regulates the fate of hair follicle progenitor cells through the control of β-catenin turnover [96].

These findings demonstrate that balanced Rho signaling is required for the homeostasis of epidermal stem cells, but also underscore how little is currently known of the mechanisms and agents that physiologically mediate such balance. In this regard, a number of indirect evidences coming from both in silico and in vivo models suggest that Rho GEFs might play an instrumental role [95, 97, 98].

4.3. RHO GTPASES IN SQUAMOUS CELL CARCINOMA

The first evidences pointing towards an implication of Rho GTPases in cancer cell growth came from the transforming activity that some of them displayed in vitro [99]. This finding was then followed by extensive cell biology data showing that Rho

GTPases were key regulators of cancer-associated processes [81, 82]. However, the assumption that these proteins were actually relevant for human cancer was for a long time challenged by the fact that, unlike RAS proteins, mutations in RHO GTPases were rarely found in human cancers. It was not until the recent development of Next Generation Sequencing technologies and the conduction of large high-throughput genomic and transcriptomic studies of human tumors that this paradigm shifted [83]. Currently, both human- and mouse-derived data demonstrate that Rho GTPases play crucial roles in various cancer types, including cSCC and hnSCC (**Figure IX**).

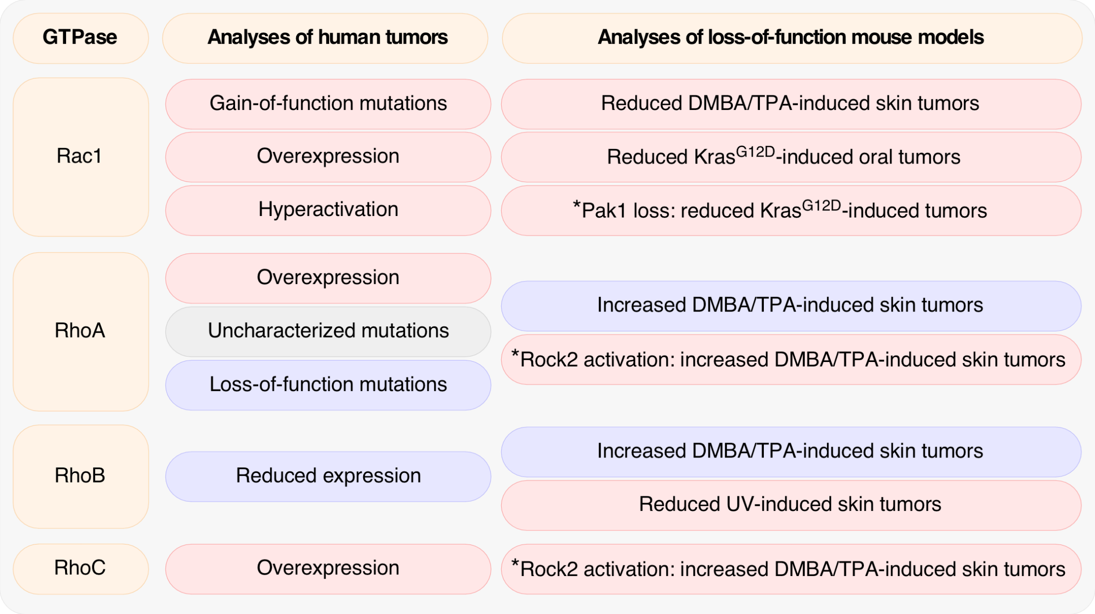

GTPase	Analyses of human tumors	Analyses of loss-of-function mouse models
Rac1	Gain-of-function mutations	Reduced DMBA/TPA-induced skin tumors
	Overexpression	Reduced Kras^{G12D}-induced oral tumors
	Hyperactivation	*Pak1 loss: reduced Kras^{G12D}-induced tumors
RhoA	Overexpression	Increased DMBA/TPA-induced skin tumors
	Uncharacterized mutations	*Rock2 activation: increased DMBA/TPA-induced skin tumors
	Loss-of-function mutations	
RhoB	Reduced expression	Increased DMBA/TPA-induced skin tumors
		Reduced UV-induced skin tumors
RhoC	Overexpression	*Rock2 activation: increased DMBA/TPA-induced skin tumors

FIGURE IX. **Implication of Rho GTPases in SCC**. Scheme summarizing the current human- and mouse-based evidences of the involvement of Rho GTPases in cSCC and hnSCC carcinogenesis. Putative pro- and anti-tumorigenic implications are highlighted in red and blue, respectively.

4.3.1. Rac family in SCC carcinogenesis

Among the Rho family, Rac1 is the most unequivocally SCC-associated member (**Figure IX**). This GTPase is recurrently found upregulated in cSCC and hnSCC, where its GTP-bound levels are also elevated [86, 87, 100, 101]. In addition, RAC1 is the RHO GTPase with the highest frequency of mutation in these tumors [83, 86]. These mutations frequently target the P29 residue and turn RAC1 into a hyperactive fast-cycling GTPase [83, 86].

Such tumor-derived evidences suggest that RAC1 plays a protumorigenic role in SCC. In line with this, Rac1 deletion in mouse models confers protection from DMBA+TPA-induced skin tumors and K-Ras^{G12D}-induced oral tumors [102, 103]. The loss of Rac1 downstream effectors such as Pak1 also abrogates the development of tumors in these carcinogenic models, further demonstrating the implication of the Rac1 signaling axis in SCC carcinogenesis [104, 105].

4.3.2. Rho family in SCC carcinogenesis

Rho subfamily members seem to play both pro- and anti-tumorigenic roles in different biological settings (**Figure IX**). Although many of them are yet to be characterized, most RHOA mutations found in hnSCC seem to induce a loss of function of the protein [83, 106]. In line with this, loss of RhoA in mouse models of DMBA+TPA-induced skin tumors translates to an increased tumor multiplicity, an indication that this GTPase functions as a tumor suppressor in SCC development [86, 107]. Nevertheless, both *RHOA* and *RHOC* have been found upregulated in squamous cell carcinomas, where they have been associated with poor prognosis [108]. This suggests that RHOA might also play prooncogenic functions in some context of SCC development. Consistent with the latter possibility, the activation of the RhoA downstream effector Rock2 results in an increased development of skin tumors in DMBA+TPA- and HRas^{G12V}-based SCC mouse models [83, 109].

Similarly puzzling observations are made in the case of RHOB. Although it is rarely mutated, reduced expression of *RHOB* is observed in hnSCC [86], which would suggest that this GTPase plays anti-tumorigenic roles. However, mouse models studies suggest that the picture is more complex, as loss of RhoB enhances and abrogates skin SCC tumorigenesis induced by DMBA+TPA and ultraviolet radiation, respectively [110, 111].

4.3.3. Cdc42 family in SCC carcinogenesis

Among the three main RHO GTPases, CDC42 seems to be the least relevant for SCC carcinogenesis. Very few mutations or transcriptional alterations have been detected in this gene so far, and the ones found are yet to be functionally characterized. Up to now, it has been implicated in other tumors such as melanoma, breast, lung and colorectal carcinomas [83, 86].

4.4. RHO GEFS IN SQUAMOUS CELL CARCINOMA

The pivotal role of Rac and Rho GTPases in SCC carcinogesis makes them appealing targets for anti-cancer therapeutics. However, GTPases are poorly druggable proteins, so their function cannot be pharmacologically blocked directly [100]. For this reason, the identification of the mediators that regulate the activity of these proteins in the carcinogenic context might provide valuable tools to harness Rho activity towards potential novel therapeutic avenues.

Since the activation of Rho GTPases relies on Rho GEFs, it is reasonable to hypothesize that the latter might be responsible for some of the Rho signaling deregulation events that occur in cancer. Nevertheless, experimentally-validated roles associated to SCC carcinogenesis have only been found for a reduced number of GEFs, namely, Ect2, Tiam1 and some members of the Vav family.

4.4.1. Ect2

Ect2 is a nuclear exchange factor for Rac, Rho and Cdc42 GTPases with a key role in cytokinesis and rRNA synthesis [106, 112, 113]. This GEF is a well-established oncogene that is found upregulated in a high number of cancers, including hnSCC [85, 106, 114]. Such upregulation is, at least in some tumors, accompanied by the mislocalization of the protein, which migrates from the nucleus to the cytoplasm where it promotes ectopic Rac activation [85, 106, 114]. Despite these preliminary evidences, the actual role that this GEF might play in SCC carcinogenesis is not known as currently there are no mouse-model-based studies.

4.4.2. Tiam1

Tiam1 is a Rac-specific GEF that was initially identified due to its relevance in T-cell lymphoma invasion [115]. Years later, HRas-driven mouse models of skin cancer showed that this GEF is also relevant for SCC tumorigenesis. Upon DMBA+TPA treatment, Tiam1-deficient mice develop fewer tumors, of smaller size and with longer latency than the wild-type counterparts [98] (**Figure X**). However, the tumors that eventually develop in this model display an exacerbated malignancy. These results suggest that in some biological scenarios this GEF might conceal an anti-tumorigenic role. Consistent with this notion, *TIAM1* levels decrease with the progression of some cancers, including SCC and breast carcinomas [98, 116].

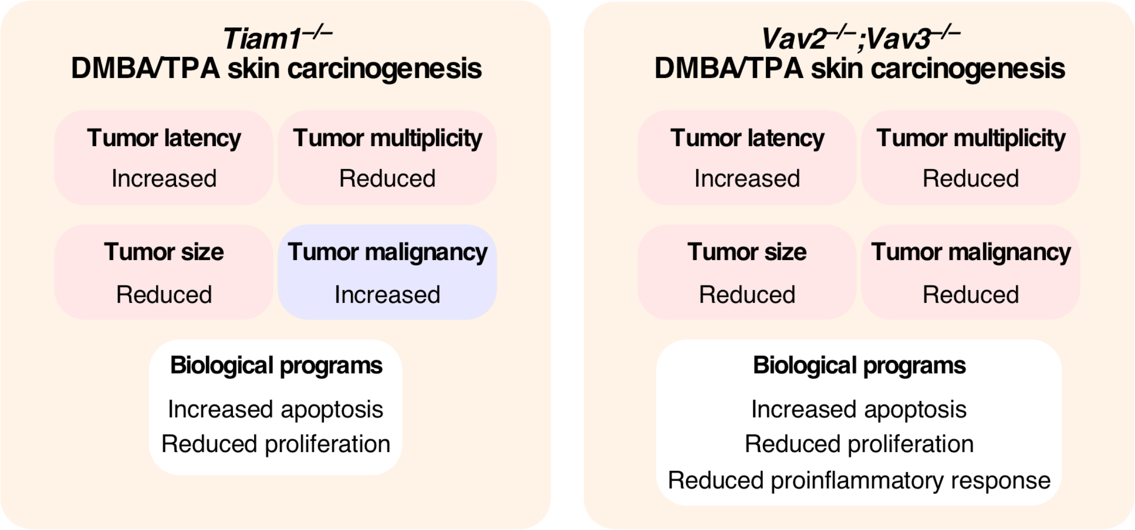
Tiam1−/−
DMBA/TPA skin carcinogenesis
Tumor latency
Increased
Tumor multiplicity
Reduced
Tumor size
Reduced
Tumor malignancy
Increased
Biological programs
Increased apoptosis
Reduced proliferation
Vav2−/−;Vav3−/−
DMBA/TPA skin carcinogenesis
Tumor latency
Increased
Tumor multiplicity
Reduced
Tumor size
Reduced
Tumor malignancy
Reduced
Biological programs
Increased apoptosis
Reduced proliferation
Reduced proinflammatory response

FIGURE X. **Tiam1 and Vav GEFs play crucial roles in SCC development**. Scheme summarizing the findings derived from the two only mouse models that so far have been used to assess the relevance of Rho GEFs in SCC development [97, 98]. Putative pro- and anti-tumorigenic implications are highlighted in red and blue, respectively.

4.4.3. Vav family

Vav proteins are tyrosine-phosphorylation-regulated GEFs that catalyze the activation of Rac1 and RhoA GTPases. Despite their similarity, the three members of the family are characterized by fairly divergent spectra of physiopathological roles (for a review, see [117]).

Vav2 and Vav3 display a ubiquitous expression pattern and play key homeostatic functions in a number of tissues, including the cardiovascular system and the brainstem, respectively [117-122]. Although these GEFs have been associated to a number of solid tumors [123-127], the only findings currently validated by mouse models are circumscribed to skin and breast cancer [97, 128]. Since traditionally these two GEFs have been deemed to play partially overlapping functions, such studies have been performed in a *Vav2*$^{-/-}$;*Vav3*$^{-/-}$ double knockout mouse model. These animals allowed to discover that Vav2 and Vav3 cooperate in the epidermal compartment to control an autocrine and paracrine program linked to proliferation and the creation of a proinflamatory environment that impinges on cSCC development [97]. As a result, when subjected to DMBA+TPA-induced skin carcinogenesis, *Vav2*$^{-/-}$;*Vav3*$^{-/-}$ mice develop fewer, smaller and more benign tumors than the wild-type couterparts [97] (**Figure X**).

Unlike Vav2 and Vav3, the first member of the Vav family is not thought to participate in SCC carcinogenesis, as it is primarily expressed in hematopoietic cells. In this cell compartment Vav1 plays essential roles in lymphocyte development and tumorigenesis [117, 129, 130]. It should be noted, however, that ectopic expression of VAV1 has been detected in some solid tumors [131-133], and thus a potential contribution of this GEF to SCC tumors cannot be entirely ruled out.

4.5. DO RHO GEFS HARBOR THERAPEUTIC VALUE?

Although the aforementioned studies provide valuable data demonstrating that some Rho GEFs can play relevant roles in SCC carcinogenesis, the lack of appropriate models leaves unanswered some of the most fundamental questions so as to exploit this knowledge in a biomedical scenario. Can the gain of function of a single GEF promote SCC? Are the results obtained from mouse models valid for human tumors? Are GEFs approachable as therapeutic targets? How would such therapy interfere with their physiological roles?

In order to address these questions, focusing on Rac1 GEFs seems prima facie the most promising approach. This is due to the fact that, as mentioned before: **i)** Rac1 is the only Rho GTPase to unequivocally play a protumorigenic role in SCC, **ii)** the activity of this GTPase is consistently increased in SCC tumors, **iii)** the mutation frequency in the *RAC1* gene cannot account for such increased activity and **iv)** the abrogation of Rac1 signaling abrogates SCC development in mouse models. Interestingly, previous reports suggest that this increase in RAC1 activity in SCC cells is mediated, at least in part, by the GEF VAV2 [124]. Such observation is in keeping with the fact that *Vav2*$^{-/-}$;*Vav3*$^{-/-}$ mice are resistant to SCC development in skin carcinogenesis models [97]. For these reasons, we thought Vav2 would be an ideal candidate to investigate the significance and exploitability of Rho GEF signaling in the homeostasis and carcinogenesis of the squamous epithelium.

OBJECTIVES

Based on the preceding evidence, the research presented in this Ph.D. thesis pursues the following main objectives:

1. To characterize the implication and role of the Rho GEF Vav2 in the carcinogenesis of cutaneous and head–and–neck squamous cell carcinomas.

2. To evaluate the therapeutic value of the inhibition of Vav2 catalytic activity in squamous cell carcinoma.

3. To investigate the physiological roles of Vav2 associated to the homeostatic maintenance of the squamous epithelium.

4. To identify and validate additional Rho exchange factors with relevant functions in head–and–neck squamous cell carcinoma.

METHODS

EXPERIMENTAL MODEL AND SUBJECT DETAILS

Ethics statement

Animal work was done according to protocols approved by the Bioethics committee of Salamanca University. The use of patient samples was done according to methods and informed patient consent policies approved by the Bioethics committees of both the Institute for Research in Biomedicine and Vall d'Hebron Research Institute.

Mouse experiments

Vav2$^{\text{Onc}}$, *Vav2*$^{-/-}$, *Vav3*$^{-/-}$, *Vav2*$^{-/-}$;*Vav3*$^{-/-}$, and *Vav1*$^{-/-}$;*Vav2*$^{-/-}$;*Vav3*$^{-/-}$ mice have been described elsewhere [97, 122, 134, 135]. The *Vav2*$^{\text{L332A}}$ knock–in mouse strain was generated by GenOway using the indicated vector in **Figure 8.1** following standard homologous recombination techniques in embryonic stem cells.

For carcinogenesis experiments in newborn mice, 3–day–old mice received a single application of 5 μg of DMBA (Sigma, Catalog No. D3254) in 200 μl of acetone. For complete carcinogenesis experiments in adult mice, the backs of 6– to 8–week–old animals of the indicated genotypes were shaved and treated biweekly with 5 μg of DMBA in 200 μl of acetone for 20 weeks. The two–step carcinogenic DMBA/TPA protocol was initiated with a single topic application of 200 μl of 0.013% DMBA dissolved as above followed by biweekly applications of 200 μl of 1×10^{-4} M TPA (Sigma, Catalog No. P8139) dissolved in acetone for the indicated period of time. The number, size and incidence of tumors were monitored weekly. Time–course studies of the in vivo response of the epithelia of WT and *Vav2*$^{\text{Onc}}$ mice to TPA using both determination of epithelial hyperplasia and BrdU incorporation were carried out as indicated before [97]. Upon euthanasia, tumors and tissue samples were collected and processed for both histological and immunohistochemical analyses.

For the tongue orthotopic xenograft experiments, exponentially growing oSCC patient derived cells were detached using accutase (CELLnTEC, Catalog No. CnT–Accutase–100), centrifuged at 300 xg for 5 min, and resuspended in culture medium at a density of 1.7×10^{6} cells per ml. 5×10^{4} SCC cells were then introduced orthotopically using an ultrafine 8–mm–needle (BD, Catalog No. 320927) in the tongues of 6– to 8–week–old *Vav1*$^{-/-}$;*Vav2*$^{-/-}$;*Vav3*$^{-/-}$ mice previously anesthetized by injecting intraperitoneally 200 µl of a mixture of 10 mg/ml ketamine (Merial, Catalog No. Imalgene 1000) and 2 mg/ml xylazine (Bayer, Catalog No. Rompun) in phosphate buffered saline solution. Growth of tumors was then periodically visualized using an IVIS Lumina In Vivo Imaging System (PerkinElmer, Catalog No. CLS136334) upon administering 50 µl of a 5 mg/ml solution of D–luciferine (Goldbio, Catalog No. LUCK–500) to mice. This procedure was performed with animals anesthetized as above. Mice were reanimated after finishing the recordings by injecting intraperitoneally 200 µl of a 1 mg/ml atipamezole (Ecuphar, Catalog No. Antisedan) solution in phosphate buffered saline solution. Upon euthanasia, tumors were collected and processed for pathological and immunohistochemical analyses.

Cardiovascular and renal parameters were determined as previously described in 4-month-old male mice [118].

Wound healing assays were performed in 8/10-week-old mice using a scalpel (Swann-Morton, Catalog No. 0508) or a biopsy punch (Stiefel, Catalog No. BI1500). Two days after shaving, a 1-cm incision was made in the dorsal skin and its healing was monitored daily. For hair regeneration assays, 8/10-week-old mice were shaved and hair growth was followed up daily.

For label-retaining cell (LRC) pulse-chase experiments, 50 mg/kg of BrdU (5-bromo-2’-deoxyuridine) (ThermoFisher, Catalog No. B23151) were injected intraperitoneally in 10-day-old mice every 12 hours for a total of 4 injections and chased after 80 days. For epidermal cell proliferation assays, 1 mg of BrdU (5-bromo-2’-deoxyuridine) (ThermoFisher, Catalog No. B23151) or EdU (5-ethynyl-2’-deoxyuridine) (Invitrogen, Catalog No. A10044) was injected intraperitoneally 1 hour before euthanasia in mice of the indicated ages.

For skin stimulation experiments, the dorsal skin of shaved animals was treated with 200 µL of an acetone solution of 3.3×10^{-5} M TPA (12-O-tetradecanoyl-phorbol-13-acetate) (Sigma, Catalog No. P8139). Mice were euthanized 24 hours later.

For skin xenograft experiments, keratinocytes and fibroblasts were isolated from donor mice as indicated previously [97]. Briefly, the skin from newborn mice was isolated and incubated in CnT-07 medium (CELLnTEC, Catalog No. CnT-07) with 5 mg/mL of dispase (Roche, Catalog No. 04942078001) overnight at 4ºC to separate the epidermis from the dermis. For keratinocyte isolation, the epidermis was then incubated with accutase (CELLnTEC, Catalog No. CnT-Accutase-100) for 30 minutes at 37ºC. For fibroblast isolation, the dermis was digested in DMEM (ThermoFisher, Catalog No. 11995065) with 0.25% collagenase (Sigma, Catalog No. C5138) for 1 hour at room temperature. All the keratinocytes resulting from one newborn mouse plus 4 x10^6 dermal cells were combined in a cell suspension for each xenograft. 8-week-old nude mice (Charles River, Catalog No. NU/NU) were anesthesized with 100 μL of a mixture of 25 mg/mL ketamine (Merial, Catalog No. Imalgene 1000), 2 mg/mL diazepam (Roche, Catalog No. Valium) and 0.1 mg/mL atropine (Braun, Catalog No. Atropine B) and placed on a heating pad. After cleaning the dorsal surface with iodopovidone, a 1-cm incision in the skin was made to insert a skin xenograft chamber as reported before [136]. The chamber was then secured with stitches and the cell suspension was introduced. One week after the intervention, mice were anesthesized and the chamber was removed. Six weeks later, skin reconstitution was considered completed and animals were injected intraperitoneally with 50 mg/kg of BrdU and sacrificed 1 hour later. Xenografted skin was taken for histological studies (see below). [130]

Primary mouse keratinocytes

Primary keratinocytes were isolated as described elsewhere [97]. Briefly, the skin from newborn mice of the indicated genotypes was treated with 250 U/ml of dispase (Roche, Catalog No. 04942078001) overnight at 4 °C. Next day, the epidermis was separated from the dermis and treated with accutase for 30 min at 37 ºC to extract the keratinocytes. Cultures were maintained in CnT07 medium (CELLnTEC, Catalog No. CnT–07) on type I collagen–precoated plates (BD Biosciences, Catalog No. 356400).

Commercially–available cell lines

Immortalized, primary neonatal human keratinocytes (KerCT cells) were purchased from the American Type Culture Collection (Catalog No. CRL–4048) and cultured in KGM–Gold medium (Lonza, Catalog No. 00192060). These cells have been immortalized by ectopically expressing human TERT and CDK4. SCC–25 cells were obtained from S.A.B. and cultured in KSFM medium (Thermo Fisher, Catalog No. 17005–042) supplemented with 25 µg/ml bovine pituitary extract (Thermo Fisher, Catalog No. 17005–042) and 0.5 ng/ml human epidermal growth factor (Thermo Fisher, Catalog No. 17005–042). COS1 cells were obtained from the American Type Culture Collection and grown in DMEM supplemented with 10% fetal calf serum, 1% L–glutamine, penicillin (10 µg/ml) and streptomycin (100 µg/ml). Unless otherwise indicated, all tissue culture reagents were obtained from Gibco.

oSCC patient–derived cells

These cells were obtained by S.A.B and described elsewhere [137]. VdH15 cells were cultured in KSFM medium supplemented with 25 µg/ml bovine pituitary extract and 0.5 ng/ml human epidermal growth factor. VdH01 and VdH02 cells were cultured in FAD^{+} medium that is composed of three parts of DMEM (Gibco, Catalog No. 21969) and one part of Ham's F12 medium (Thermo Fisher, Catalog No.11765054) supplemented with 10% fetal bovine serum (Gibco, Catalog No. 10270106), 1.8 x 10^{-4} M adenine (Sigma, Catalog No. A2786–5G), 0.5 µg/ml hydrocortisone (Sigma, Catalog No. H4001–1G), 5 µg/ml insulin (Thermo Fisher, Catalog No. 12585014), 10 ng/ml EGF (PreproTech, Catalog No. AF–100–15), 10^{-10} M cholera toxin (Sigma, Catalog No. C8052–5MG), and 2 mM L–glutamine (Gibco, Catalog No. 25030024).

METHOD DETAILS

Plasmid generation

To generate the lentiviral vector encoding HA–tagged Vav2^{Onc} (pCCM34), a cDNA fragment encoding the HA–tagged version of Vav2 (fragment 187–868) was amplified by PCR using the primers 5'–AAT AAC TAG TGC CAC CAT GTA CCC ATA CGA CGT CCC AGA CTA CGC TAA AAT GGG AAT GAC TGA GGA CGA C–3' and 5'–ATA GAC CGC GGC CGC TCA CTG GAT GCC CTC CTC TTC TAC GTA–3' (restriction sites underlined) and the pCMV–Vav2–HA vector as template [138]. Upon digestion with SpeI and NotI, the cDNA fragment was cloned into the linearized pLVX–IRES–Hyg vector (Clontech, Catalog No. 632185). To generate the vector encoding HA–Vav2$^{\text{Onc+E200A}}$ (pFLM12), the pCCM34 vector was subjected to site–directed mutagenesis using the primers 5’–GAC AAG AGA AGC TGC TGC TTG TTA GCG ATT CAG GAG ACC GAG GCC AAG TAC–3’ and 5’–CAT GAA CCG GAG CCA GAG GAC TTA GCG ATT GTT CGT CGT CGA AGA GAA CAG–3’ (changes used to generate the mutated codon are underlined). The pMIEG3, pMIEG3–Rac1$^{\text{F28L}}$, pMIEG3–RhoA$^{\text{F30L}}$ and pMIEG3–Cdc42$^{\text{F28L}}$ plasmids have been reported before [139]. To generate the plasmid encoding EGFP–Vav2$^{\text{Onc}}$ (pNM115), the plasmid pKES19 [140] was digested with BstXI, filled–in, and cloned into the SmaI–linearized pEGFP–C2 vector (Clontech, Catalog No. 632481). The plasmid encoding EGFP–Vav2$^{\text{Onc+E200A}}$ (pFLM07) was obtained by site–directed mutagenesis of pNM115 using the primers 5’–GAC AAG AGA AGC TGC TGC TTG TTA GCG ATT CAG GAG ACC GAG GCC AAG TAC–3’ and 5’–CAT GAA CCG GAG CCA GAG GAC TTA GCG ATT GTT CGT CGT CGA AGA GAA CAG–3’ (the altered nucleotides used to create the E200A mutation are underlined). The plasmid encoding EGFP–Vav2$^{\text{L332A}}$ (pSAF3) was obtained by site–directed mutagenesis of a homemade EGFP–Vav2–encoding vector (pAA7) [141] using the primers 5’–GGT GCC CAT GCA ACG GGT GGC GAA GTA CCA CCT GCT GCT C–3’ and 5’–GAG CAG CAG GTG GTA CTT CGC CAC CCG TTG CAT GGG CAC C–3’ (the altered nucleotides used to create the L332A mutation are underlined). The plasmid encoding EGFP–Vav2$^{\text{del309–339}}$ (pSAF2) was generated by SacI–flanked PCR amplification of the first 1285 bp (amino acids 1–308) of Vav2 cDNA using the plasmid pAA7 as template and the primers 5’–CCG GGC GAG CTC AAT GGA GCA GTG GCG GCA ATG CGG C–3’ and 5’–CCG GGC GAG CTC TGT GCA CTC CTC CAC TTT CTG–3’ (restriction sites underlined). Upon SacI digestion, the cDNA fragment was cloned into the linearized pNM115 vector containing Vav2 sequence from nucleotide 1378 to end (amino acids 340–868). The plasmid encoding EGFP–Vav2$^{\text{Onc+L332A}}$ (pSAF1) was obtained by site–directed mutagenesis of pNM115 using the primers indicated for pSAF3. The plasmid encoding EGFP–Vav2$^{\text{Onc+}\Delta\text{309–339}}$ (pSAF4) was generated as indicated for pSAF2 using the plasmid pNM115 as template and the primers 5’–CCG GGC GAG CTC AAT GGG CAT GAC TGA GGA CGA CAA G–3’ and 5’–CCG GGC GAG CTC TGT GCA CTC CTC CAC TTT CTG–3’ (restriction sites underlined). Plasmids encoding c–Myc and the Yamanaka’s factors (Oct4, Sox2, Klf4 and c–Myc) were provided by P.M. Fernández–Salguero (Department of Biochemistry and Molecular Biology, Extremadura University, Badajoz, Spain).

The luciferase plasmids used to assay promoter activation included: pAP1–Luc (AP1 reporter, obtained from Stratagene), pBV–Myc–Del1–Luc (c–Myc reporter, obtained from Addgene, Catalog No. 16601), pGL2–Chk1–WT–Luc (E2F reporter, obtained from A.M. Zubiaga, Department of Genetics, Physical Anthropology and Animal Physiology, University of the Basque Country, Bilbao, Spain), p8xGTIIC–Luc (TEAD reporter, obtained from Addgene, Catalog No. 34615), pFA2–cJun (JNK reporter, obtained from Stratagene), pSRE–Luc (SRF reporter, Agilent, Catalog No. 219081), and pRL–SV40 (*Renilla* luciferase, obtained from Promega, Catalog No. E2231). All plasmids were DNA sequence verified.

In silico analyses of public gene expression data

R (version 3.5.1) and Perl were used to carry out the statistical analyses and data processing, respectively. Signal intensity values were obtained from CEL files after robust multichip average (RMA). Differentially expressed genes were identified using linear models for microarray data (Limma). Adjusted *P* values for multiple comparisons were calculated applying the Benjamini–Hochberg correction (false discovery rate, FDR). The GEO datasets GSE45216 and GSE13355 (human cSCC), GSE30784 (human oSCC) and GSE21264 (mouse cSCC) were used to identify the RHO GEFs differentially expressed in SCC tumors as well as to obtain the mRNA expression levels according to pathological status. The dataset GSE52954 was used to assess the expression of RHO GEFs during keratinocyte differentiation. The TCGA hnSCC dataset was accessed and analyzed through the TCGAbiolinks R package. In all cases, a 0 to 1 normalization of the expression values was applied for representation purposes. A T–ALL dataset GSE26713 was used as control for SCC–specific deregulation. Overall survival analyses were performed through Kaplan–Meier estimates using the GSE41613 dataset. The median of the expression distribution for each transcript was used to establish the low and high expression groups and, subsequently, the Mantel–Cox test was applied to statistically validate the differences between the survival distributions. Correlation matrices were calculated from the indicated expression matrices using the corrplot R package. Circos plots were generated using the OmicCircos R package implemented with human genomic data from the UCSC Genome Browser and public copy-number variation data from GISTIC analyses of the TCGA hnSCC dataset. The GEF-based gene network reverse engineering was performed through ARACNE [142] using the adaptative partitioning algorithm for mutual information inference, and setting the indicated GEFs as hubs and a *P* value threshold of 10^{-10}. The resulting networks were represented using the Cytoscape software [143] and functionally analyzed through Metascape [144]. For the discovery of transcription factor binding motifs in the promoters of the coregulated genes, the iRegulon software was used [145]. A collection of 9,713 position weight matrices (PWMs) was applied to analyze 10 kb–long DNA sequences that were centered around the transcriptional start sites. Using as criteria a maximum false discovery rate (FDR) on motif similarity below 0.001, we performed motif detection, track discovery, motif–to–factor mapping, and target detection. The ternary and radar plots used to represent GEF catalytic specificity and subcellular localization were generated with the R Ternary and fmsb packages and the data available in [146].

Immunoprecipiation experiments

Healthy mucosa, when included in the experiments, where obtained from the hnSCC patients (due to this, they were assigned the same identification number shown in **Figure 1.3**). Tumoral and healthy tissues were mechanically homogenized in RIPA buffer (10 mM Tris–HCl [pH 8.0], 150 mM NaCl, 1% Triton X–100 (Sigma, Catalog No. X100), 1 mM Na_3VO_4 (Sigma, Catalog No. S6508), 1 mM NaF (Sigma, Catalog No. S7920), and a mixture of protease inhibitors (Roche, Catalog No. 11836145001) using a gentleMACS dissociator (Miltenyi Biotec, Catalog No. 130–093–235) and gentleMACS M tubes (Myltenyi Biotec, Catalog No. 130–096–335). Extracts were precleared by centrifugation at 13,200 rpm for 10 min at 4 ºC. Protein concentration in the resulting supernatants was quantified using the Bradford reactive (Bio–Rad, Catalog No. 5000006). 400 μg of protein extracts in a final volume of 500 μl of RIPA buffer were incubated with 1.5 μl of a homemade antibody to Vav2 (Lab catalog No. 580–2) for 2 hours at 4 ºC in a rotating wheel. Immunocomplexes were collected with 35 μl of Gammabind G–Sepharose beads (GE Healthcare, Catalog No. GE17–0885–01) at 50% concentration for another 2 hours at 4 ºC in a rotating wheel. After three times washes with the lysis buffer at 4 ºC, the beads were resuspended in

SDS–PAGE buffer, boiled for 5 min, and subjected to Western blot analyses as indicated below.

Western blotting

In the case of tissue extracts, samples were transferred to RIPA buffer and mechanically homogenized using the gentleMACS dissociator. In the case of keratinocytes maintained in culture, cells were washed with chilled phosphate buffered saline solution and then directly lysed in RIPA buffer at 4 ºC. Extracts were precleared by centrifugation at 13200 rpm for 10 min at 4°C, denatured by boiling in SDS–PAGE sample buffer, separated electrophoretically, and transferred onto nitrocellulose filters using the iBlot Dry Blotting System (ThermoFisher, Catalog No. IB21001). Membranes were blocked in 5% bovine serum albumin (Sigma, Catalog No. A7906) TBS–T (25 mM Tris–HCl (pH 8.0), 150 mM NaCl, 0.1% Tween–20 (Sigma, Catalog No. P7949) for at least 1 hour and then incubated overnight at 4 ºC with the appropriate antibodies to Vav2 (1:1000 dilution, homemade), GFP (1:5000 dilution, Covance, Catalog No. MMS–118P), the hemagglutinin (HA) epitope (1:1000 dilution, Cell Signaling, Catalog No. 3724), Rac1 (1:1000 dilution, BD Biosciences, Catalog No. 610651), RhoA (1:1000 dilution, Cell Signaling, Catalog No. 2117), Cdc42 (1:1000 dilution, Santa Cruz Biotechnology, Catalog No. sc–87), c–Myc (1:1000 dilution, Merck, Catalog No. 06–340), and tubulin α (1:2000 dilution, Calbiochem, Catalog No. CP06). After three washes with TBS–T to eliminate the primary antibody, the membrane was incubated with the appropriate secondary antibody (1:5000 dilution, GE Healthcare) for 30 min at room temperature. Immunoreacting bands were developed using a standard chemiluminescent method (ThermoFisher, Catalog No. 32106). Blots were quantified using the ImageJ software. When indicated, filters were stained with Ponceau S solution (Sigma, Catalog No. P7170).

Analysis of mRNA abundance

Total RNA was extracted using NZYol (NZYtech, Catalog No. MB18501) and quantitative RT–PCR performed using the Power SYBR Green RNA–to–CT 1–Step Kit (Applied Biosystems, Catalog No. 4389986) and the StepOnePlus Real–Time PCR System (Applied BioSystems, Catalog No. 4376600). Raw data were analyzed using the StepOne software (Applied Biosystems). We used the abundance of the endogenous *GAPDH* mRNA as internal normalization control. Primers used for transcript quantitation included: 5'–GAC GGG GAA CTG AAA GTC CG–3' (forward, *VAV2*), 5'–TTT TCC CGT GAG ACT TCT TGA C–3' (reverse, *VAV2*), 5'–ATG GCC TTC CGT GTC CCC ACT G–3' (forward, *GAPDH*), 5'–TGA GTG TGG CAG GGA CTC CCC A–3' (reverse, *GAPDH*), 5'–AAG TAC CTC AGC CTC CAG CA–3' (forward, *Nanog*), 5'–GTG CTG AGC CCT TCT GAA TC–3' (reverse, *Nanog*), 5'–TGC ACC ACC AAC TGC TTA GC–3' (forward, *Gapdh*), 5'–TCT TCT GGG TGG CAG TGA TG–3' (reverse, *Gapdh*), 5'–TCC TCT TCC AGT CCT TAA AGC–3' (forward, *ECT2*), 5'–GTT TCA ATC TGA GGC ATC TCT TCT–3' (reverse, *ECT2*), 5'–GCT CCT AGA GAT TGC CCG TC–3' (forward, *FARP1*), 5'–CCT GGT ACG CAC TAT TGG CA–3' (reverse, *FARP1*), 5'–CCT CTG TGC ACC GGA GTA TG–3' (forward, *FGD6*), 5'–CTG GGA TGC TCC TGA ACT GG–3' (reverse, *FGD6*), 5'–CGG GAA GGA CTC AGC AAC AA–3' (forward, *TRIO*), 5'–GCC TCT CCC AGG TCA CTG TA–3' (reverse, *TRIO*), 5'–GAT CCA GCA GCT GAC CAA GA–3' (forward, *ARHGEF10L*), 5'–CTG GCC CCT GTG GTT GG–3' (reverse, *ARHGEF10L*), 5'–ACA GGC TAC GCA ACA GGT TC–3' (forward, *ITSN2*), 5'–AGC CCC CAG CAT TAA CCA TT–3' (reverse, *ITSN2*), 5'–GAC CCC TCT CAG ACA AAA GC–3' (forward, *KALRN*), 5'–ATC TGC TCG AAG AGG AAC ACG–3' (reverse, *KALRN*), 5'–TGG GAC ATG TGA AGC CAG AC–3' (forward, *TIAM1*), 5'–GAA TGC GCC AAA AAC CCC AT–3' (reverse, *TIAM1*), 5'–GCT TAA CAA CCT CCG GGC G–3' (forward, *VAV3*), 5'–GAA GGG CCT GAT TCC TGT GG–3' (reverse, *VAV3*).

Histological studies

Tissues were extracted, fixed in 4% paraformaldehyde, paraffin embedded, cut in 2–3 µm thick sections, and stained with hematoxylin–eosin. Images were captured using an Olympus BX51 microscope coupled to an Olympus DP70 digital camera. The thickness of the epidermal and/or dermal layers was measured in vertical cross–sections using the software ImageJ. In the case of tumor sections, they were analyzed blindly by a pathologist to classify them according to malignancy grade and level of differentiation.

Immunohistochemical studies

Immunohistochemical staining was performed using a Ventana Discovery Ultra instrument (Roche, Catalog No. 05987750001). Paraffin–embedded sections were dewaxed, subjected to either citrate buffer [pH 6.0] or Tris EDTA [pH 8.0] for heat–induced antigen retrieval, and incubated for 40 min with the appropriate primary antibody to c–Fos (1:50 dilution, Santa Cruz Biotechnology, Catalog No. sc–166940), c–Myc (1:50 dilution, Abcam, Catalog No. ab32072), YAP (1:200 dilution, Novus Biologicals, Catalog No. NB110–58358), Cyclin D1 (1:200 dilution, Roche, Catalog No. 790–4508), keratin 14 (1:300 dilution, Biolegend, Catalog No. 905301), involucrin (1:100 dilution, Sigma, Catalog No. I9018) or BrdU (1:100, BD, Catalog No. 347580). For standard staining, the Discovery OmniMap anti–Rb HRP detection system (Roche, Catalog No. 760–4311) was used for detection and hematoxylin for counterstaining as indicated by the manufacturer. For immunofluorescent studies, we incubated the sections in a humid chamber for 1 hour with secondary antibodies to rabbit and mouse IgGs labeled with Alexa Fluor 488 (1:200 dilution, ThermoFisher, Catalog No. A21206) and Cy3 (1:200 dilution, Jackson ImmunoResearch, Catalog No. 115–165–146), respectively. A 5–minute incubation with DAPI (Sigma, Catalog No. D9542) or rhodamine-labeled phalloidin (Invitrogen; diluted 1:200 in TBS–T and 2% bovine serum albumin) was performed for counterstaining. Samples were analyzed with a Leica TCS SP5 confocal microscope. Images were captured with LAS AF software (version 2.6.0.72266, Leica). Quantitation of immunohistochemical signals were done using the ImageJ software by adjusting the signal threshold to the staining intensity and measuring the area of the resulting particles.

Three–dimensional histotypic cultures

Exponentially growing keratinocytes maintained in CnT–Prime medium were detached using accutase, centrifuged at 300 xg for 5 min at room temperature, and counted. 2 x 10^5 cells were seeded onto polycarbonate inserts (ThermoFisher, Catalog No. 140620) and cultured for two days in CnT–Prime medium. Upon confluency, the medium was changed to 3D–Barrier (CellnTec, Catalog No. CnT–PR–3D) and the air–lift was performed according to the manufacturer's instructions. 3D cultures were maintained for 12 days with three medium changes per week and finally processed for histological study as indicated above. When indicated, the inhibitors and corresponding vehicles were applied in the sixth day after carrying out the airlift and refreshed with the medium changes indicated above. Inhibitors used included FRAX597 (5 nM, Selleckchem, Catalog No. S7271), Y–27632 2HCl (1 µM, Selleckchem, Catalog No. S1049), 1A116 (500 nM) [147], 10058–F4 (500 nM, Selleckchem, Catalog No. S7153), and verteporfin (200 nM, Selleckchem, Catalog No. S1786). Concentrations of inhibitors were selected based on the induction of minor effect in the histotypic structures formed by control cells.

Lentiviral–mediated expression of proteins in human keratinocytes

For the generation of stable cell clones, lentiviral particles were produced in HEK293T cells cultured in DMEM (supplemented with 10% fetal bovine serum and 2 mM L–glutamine) and subsequently concentrated using the LentiX concentrator kit (Clontech, Catalog No. 631232). Keratinocytes were then infected with control and protein–encoding lentiviral particles in KGM–Gold medium in the presence of 8 µg/ml of polybrene (Sigma, Catalog No. H9268) and selected by either antibiotic resistance or EGFP expression by flow cytometry. In the latter case, we used a FACSAria III flow cytometer (BD Biosciences) for cell purification. Proper protein expression was assessed by Western blot.

Rho GTPase activation assays

Total cellular lysates were obtained as above, snap frozen, thawed, quantified for total protein concentration, and analyzed using the Rac1, RhoA and Cdc42 G–LISA assay kits according to the manufacturer's instructions (Cytoskeleton, Catalog No. BK135).

RNA extraction and transcriptome profiling

Whole epidermis or FACS-purified epidermal stem cells were lysed in RLT buffer and RNA was extracted using the QIAGEN RNeasy Mini (QIAGEN, Catalog No. 74104) or Micro Kit (QIAGEN, Catalog No. 74004), respectively, according to manufacturer’s instructions. Purified RNA was processed as indicated elsewhere [97] and hybridized to Affymetrix GeneChip Mouse Gene 1.0 ST microarrays.

In silico analyses of mouse epidermis expression microarray data

Initial data processing was carried out as indicated for the human data (see above). Gene Ontology and KEGG pathways enrichment analyses were performed using DAVID and ToppFun. GSEA was performed using gene set permutations ($n = 1000$) for the assessment of significance and signal–to–noise metric for ranking genes. The gene sets used included signatures related to: epidermal differentiation (GSE52954); SCC stem cells (GSE29328); embryonic stem cells (GSE10423); cSCC cells (GSE5576); and metastatic oSCC cells (GSE72939). We also used lists for transcriptional targets for AP1 [148], c-MYC [149], E2F (signature #M40 from the Molecular Signatures Database, Broad Institute), NFY (signature #C3:TFAC:0178 from the Molecular Signatures Database, Broad Institute), YAP/TAZ/TEAD (GSE66083), and FOXO (signature #C3:TFAC:0256 from the Molecular Signatures Database, Broad Institute). To evaluate the similarity between the transcriptional programs activated by Vav2^{Onc} and those differentially regulated in the indicated SCC and clinical conditions, the datasets GSE45216 and GSE13355 (human cSCC), GSE30784 (human oSCC) and GSE21264 (mouse cSCC) were used as indicated above. To assess conservation of the Vav2^{Onc} transcriptional signature across tumors, a 1.5–fold change threshold was used. Heatmaps were generated using the heatmap3 package. To evaluate the enrichment of the Vav2^{Onc} gene signature across SCC tumors, ssGSEA were used. To assess the specificity of the Vav2^{Onc}–Sig, a principal component analysis was performed using the datasets indicated in the corresponding figure legend. For the identification of the Vav2^{Onc}–driven prognostic signature, the Cox proportional–hazards regression model was applied using the survival R package. Survival analyses according to the Vav2^{Onc}–driven prognostic signature enrichment were performed as indicated above, using datasets from the GEO (GSE41613) and the TCGA (hnSCC collection). For the discovery of transcription factor binding motifs in the promoters of the coregulated genes, the iRegulon software was used as indicated above [145]. Circos plots were generated using the OmicCircos package implemented with mouse genomic data from the UCSC Genome Browser (https://genome.ucsc.edu), gene ontology annotation from the Gene Ontology Consortium (http://www.geneontology.org), and transcription factor annotation from the iRegulon tool. To evaluate the correlation of c–MYC or YAP gene signature with *VAV2* mRNA levels in tumors, we stratified patients according to *VAV2* expression levels (low, medium, and high, established by quantiles) and calculated the ssGSEA enrichment score for the aforementioned signatures.

Generation of induced pluripotent stem cells from primary keratinocytes

Retroviral particles encoding the Yamanaka's factors were used to infect primary keratinocytes obtained from neonate mice in the presence of polybrene (8 µg/ml) and, after two days, transferred to an iPSC medium composed of DMEM–GlutaMAX (ThermoFisher, Catalog No. 31966–021), 15% knockout serum replacement (ThermoFisher, Catalog No. 10828–028), 1x nonessential amino acids (ThermoFisher, Catalog No. 11140–035), 100 µM 2–mercapthoethanol (ThermoFisher, Catalog No. 31350–010), and 1 x 10^3 u/ml LIF (Millipore, Catalog No. ESG1107). Three days later, cells were collected using accutase and seeded on feeder cell layers generated as indicated elsewhere [150]. iPS cell colonies were allowed to grow for two weeks, with daily medium changes, and finally stained with an alkaline phosphatase assay kit (Sigma, Catalog No. AB0300) according to the manufacturer's instructions. The generation of bona–fide iPS cells was further confirmed using qRT–PCR analysis to detect *Nanog* expression.

Promoter activation assays

We utilized luciferase reporter plasmids to evaluate the activation status of the interrogated transcriptional factors of our study. To this end, exponentially growing human keratinocytes were transiently transfected with 40 ng of the pRL–SV40 vector encoding the *Renilla* luciferase for intersample normalization, 2 µg of the appropriate EGFP and EGFP–Vav2 encoding vector, and 2 µg of the appropriate firefly reporter plasmids containing the firefly luciferase gene under the regulation of AP1– (pAP1–Luc), c–Myc– (pBV–Myc–Del1–Luc), E2F– (pGL2–Chk1–WT–Luc), and TEAD– (p8xGTIIC–Luc) responsive promoters. After 24 hours, cells were lysed with Passive Lysis Buffer (Promega, Cat No. E1960) and luciferase activities determined using the Dual Luciferase Assay System (Promega, Cat No. E1960). In all cases, the values of firefly luciferase activity obtained in each experimental point were normalized taking into account the activity of the *Renilla* luciferase obtained in the same samples. In addition, we analyzed aliquots of the same lysates by Western blot to assess the appropriate expression of the ectopically expressed proteins in each case. Values are represented in the figures as the n–fold change of the experimental sample relative to the activity shown by control cells (which was given an arbitrary value of 1 in each case). When needed, these experiments included the use of chemical inhibitors in concentrations identical to those used in the 3D histotypic cultures.

shRNA–mediated transcript knockdown

To target the mRNAs encoding the different GEFs, we infected the indicated cell lines with lentiviruses encoding either empty (TR1.5–pLKO–1–puro, Sigma, Catalog No. SHC001) or a number of independent shRNAs against *VAV2* (TRCN0000435647, referred to in the figures as shRNA#1; TRCN0000436728, referred to in the figures as shRNA#2; TRCN0000048227, referred to in the figures as shRNA#3; TRCN0000418821, referred to in the figures as shRNA#4 and TRCN0000419630, referred to in the figures as shRNA#5), *ECT2* (TRCN0000047686, referred to in the figures as shRNA#1; TRCN0000299365, referred to in the figures as shRNA#2), *FARP1* (TRCN0000303352, referred to in the figures as shRNA#1; TRCN0000047243, referred to in the figures as shRNA#2), *FGD6* (TRCN0000420570, referred to in the figures as shRNA#1; TRCN0000418076, referred to in the figures as shRNA#2), *TRIO* (TRCN0000010561, referred to in the figures as shRNA#1; TRCN0000000871, referred to in the figures as shRNA#2), *ARHGEF10L* (TRCN0000433949, referred to in the figures as shRNA#1; TRCN0000416149, referred to in the figures as shRNA#2), *ITSN2* (TRCN0000381122, referred to in the figures as shRNA#1; TRCN0000002385, referred to in the figures as shRNA#2), *KALRN* (TRCN0000001428, referred to in the figures as shRNA#1; TRCN0000001429, referred to in the figures as shRNA#2), *TIAM1* (TRCN0000256946, referred to in the figures as shRNA#1; TRCN0000256948, referred to in the figures as shRNA#2) or *VAV3* (TRCN0000047701, referred to in the figures as shRNA#1; TRCN0000047702, referred to in the figures as shRNA#2). These lentiviral vectors were obtained from Sigma. Lentiviral particle production and infections were done as indicated above. Transduced cells were puromycin selected as described elsewhere [97]. Transcript knockdown was assessed by qRT–PCR.

JNK and SRF activity assays in COS1 cells

For JNK activation assays, exponentially growing COS1 cells were transfected with liposomes (Lipofectamine 2000, ThermoFisher, Catalog No. 11668019) with 1, 0.5, and 2 μg of the pFR–Luc, pFA2–cJun, and the appropriate experimental expression vector, respectively. For SRF activation assays, COS1 cells were transfected as above with 1 μg of pSRE–luc, 1 ng of pRL–SV40, and 1 μg of the appropriate experimental vectors. Luciferase activities were determined 36 hours after the transfection step as described earlier. In all cases, the abundance of the ectopically expressed proteins under each experimental condition was verified by analyzing aliquots of the cell extracts used in the luciferase experiments by immunoblot.

Cytoskeletal change assays

COS1 cells exponentially growing in 6–well culture plates were transfected with 1 μg of the plasmid of interest with Lipofectamine 2000. After 24 hours, cells were trypsinized, plated onto 12–mm diameter coverslips (Menzel–Glaser, Catalog No. 11778691) pre–treated for 10 min with poly–L–Lysine (1 μg/ml, Sigma, Catalog No. P4707), and then cultured for 12 to 24 hours. Cells were then fixed in 4% formaldehyde in phosphate buffered saline solution for 15 min, washed twice with phosphate buffered saline solution, permeabilized in 25 mM Tris–HCl (pH 8.0) containing 0.5% Triton X–100 (Sigma) for 10 min, washed three times with TBS–T, and blocked for 15 min with 2% bovine serum albumin in TBS–T. After a 20–min long incubation with rhodamine–labeled phalloidin (Invitrogen; diluted 1:200 in TBS–T and 2% bovine serum albumin) to visualize the F–actin cytoskeleton, cell preparations were washed thrice with TBS–T, stained with DAPI (Invitrogen, Catalog No D1306) for 5 min to visualize the nuclei, and mounted onto microscope slides with Mowiol (Calbiochem, Catalog No 9002–89–5). Samples were analyzed with a Leica TCS SP5 confocal microscope. Images were captured with LAS AF software (version 2.6.0.72266, Leica).

Whole mount immunohistochemical analyses

Tail skin was incubated in 5 mM EDTA (ethylenediaminotetraacetic acid) in PBS at 37ºC for 4 hours in order to separate de epidermis from the dermis. At room temperature, the epidermis was then fixed in 4% paraformaldehyde for 2 hours, permeabilized in 0.2% Triton X-100 (Sigma, Catalog No. T8787) for 15 min and blocked in 2% horse serum (ThermoFisher, Catalog No. 16050122) for 30 minutes, with 10-minute washing intervals in PBS between each step. Incubation with the primary antibody was performed in 2% horse serum overnight at room temperature using the following antibodies: BrdU (1:100, BD, Catalog No. 347580), Ki67 (1:100, Novocastra, Catalog No. NCL-L-Ki67-MM1), K14 (1:400, Covance, Catalog No. PRB-155P). Secondary antibody incubation was performed on the next day under the same conditions with Alexa Fluor 488 (1:400, Invitrogen, Catalog No. A21202) and Cy3 (1:400, Jackson Immunoresearch, Catalog No. 111-165-144). After washing, the preparations were stained with DAPI for 1 hour and mounted using Mowiol (Calbiochem, Catalog No 9002–89–5). Samples were analyzed with a Leica TCS SP5 confocal microscope. Images were captured with LAS AF software (version 2.6.0.72266, Leica).

Epidermal stem cell isolation

The isolation of epidermal stem cells was carried out as previously described [151]. Briefly, back skin was digested in 0.25% trypsin (ThermoFisher, Catalog No. 25200056) overnight at 4ºC to collect the keratinocytes from the epidermis. This cell suspension was then filtered, resuspended in EMEM (Lonza, Catalog No. BE06-174G) with 15% fetal bovine serum (ThermoFisher, Catalog No. 10500064) and incubated for 30 minutes on ice with biotin-conjugated anti-CD34 (1:50, eBioscience, Catalog No. 13-0341-85) followed by another 30-minute incubation with APC-conjugated streptavidin (1:300, BD Biosciences, Catalog No. 554067) and PE-conjugated anti-CD49f (1:200, AbD Serotec, Catalog No. MCA699PE). DAPI (4’,6-diamidino-2-phenylindole) staining was used to exclude dead cells. Positive cells for CD34 and CD49f were isolated using a FACSAria III flow cytometer (BD Biosciences) and analyzed with the FlowJo software.

Epidermal stem cell proliferation

DNA replication in proliferating cells was assessed using the Click-iT EdU Alexa Fluor 647 Flow Cytometry Assay Kit (ThermoFisher, Catalog No. C10424) according to manufacturer’s instructions.

Colony formation assays

Keratinocytes were isolated as indicated before, counted and plated in six-well plates at a density of 500 cells per well in CnT07 medium. Upon colony formation after 10-14 days, cells were fixed with 4% paraformaldehyde for 10 minutes and stained with Giemsa (1:10, Merck, Catalog No. 32884) for another 10 minutes. Plates were washed with distilled water, left to dry and colonies were quantified.

Standardized in silico analyses of epidermal stem cell expression microarray data

Initial data processing was carried out as indicated for the human and mouse epidermis data (see above). The *heatmap3* package was used to generate the expression heatmaps for the indicated genes. Functional annotation was performed using Metascape [144] for biological processes and ToppFun [152] for molecular functions. A FDR q-value of 0.05 was set as threshold for statistical significance. GSEA was carried out as described above with the EpSC-associated gene sets obtained from [153]. Single-sample Gene Set Enrichment Analysis (ssGSEA) [154, 155] was used to calculate the fitness of different hallmark [156] and epidermal stem cell signatures [153] across time and genotypes. The time-course enrichment scores for either these signatures or individual transcripts were used to build the signature correlation matrices, obtained through the *corrplot* R package. Correlations were considered statistically significant when the Pearson coefficient corresponded to a P value below 0.05. Functional clusters were established when every pair-wise correlation within a group of signatures was found significant. Known functional interactions among relevant genes were obtained through the String tool [157]. Cytoscape software was used to perform network data integration and visualization [143]. For the discovery of transcription factor binding motifs in the promoters of the co-regulated genes, the iRegulon software was used as indicated above [145].

Establishment of time-course gene expression patterns in epidermal stem cells

As described before [158], both Chi-squared and fold change thresholds were used to establish static and dynamic probesets. Briefly, for each probeset, a Chi-squared test with N-1 degrees of freedom was applied as follows:

$$\chi^2 = \sum_{i}^{n} \frac{(\overline{X_i} - \overline{X})^2}{\overline{X}} =$$

$$= \frac{(\overline{X_{0.6}} - \overline{X})^2}{\overline{X}} + \frac{(\overline{X_1} - \overline{X})^2}{\overline{X}} + \frac{(\overline{X_{2.5}} - \overline{X})^2}{\overline{X}} + \frac{(\overline{X_4} - \overline{X})^2}{\overline{X}} + \frac{(\overline{X_6} - \overline{X})^2}{\overline{X}} + \frac{(\overline{X_{12}} - \overline{X})^2}{\overline{X}}$$

where $\overline{X_i}$ is the mean expression of the gene for the microarray triplicates for each time point i, $\overline{X}$ is the overall mean expression across all time points, and n is the number of time points. For those probesets satisfying $P(\chi^2) < 0.01$, a fold change >= 2 requirement was empirically established.

Unsupervised soft clustering with the Mfuzz R package [159] was used for the identification of time-course expression profiles. After standarization of the expression values for Euclidian space clustering, we applied the *mfuzz* function with a fuzzifier value of 1.25 and a ranging number of cluster centers to determine the optimal number of non-overlapping expression patterns. For the inclusion of a probeset in a particular cluster, the membership value threshold was set to 0.5. The resulting expression profiles were named according to the position of the main positive (+) and negative (–) enrichments (peaks), i.e., 0.6 = 0.6 months old, 1 = 1 month old, 2.5 = 2.5 months old, 4 = 4 months old, 6 = 6 months old, 12 = 12 months old.

To evaluate how $Vav2^{Onc}$ activity affects EpSC transcriptional dynamics, the fluctuation of each dynamic probeset between WT and $Vav2^{Onc}$ genotypes was analyzed. Using the Cytoscape software [143], we represented the results as a network where the nodes represent expression patterns and the edges (arrows) indicate how dynamic transcripts behave in the $Vav2^{Onc}$ context when compared to the WT. Node color, hue and size were set according to genotype, connectivity and number of probesets, respectively. The inner ring was used to specify the fraction of genotype-specific dynamic probesets within the pattern. Edge thickness was established according to the number of transcripts that are shared between two nodes. The sensitivity for edge representation was set to 10% of the pattern size.

For the visualization of expression and enrichment data, a 0–1 normalization was used according to the minimum and maximum WT values:

$$x_{norm} = \frac{x - x_{min}}{x_{max} - x_{min}}$$

Weighted correlation network analyses

In order to find the best representatives of every gene expression pattern, the *WGCNA* R package was applied [160]. We constructed each weighted gene network from the corresponding expression matrix through the *blockwiseModules* function. The *pickSoftThreshold* function was used to select the soft thresholding power according to network topology. Consensus module detection within each expression pattern was omitted and kept to one module as the number of clusters had been already optimized. The heatmap plot depicting the adjacency matrix was created with the *TOMplot* function. To calculate the intramodular connectivity for each gene, we computed the whole network connectivity for each expression pattern through the *intramodularConnectivity* function. Hubs were defined as the 10% most connected genes within each expression pattern. The known functional interactions among hubs were obtained through the String tool [157] and represented using Cytoscape [143].

Determination of cell proliferation in vitro

Proliferation was measured at the indicated time points using the 3-(4,5-dimethylthiazol-2-yl) 2,5-diphenyltetrazolium bromide (MTT) method. To this end, the culture medium of each 200-mm^2 well was replaced by 250 μL of the MTT solution (0.5 mg/mL). After 1 hour at 37ºC in a 5% CO_2 atmosphere, the MTT solution was replaced by 500 μL of DMSO in order to dissolve the formazan crystals formed. 10 minutes later the absorbance at 570 nm was measured in an Ultraevolution reader.

QUANTIFICATION AND STATISTICAL ANALYSES

Statistics

The number of biological replicates (*n*), the type of statistical tests performed, and the statistical significance are indicated for each experiment either in the figure legends or in the main text. Data normality and equality of variances were analyzed with Shapiro–Wilk and Bartlett's tests, respectively. Parametric distributions were analyzed using Student's *t*–test (when comparing two experimental groups) or one-way ANOVA followed by either Dunnett’s (when comparing more than two experimental groups with a single control group) or Tukey’s HSD test (when comparing more than two experimental groups with every other group). For those analyses where two independent variables were considered, two-way ANOVA followed by Sidak’s multiple comparisons test was applied. Nonparametric distributions were analyzed using either Mann–Whitney (for comparisons of two experimental groups) or the Kruskal–Wallis followed by Dunn’s (for comparisons of three or more than three experimental groups) tests. The chi–squared test was used to determine the significance of the differences between expected and observed frequencies. In all cases, values were considered significant when $P \leq 0.05$. Data obtained are given as the mean ± SEM.

RESULTS

DISCUSSION

Vav2 upregulation is a functionally relevant event in SCC carcinogenesis

We have demonstrated in this thesis that the RHO GEF VAV2 constitutes a signaling modifier intrinsically associated with the maintenance of stem cell-like traits in different populations of epidermal and oral squamous cells. This VAV2-driven stemness-associated molecular program is frequently exploited by cSCC and hnSCC tumor cells, where the abundance of both VAV2 and *VAV2* transcripts becomes strongly upregulated. Importantly, we have proved using histotypic cultures and xenotransplantation experiments that patient-derived SCC cells require these high levels of endogenous VAV2 for their tumorigenic fitness. Consistent with this, we have also found that the abundance of *VAV2* and its molecular signature correlates with the poor prognosis of oSCC patients in a comparable manner to bona–fide SCC drivers such as the *EGFR*, *KRAS*, *ACTL6A*, *c–MYC*, and *NOTCH* family members [54, 60]. However, unlike those cases, the deregulation of the VAV2 pathway in SCC is not associated with locus-specific genetic alterations. In this regard, the molecular basis for the aberrant upregulation of VAV2 in these tumors remains to be addressed. Possible explanations include the amplification of super–enhancers and the spurious activation of transcriptional factors. Given that the fold changes in VAV2 protein are much larger than those found in its transcripts in both patient samples and patient–derived cells, it is also possible that processes associated with increased mRNA translation could contribute to the enhancement of VAV2 signaling.

Regardless of the mechanism mediating such VAV2 upregulation, it targets the *VAV2* locus specifically as the genes located in its vicinity do not share the same dysregulation pattern. This phenomenon is also tumor-specific since it is virtually restricted to cSCC and hnSCC, while other squamous tumors such as lSCC or ceSCC, as well as most of the tumors from pan-cancer collections, do not show alterations in *VAV2* levels. Importantly, this deregulation takes place very early during cSCC and hnSCC tumor evolution, as inferred from the detection of upregulated *VAV2* in premalignant lesions such as actinic keratosis and oral epithelial dysplasias. This indicates that the upregulation of *VAV2* is not the mere consequence of the genomic- and transcriptomic-wide turmoil present in full-blown cancer settings, but rather a protumorigenic event that assists pre-cancer cells in their malignant transformation.

Consistent with the aforementioned findings, we have shown using a knockin gain-of-function mouse model that upregulated Vav2 signaling promotes a hyperproliferative and undifferentiated phenotype in epidermal and oral squamous epithelia. In the case of the skin, this is also accompanied by epidermal inclusion cysts, orphan sebaceous glands and an abnormally high density of hair follicles. Even though these alterations do not lead per se to tumorigenesis in the cancer-resistant C57BL/6 mouse strain, aged *Vav2*^{Onc} mice in mixed genetic backgrounds do develop skin tumors, thus demonstrating that in some contexts upregulation of Vav2 activity can be sufficient to drive tumor formation (data not shown). Perhaps more importantly, hyperactivation of Vav2 favors tumor formation, progression and poor prognosis regardless of the mouse model tested when it is combined with additional genetic lesions. This mutated scenario mimics the genomic erosion intrinsic to human SCC tumors, offering a more faithful and clinically-relevant model on the impingement of VAV2 signaling on SCC carcinogenesis.

We are fully aware of the inherent limitations of using a constitutive knockin mouse model for a gene as widely expressed as *Vav2*. However, through skin xenograft experiments we have demonstrated that the epidermal phenotype of *Vav2*^{Onc} mice stems exclusively from keratinocytes. Furthermore, when grown in 3D histotypic cultures, both mouse and human keratinocytes expressing hyperactive Vav2 recapitulate the hyperplastic condition seen in the skin of the *Vav2*^{Onc} mouse model. Importantly, not only does the latter finding reflect the autonomy of such phenotype, but it also proves formally that it stems from keratinocytes that are not associated to the hair follicle.

Besides its role in keratinocytes, it should be indicated that both published and unpublished data from our group have shown that Vav2 can signal from many other cell lineages and cause an array of pathological disorders ([118, 119, 134]). Among these, hyperactivation of Vav2 in fibroblasts leads to dermal dysplasia and, interestingly, to the spurious formation of hair follicles and epidermal inclusion cysts. Although the underpinnings of this phenotype have yet to be addressed, the intimate crosstalk that takes place between keratinocytes and fibroblasts via growth factors and cytokines seems prima facie a promising lead [186]. Consistent with this possibility, Vav2 is known to regulate the expression of a large number of these paracrine factors in several cell types and tissues, including the skin ([97] and data not shown). Whether this represents an additional mechanism by which this GEF can contribute to SCC carcinogenesis will be investigated in the future.

Vav2 is a key mediator of stemness in epidermal and oral squamous cells

Our 3D histotypic models have allowed us to explore the molecular apparatus mediating Vav2 signaling in the squamous cell context. We have found that Vav2 elicits its epidermal phenotype in a catalysis-dependent manner through the activation of Rac1 and RhoA. Importantly, the activation of these two GTPases has to occur concurrently in order to fully recapitulate the $Vav2^{Onc}$ phenotype. In line with this, we have encountered that their respective effector kinases, such as Pak or Rock, are necessary but not sufficient to trigger the $Vav2^{Onc}$-induced epidermal disorders (data not shown). Since Rac1 and RhoA signaling pathways engage mutually inhibitory loops in several cellular contexts [187], the cooperation between both GTPases driven by Vav2 probably involves some kind of spatial segregation.

The activation of this Vav2-governed signaling cascade triggers a downstream transcriptional program intimately involved in the promotion of keratinocyte proliferation and undifferentiation. As a result, keratinocytes endowed with high Vav2 activity develop a stem cell-like molecular profile. In line with this, we have found that endogenous Vav2 is highly expressed in epidermal progenitors located at the basal layer of the squamous epithelium (data not shown). Such Vav2-driven transcriptional program is frequently engaged by human SCC tumor cells and, importantly, is strongly associated to patient survival. Using a series of bioinformatic approaches, we have been able to distill this association into a robust 41-gene minimal prognostic signature that has been validated using data from over 600 hnSCC patients.

Further in silico analyses have revealed that the Vav2–driven transcriptional program is triggered via the stimulation of transcription factors (AP1, c–Myc, E2F, Nfy, Yap/Tead) directly involved in the orchestration of gene expression changes associated with stem cell–like regenerative proliferation and delays in cell differentiation [54, 60, 145, 188-191]. Both our gain– and loss–of–function experiments have validated the functional correlation of VAV2 activity with the expression of the aforementioned transcription factors in hyperplastic epithelia, SCCs, and patient–derived cells.

Using patient-derived data, we have found that these correlations are especially robust in the case of c–Myc and Yap factors. Consistent with this, we have proved that these two transcriptional regulators play pivotal roles in the Vav2-mediated induction of keratinocyte proliferation and undifferentiation, respectively. In this regard, while it has been previously reported that Rac1 and RhoA can drive the activation of Yap/Taz [192], the mechanism employed by Vav2 in order to trigger c–Myc activation is still to be fully understood. Although it was initially reported in mice that Rac1 regulates c–Myc negatively through Pak2-mediated phosphorilation [87], this finding has been challenged by later studies [88]. According to our data, the fast cycling versions of Rac1 and RhoA are only able to induce a mild upregulation of c–Myc in histotypic cultures, much lower than in the case of *Vav2*^{Onc} cells. However, when both hyperactive GTPases are expressed simultaneously, the abundance of this transcription factor becomes exacerbated, thus suggesting that the synergism between Rac1 and RhoA pathways might mediate the induction of c–Myc. In any case, formal demonstration of this hypothesis will require further validation.

VAV2 is a potential therapeutic target in squamous cell carcinoma

Cross–platform comparative analyses of the *Vav2*^{Onc}–driven transcriptional program has revealed that around 40% of its transcripts show the opposite transcriptional behavior in the TPA-treated skin of *Vav2*$^{-/-}$;*Vav3*$^{-/-}$ mice [97]. This high degree of reciprocity in spite of the different experimental conditions and genetic backgrounds of *Vav2*^{Onc} (this work) and *Vav2*$^{-/-}$;*Vav3*$^{-/-}$ [97] mice shows that Vav2 is able to trigger this stem cell-like program in a signaling autonomous manner. This finding, together with the fact that Vav2 mediates its protumorigenic function catalytically and the recent observations indicating that the depletion of RAC1 restores chemo and radiosensitivity to hnSCC cell lines [193], suggest that the inhibition of the enzyme activity of this GEF could be a potential therapeutic avenue in a significant percentage of SCCs. This idea, which is at the heart of the study of most RHO GEFs in cancer settings, had not been ever demonstrated in vivo with properly designed mouse models [83]. To address this issue, we have generated cohorts of knock–in mice exhibiting varying amounts of Vav2 catalytic activity. With this strategy, we aimed at mimicking the usual conditions found with drug-based therapies in which the 100% inactivation of the target is hardly achieved. Using this approach we have found that effective therapeutic impacts can be obtained even under conditions in which some remaining GEF catalytic activity ($Vav2^{L332A}$, ≈20% GEF activity) is preserved. Perhaps more importantly, these studies have unveiled the existence of therapeutic windows in which the homeostasis of the healthy tissues can be maintained. These preclinical results validate VAV2 as a potential therapeutic target to drive the differentiation and growth arrest of specific SCC subtypes.

Vav2 regulates stemness in the hair follicle

Understanding the physiological role of VAV2 in the homeostasis of the squamous epithelium will be of paramount importance for the design of the aforementioned potential therapeutic approaches. We have shown that Vav2 activity impinges on the epidermal fitness to adapt to challenges such as skin or hair regeneration, a phenotype that is associated with the abundance of EpSC and their responsiveness to activation cues. Interestingly, upregulated Vav2 activity leads to the perennial expansion of the EpSC reservoir while favoring a transcriptional status associated to quiescence. It should be noted that such quiescence is defined according to the transcriptomic profile of EpSC during telogen, and thus the term ‘quiescent’ can be misleading since the fact that these cells are not proliferating does not imply lack of cellular activity [153]. In fact, such quiescent cells upregulate a large transcriptional program involved in survival, the regulation of differentiation and proliferation, and the control of the metabolic status of the cell [153]. In terms of cellular functionality, our experiments have shown that this transcriptional endowments lead to a ready-to-go state in the expanded population of $Vav2^{Onc}$ EpSC.

In order to understand how upregulated Vav2 signaling is able to regulate epidermal stem cell homeostasis, here we have presented an EpSC transcriptomic time-course analyses. These studies have not only revealed how this GEF reshapes the EpSC transcriptome, but also provided valuable insights into the controversial topic of epidermal stem cell ageing. While a series of studies have unambiguously shown that skin from young and aged mice have the same number of EpSC, assessment of how the passing of time affects their functionality has led to conflicting reports [175, 194, 195]. The lack of comprehensive time-course approaches specifically targeting the purified population of EpSC has precluded the elucidation of such controversy, and thus the molecular events that occur within the EpSC niche as it ages have remained hitherto largely unknown.

Our in silico time-course study has revealed that around one third of the EpSC transcriptome is reconfigured throughout the first year of age. Although such figure is certainly influenced by disparities in the hair cycle phase among the differently aged EpSC, our data indicate that the overall contribution of the hair cycle-related genes to the dynamic patterns here described is rather limited. In fact, the overlap between our dynamic gene collection and the hair cycle-related genes [196] amounts to a mere 15% (data not shown). Interestingly, this collection of time-sensitive transcripts doubles in size in the presence of hyperactive Vav2. Such amplification of transcriptional dynamism is an event that occurs late in the *Vav2*^{Onc} EpSC lifetime, probably as a result of the dynamic remodeling that occurs at earlier stages.

The Vav2-driven transcriptomic rewiring leads to the alteration of age-specific transcriptional signatures, modifying the native functional enrichment of key time-driven biological processes. At a prime stage (18 days old), WT epidermal stem cells boost cell division and growth programs. Consistent with this, pathways associated with proliferation (E2F), stem cell activation (Hedgehog) and metabolic anabolism (Myc, MTOR) become strongly enriched. This occurs with the concomitant abrogation of quiescence-related signatures (TGFβ). Hyperactive Vav2 favors stem cell quiescence even at these early stages, while increasing the transcriptional coordination between proliferation and anabolism pathways. By postnatal day 30 (mid-anagen) a drastic transcriptional rewiring takes place in WT EpSC, abolishing and promoting these cell proliferation and quiescence programs, respectively. This phenomenon, however, is largely dampened in the context of *Vav2*^{Onc} signaling, where proliferation and activation signatures remain overly enriched. This is in agreement with the rest of evidence indicating that upregulated Vav2 signaling, while preserving the EpSC in a quiescent state, also favors EpSC activation in the presence of activation stimuli.

After this initial dynamic burst, WT EpSC experience a phase of transcriptomic stillness during adulthood. Few genes display transcriptional fluctuations at this point, whose functional analyses reveal a modest enrichment in differentiation-related processes. In the *Vav2*^{Onc} context, however, EpSC display the spurious deregulation of transcripts associated to ribosome biogenesis, signaling through RTKs and metabolic processes. In addition, *Vav2*^{Onc} EpSC still preserve a highly quiescent transcriptional profile at this stage.

The transcriptional calm in WT EpSC is lost by one year of age, when signatures associated to epidermal differentiation and stemness become markedly up- and downregulated, respectively. These data show the progressive deterioration of stemness-associated features, which is in agreement with the loss of clonogenic potential that other studies have reported in old EpSC [175]. We have also found the previously described age-driven transcriptional upregulation of the Jak-Stat and Notch signaling pathways [175]. However, our work has revealed that these phenomena are accompanied by an additional set of transcriptional events that had not been identified before. In our view, our increased resolution is due to the circumvention of some of the limitations of the preceding studies by **i)** performing a time-course approach instead of a two-point (young versus old) analysis, **ii)** including younger EpSC, and **iii)** isolating CD34$^+$ Itga6$^+$ bulge stem cells instead of using other less specific EpSC markers [175]. Importantly, this approach has allowed us to unveil that aged *Vav2*^{Onc} EpSC upregulate transcriptional programs associated to epidermal morphogenesis and metabolic activity, thus suggesting that Vav2 signaling might help preserve the fitness of the EpSC population.

Further in silico analyses have revealed that this whole Vav2-induced conditioning of key EpSC signaling pathways and biological processes stems from the enhancement of transcriptional coordination. In pursuit of the factors driving such phenomenon, we have applied weighted correlation network algorithms to each coexpression cluster to identify its transcriptional hubs, i.e., the transcripts that are more closely related to every other transcript in terms of coexpression. These hubs constitute the heart of each coexpression cluster and, according to their transcriptional profiles, are in direct or close proximity to its transcriptional drivers. Consistent with this, many of the hubs we have identified are able to interact or regulate transcription factors, or are even transcription factors themselves (data not shown).

Even though most WT dynamic transcripts (84.6%) are also dynamic in *Vav2*^{Onc} EpSC, we have encountered that only 26.5% of the WT transcriptional hubs occupy this position in *Vav2*^{Onc} cells. This transcriptional hubs shift, which occurs throughout the entire time course we have analyzed, indicates that upregulated Vav2 signaling emphasizes the activity of a particular set of transcriptional drivers that remodel the EpSC transcriptome. Interestingly, by focusing on those transcriptional hubs able to drive transcription directly, we have found that the Vav2-driven transcriptional program revolves around a collection of transcription factors strongly associated to the maintenance of quiescence within the EpSC niche. Although our data suggest the participation of both transcriptional and non-transcriptional mechanisms, how Vav2 controls the activity of these transcription factors will have to be further explored. In this regard, we are fully aware of the limitations of our in silico approach, which surely cannot capture the whole complexity of the regulatory networks governing the EpSC molecular landscape. Nevertheless, our data does provide sound evidence and directions to implement new multifaceted experimental approaches and lead to an unprecedented comprehension of the role of Rho exchange factors in the homeostasis of epidermal stem cells.

Vav2 signaling in the skin: stemness in two flavors

Collectively, these findings reveal that Vav2 signaling leads to the activation of divergent molecular programs in different epidermal cell compartments. While it promotes an undifferentiated and highly proliferative stem cell-like state in interfollicular keratinocytes, it favors quiescence within the epidermal stem cell niche. These programs are barely related, since the interfollicular Vav2-driven protumorigenic signature is not conserved in *Vav2*^{Onc} EpSC, nor is the Vav2-governed collection of EpSC-associated transcription factors functionally enriched in interfollicular *Vav2*^{Onc} keratinocytes (data not shown). However, despite their apparent dissimilarity, both programs orbit around the same biological concept: stemness. Interestingly, cross-transcriptomic analyses aimed at this circumstance have revealed that underneath the cell compartment-specific molecular layers, Vav2 is driving a core of stemness-associated genes that is shared by interfollicular keratinocytes and epidermal stem cells (**Figure XI**). Such core is mainly involved in the regulation of DNA metabolism, replication and repair, and in the control of cell cycle progression (data not shown).

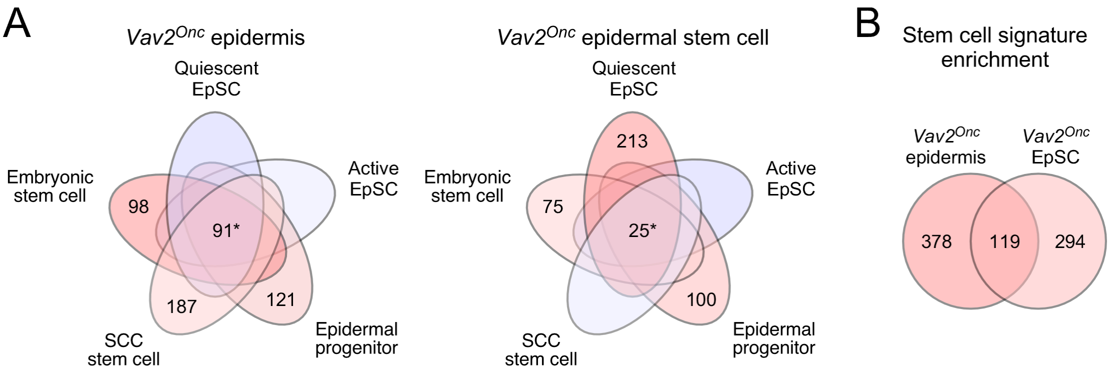
A
Vav2Onc epidermis
Quiescent EpSC
Embryonic stem cell
Active EpSC
98
91*
187
121
SCC stem cell
Epidermal progenitor
Vav2Onc epidermal stem cell
Quiescent EpSC
213
Embryonic stem cell
Active EpSC
75
25*
100
SCC stem cell
Epidermal progenitor
B
Stem cell signature enrichment
Vav2Onc epidermis
Vav2Onc EpSC
378
119
294

FIGURE XI. Vav2 signaling in the skin: stemness in two flavors. (A) Venn diagrams showing the overlap among the genes belonging to different stem cell-associated signatures that are enriched in the epidermis (left) and EpSC (right) of *Vav2*^{Onc} mice. Red and blue colors represent positive and negative signature enrichments, respectively. *, number of overlapping genes between, at least, two transcriptional signatures. **(B)** Venn diagram showing the overlap between the stem cell-associated genes enriched in *Vav2*^{Onc} epidermis and EpSC according to the data shown in panel A. EpSC, epidermal stem cell.

This finding demonstrates that the two Vav2-directed molecular programs are based on common foundations, and thus exemplifies how different cells can funnel the same molecular essence into vastly different cellular programs. Understanding the underpinnings of these context-dependent engagements of Vav2 signaling will undoubtedly bring us one step closer to the rational design of strategies aimed at harnessing GEF activity.

VAV2 belongs to a group of RHO GEFs with key roles in SCC carcinogenesis

Besides our study of VAV2, recent data gathered from animal models, genome–wide expression analyses, and Pan–Cancer projects are beginning to illuminate new, and in some cases quite unsuspected roles for additional RHO GEFs [83, 129]. In such context, we have performed in silico analyses of SCC transcriptomic data in order to identify recurrent alterations in RHO GEF transcripts as an indicator of potential functional relevance in carcinogenesis. Such analyses have revealed that, in addition to *VAV2*, only a small number of GEF-encoding mRNAs are consistently deregulated in these tumors. Importantly, we have found the same numbers of putative pro- (ECT2, FARP1, FGD6, TRIO, VAV2) and anti-tumorigenic (ARHGEF10L, ITSN2, KALRN, TIAM1, VAV3) GEFs in terms of differential expression and association with patient survival. This finding challenges the long-held notion that RHO GEFs are tumor driving proteins [83].

Our data indicate that both the putative pro- and anti-tumorigenic GEFs are transcriptionally regulated in a coordinated manner. It is important to emphasize that such transcriptional coordination is unrelated to their differential expression. Illustrating this, we have identified a group of GEFs that despite being strongly coexpressed, are not differentially expressed in SCC tumors. These coexpressions are not the result of cancer-associated genomic copy number variations either, but rather transcriptional events specifically targeting these loci. In keeping with this, coexpression among the members of these GEF clusters not only occurs in cancer settings, but also during normal keratinocyte differentiation. This is probably the reflection of coordinated but non-redundant GEF-mediated physiological programs that are harnessed by tumor cells. Consistent with this, such coordinated GEF clusters lie at the heart of large coexpression networks involved in the regulation of key processes for both stem and tumor cells. The elements driving these networks remain to be identified, although enrichment analyses of transcription factor binding sites have provided a series of candidate regulators.

The putative protumorigenic function predicted by our in silico analyses for ECT2, FARP1, FGD6, TRIO and VAV2 has been biologically validated using SCC patient-derived cells in both histotypic cultures and xenograft experiments. These studies have also demonstrated that, although coordinated, these GEFs play non-redundant functions as each of them conditions the tumorigenic features of SCC cells in a distinct manner. Importantly, these differential features become apparent in the context of xenografts experiments, but they are hardly unveiled by in vitro histotypic cultures. This constitutes yet another illustrative example of how narrowing GEF studies to in vitro settings, as has occurred historically, severely cripples our understanding of the true biological role of these proteins in cancer and other physiopathological processes.

It should be noted that the immunocompromised *Vav1*$^{-/-}$;*Vav2*$^{-/-}$;*Vav3*$^{-/-}$ mouse model that we have used for our tongue xenograft experiments still has marginal levels of T-lymphocytes (data not shown). This means that tumor growth in this setting is not only the result of the intrinsic proliferative capability of the grafted tumor cell, but also of its immunogenic potential. Importantly, this feature allows our experimental model to mimic more faithfully the scenario in which human tumors grow and circumvents one of the major drawbacks of immunodeficient mouse models, i.e., that the lack of functional immune system hampers both disease modeling and clinical translation [197].

According to our experiments, TRIO could very well be considered the Achilles heel of the patient-derived SCC cells. Despite the fact that this protein does not seem to be as intimately associated to the control of cell differentiation as other protumorigenic GEFs, its downmodulation stunts tumor cell growth in vivo to an extent that is unmatched by any of the other exchange factors tested. This phenotype is much stronger than the one revealed by in vitro studies, thus suggesting that the tumor microenvironment might be playing a determinant role here. Consistent with this, previous studies have shown that TRIO mediates the proliferative response to mitogens in several cancer cells [198].

We have found that patient-derived SCC cells are also strongly dependent on ECT2 activity in order to maintain both their proliferation potential and their undifferentiated state. This observation could be expected to some extent, since this GEF is an essential component of the molecular apparatus responsible for cell cycle progression and cytokinesis [114]. Nevertheless, ECT2 has also been reported to impinge on cancer cell growth through alternative mechanisms different from direct control of cell division, including the regulation of the ribosome biogenesis [113]. Although the precise functions of ECT2 in SCC cells will have to be addressed in the future, the knockdown of this GEF in our patient-derived cells results in a conspicuous enucleation defect, thus suggesting its implication in the differentiation-driven processes that lead to nuclear degradation in keratinocytes [199].

On the other side of the spectrum, *FGD6* has proven to be a prototypical case of a gene with potential therapeutic interest according to in vitro studies that, when tested in vivo, has led to only marginal effects. This suggests that whatever deficiency the abrogation of FGD6 is originating in SCC cells cultured in vitro, it is somehow overcome in vivo. In our view, this does not necessarily rule out the possibility that this GEF plays a relevant role in SCC carcinogenesis, but could rather suggest that in order to do so it might require the presence of additional oncogenic events. It should also be noted that we have not found increased levels of *FGD6* in any of our SCC cell lines, which could indicate that they are not as dependent on the activity of this GEF. Alternatively, the catalytic specificity could also be a relevant factor, since the two GEFs that have displayed mild phenotypes in our in vivo experiments, FGD6 and FARP1, are the ones involved in the activation of CDC42 GTPase, whose role in carcinogenesis is still unclear [83]. In any case, whether some of these elements are accountable for our findings will have to be further explored in the future.

Taken together, these experiments have materialized the notion that VAV2 is but one member of a group of RHO exchange factors that govern key processes involved in SCC carcinogenesis. Importantly, our in vivo data shows that, besides VAV2, TRIO and ECT2 also constitute appealing candidates for the exploration of new therapeutic avenues against hnSCC. Since our immunohistochemical and promoter activation assays have shown that these GEFs control different distal effectors (data not shown), combined therapies targeting several of these GEFs are, theoretically, also practicable. While we have already proved the existence of therapeutically safe windows for VAV2 inhibition, this will require analog studies in the case of TRIO, ECT2 and their potential combined inhibition. One should bear in mind, however, that this is just the first step in the long journey towards RHO GEF-based therapies. The major roadblock to reach that goal lies probably right ahead, since the biochemical properties of exchange factors makes the design of efficient pharmacologic inhibitors a challenging task [83, 200]. Nevertheless, this obstacle is not insurmountable and our data provides a new rationale to focus novel drug design strategies on particular GEFs.

Unlike the preceding findings, the observation that some RHO GEFs (*ARHGEF10L*, *ITSN2*, *KALRN*, *TIAM1*, *VAV3*) are consistently downregulated in SCC tumors was a rather unanticipated discovery. Our xenograft SCC model has shown that such transcriptional downmodulation is linked to tumor suppressor-like functions for ITSN2, KALRN and VAV3. Except for VAV3, these functions are not detected in vitro, which suggests the implication of the tumor microenvironment. On the other hand, neither in vitro nor in vivo models have revealed alterations in SCC tumorigenicity upon *ARHGEF10L* or *TIAM1* knockdown. This can be attributed to several causes. Firstly, tumor suppression functions might manifest in a way not readily revealed by our models, as can be exemplified by the case of TIAM1. In keeping with a tumor-suppressive function, the deficiency of this GEF has already been shown to lead to the exacerbation of SCC malignancy in vivo [98]. However, this is accompanied by a counterintuitive decrease in tumor multiplicity and size [98]. Probably, our models are an unsuitable experimental approach to unveil such paradoxical anti-tumorigenic functions. Another possible explanation for the lack of phenotype of these GEFs is that their downmodulation has to concur with the alteration of additional signaling molecules, either within or without the RHO signaling cascade. Lastly, it should also be considered that in the case of patient-derived SCC cells, the expression levels of some of these GEFs might be natively too low to induce further effects by additional shRNA-based downmodulation. Our experimental plan will continue with the ectopic expression of these GEFs in order to shed light on these lingering issues.

In any case, without undervaluing the inherent relevance of proving that RHO GEFs can also play tumor suppressor-like roles, it is worth noting that the potential therapeutic exploitability of this finding is rather limited, as neither the pharmacologic nor the genetic induction of GEF activity is currently a viable therapeutic option. Perhaps more importantly, what this finding demonstrates is that therapies directed towards protumorigenic GEFs have to be exquisitely specific. This is of paramount relevance since our data shows that off-target GEF inhibition can result in a negative therapeutic impact.

The mechanisms underlying RHO GEF idiosynchrasy: a puzzle to be solved

The aforementioned findings show that from a shared molecular commitment, i.e., the activation of RHO GTPases, GEFs are able to elicit different and even antagonistic responses in the context of SCC carcinogenesis. This inevitably raises the most fundamental question: what differences in their activity as exchange factors account for such functional divergence?

Probably the most straightforward explanation would be that each of these GEFs activated different RHO GTPases. However, based on data from both our lab and published studies [146], we have found that GTPase specificity per se is not sufficient to explain our observations. For instance, VAV3 (anti-tumorigenic) and VAV2, ECT2 and TRIO (pro-tumorigenic) activate both RHOA and RAC1 GTPases (**Figure XII-A**). Similarly, ITSN2 (anti-tumorigenic) and FGD6 (pro-tumorigenic) share catalytic activity towards CDC42 (**Figure XII-A**). And even more puzzling, despite the fact that RAC1 has been unmistakably linked to protumorigenic functions in SCC [83], the two RAC1-specific GEFs KALRN and TIAM1 display antitumorigenic profiles (**Figure XII-A**). This puts in evidence that the catalytic specificity is a poor predictor of GEF function.

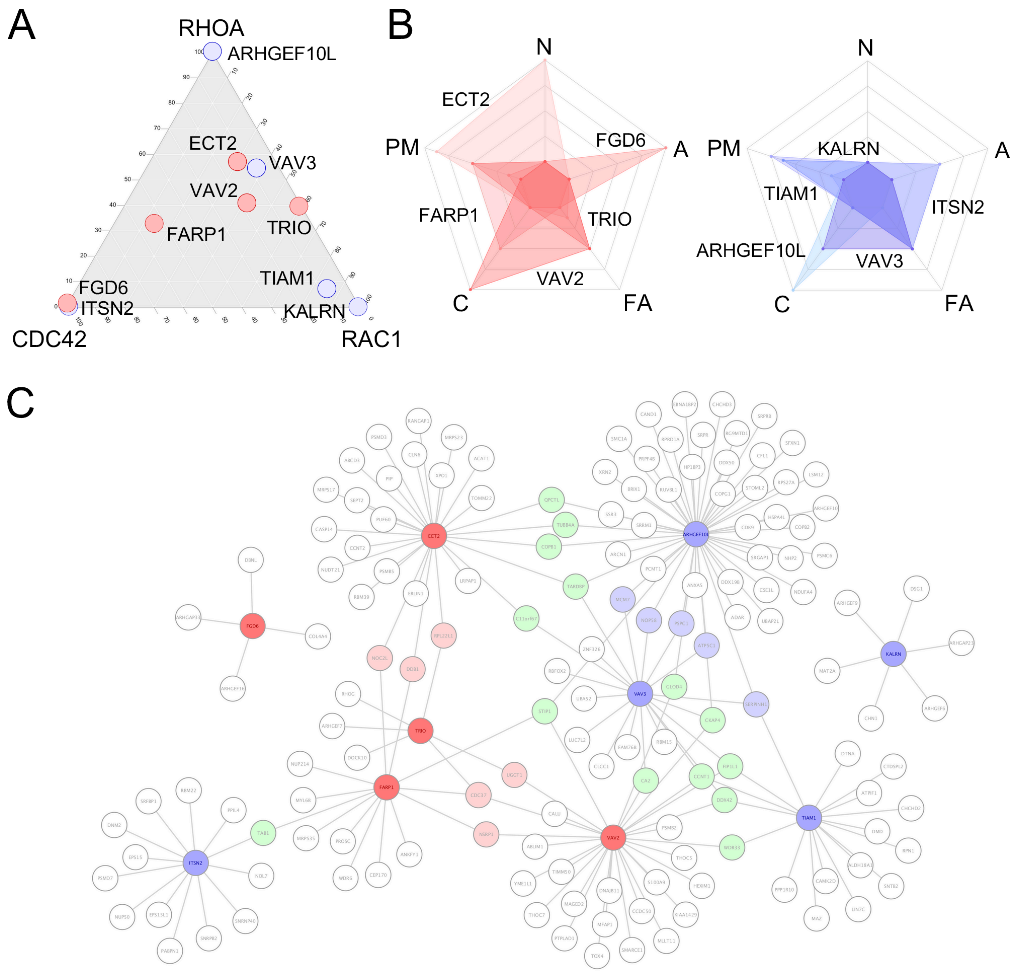

FIGURE XII. Current evidence on RHO GEF catalytic specificity, subcellular localization and interactome. (A) Ternary plot showing the catalytic specificity of the RHO GEFs that are up- (red) and downregulated (blue) in hnSCC. The affinity for a given GTPase is represented by the proximity to the corresponding coordinates. **(B)** Radar plots showing the subcellular location of the RHO GEFs that are up- (red) and downregulated (blue) in hnSCC. N, nucleus; A, actin cytoskeleton; FA, focal adhesions; C, cytosol; PM, plasma membrane. **(C)** Protein-protein interaction network of the RHO GEFs that are up- (red) and downregulated (blue) in hnSCC. Shared interacting proteins among two upregulated, two downregulated and two differentially regulated GEFs are highlighted in light red, light blue and light green, respectively. The data represented in all panels was obtained from previously published studies [146].

GTPase activation at different subcellular locations can also trigger various cellular responses [201, 202]. However, except for the localization of ECT2 in the nucleus, pro- and anti-tumorigenic GEFs share quite overlapping localizations across the cytosol, plasma membrane, actin cytoskeleton and focal adhesions (**Figure XII-B**). Therefore, these data indicate that the subcellular localization does not correlate with the idiosyncratic behavior of GEFs in SCC carcinogenesis.

As these evidences seem to suggest, linking the carcinogenesis-associated role of each GEF with its molecular function will probably require the investigation of its proximal effectors. Consistent with this, previous studies have shown that GEFs with the same catalytic specificity can elicit antagonistic cellular responses through the activation of different effectors [203]. In this regard, the analysis of publicly-available proteomics data on the interactome of RHO GEFs shows that the exchange factors we have studied only share about 15% of their interacting proteins (**Figure XII-C**). This is a clear indicator that, although they might coincide in catalytic specificities and subcellular locations, these GEFs are triggering vastly different signaling programs.

Regardless of the mechanisms underlying their idiosynchrasy, we should be aware of the fact that the approach we have used to identify RHO GEFs with potentially relevant functions in SCC tumorigenesis is exclusively based on transcriptomic data. This means that our findings still need to be complemented by studies assessing other potential non-transcriptional mechanisms involved in the regulation of RHO GEF activity. Intriguingly, DNA mutation does not seem to be one of them, as neither the pro- nor the anti-tumorigenic GEFs we have identified are significantly mutated in SCC tumors (data not shown). Why tumor cells favor transcriptional deregulation over DNA mutation in order to manipulate GEF activity is still to be understood. One possible explanation might lie in the flexibility intrinsic to gene expression control as opposed to the irreversible nature of genetic lesions. Perhaps the constitutive deregulation of GEFs throughout all stages of SCC carcinogenesis might not be as beneficial as the fine-tuned transcriptional modulation of their activity. Alternatively, genetic mutations might lead to conformations that are not as effective inducing tumorigenesis as a consequence of the impairment of non-catalytic GEF functions. Paralleled to these possibilities, the RAS-based G12 or Q61 activating mutations, which lock the GTPase in its GTP-bound state and have been used to model RAC1 activation in laboratories, are hardly found in human tumors [83, 86]. Instead, the fast-cycling P29S mutation, which is more flexible and still allows transition between the GTP- and GDP-bound states, is the one most commonly occurring [83, 86]. This supports the idea that, unlike the case of RAS GTPases, blind constitutive activation of RHO signaling might not be the most efficient protumorigenic avenue.

Vav2 and Vav3: friends and foes

The data presented here have made one conclusion redundantly clear: instead of playing cooperative roles as previous evidences seemed to indicate [97], VAV2 and VAV3 have antagonistic functions in the context of SCC carcinogenesis. This is a rather unexpected behavior for two GEFs that share 51.8% and 69.1% of sequence identity and similarity, respectively. In fact, this phenomenon seems to be cell lineage-specific as Vav2 and Vav3 do play cooperative roles in other carcinogenic contexts such as breast adenocarcinoma [128, 204]. In addition, we have found that these GEFs also play cooperative roles in the EpSC context, since the reversal of the defects elicited by *Vav2*^{Onc} in EpSC requires the elimination of both Vav2 and Vav3.

This apparent paradox in the roles of Vav2 and Vav3 in the epidermis can be attributed to several possible causes. On the one hand, one straightforward explanation is that the spectra of Vav2 and Vav3 effectors differ greatly between EpSC and interfollicular keratinocytes, allowing their cooperation in the former cell compartment. On the other hand, the possibility that such cooperation does not occur within the same cellular compartment cannot be formally ruled out. Although our skin xenograft experiments have shown that the hair-follicle-associated phenotype driven by Vav2 is keratinocyte autonomous, they are unable to resolve which epidermal cell populations are contributing to it. As such, we cannot neglect the possibility that other multipotent cell populations from the hair follicle might be participating in the phenotype seen in bulge EpSC. If this were the case, the redundancy between Vav2 and Vav3 signaling programs in any of these surrounding cell compartments could explain the lack of EpSC phenotype seen in Vav2-deficient mice. This hypothesis can be even extended to fibroblasts, since skin xenograft experiments performed with *Vav2*^{Onc} fibroblasts result in abnormally high numbers of hair follicles and epidermal inclusion cysts. As cooperation between Vav2 and Vav3 in mouse fibroblasts has already been reported [205], it is possible that the expression of Vav3 in the dermal compartment might be able to alleviate the deficiency of Vav2 in the EpSC niche in a paracrine fashion.

In any case, further work will have to be devoted to the characterization of Vav2 and Vav3 effectors in different cellular contexts in order to fully understand the relationship between their respective signaling programs.

CONCLUSIONS

Based on the preceding findings, the research presented in this Ph.D. thesis indicates that:

1. VAV2 drives a signaling-autonomous molecular program involved in the maintenance of a stem cell-like proliferative and undifferentiated state in both cutaneous and oral squamous epithelia. This program is triggered catalytically through the activation of RAC1 and RHOA GTPases.

2. The VAV2-driven molecular program is frequently engaged by malignant and premalignant cells of the squamous epithelium, promoting tumor progression and leading to poor prognosis. The tumorigenic fitness of full-blown SCC tumor cells is highly sensitive to VAV2 activity.

3. Inhibition of Vav2 catalytic activity prevents SCC tumor formation and progression. There are therapeutic windows where this effect can be achieved without triggering the side effects associated to the physiological role of this exchange factor.

4. Vav2 regulates the abundance, activity and responsiveness of hair follicle bulge epidermal stem cells. This function is at least partially coordinated with Vav3.

5. Vav2 controls the dynamic configuration of the EpSC transcriptome across time. This Vav2-governed transcriptional program impinges on the regulation of EpSC homeostasis and quiescence.

6. In addition to VAV2, the RHO exchange factors ECT2, FARP1, FGD6 and TRIO also contribute to the fitness of hnSCC tumors. These protumorigenic roles are non-redundant.

7. The RHO exchange factors ITSN2, KALRN and VAV3 play anti-tumorigenic roles in the context of hnSCC development.

REFERENCES

1. Watt, F.M., *Mammalian skin cell biology: at the interface between laboratory and clinic.* Science, 2014. **346**(6212): p. 937-40.
2. Blanpain, C. and E. Fuchs, *Epidermal stem cells of the skin.* Annu Rev Cell Dev Biol, 2006. **22**: p. 339-73.
3. Baroni, A., et al., *Structure and function of the epidermis related to barrier properties.* Clin Dermatol, 2012. **30**(3): p. 257-62.
4. Fuchs, E., *Skin stem cells: rising to the surface.* J Cell Biol, 2008. **180**(2): p. 273-84.
5. Squier, C.A. and M.J. Kremer, *Biology of oral mucosa and esophagus.* J Natl Cancer Inst Monogr, 2001(29): p. 7-15.
6. Jones, K.B. and O.D. Klein, *Oral epithelial stem cells in tissue maintenance and disease: the first steps in a long journey.* Int J Oral Sci, 2013. **5**(3): p. 121-9.
7. Cichorek, M., et al., *Skin melanocytes: biology and development.* Postepy Dermatol Alergol, 2013. **30**(1): p. 30-41.
8. Munde, P.B., et al., *Pathophysiology of merkel cell.* J Oral Maxillofac Pathol, 2013. **17**(3): p. 408-12.
9. Upadhyay, J., et al., *Langerhans cells and their role in oral mucosal diseases.* N Am J Med Sci, 2013. **5**(9): p. 505-14.
10. Sotiropoulou, P.A. and C. Blanpain, *Development and homeostasis of the skin epidermis.* Cold Spring Harb Perspect Biol, 2012. **4**(7): p. a008383.
11. Lee, J., P. Lee, and X. Wu, *Molecular and cytoskeletal regulations in epidermal development.* Semin Cell Dev Biol, 2017. **69**: p. 18-25.
12. Koster, M.I. and D.R. Roop, *Mechanisms regulating epithelial stratification.* Annu Rev Cell Dev Biol, 2007. **23**: p. 93-113.
13. Berta, M.A., et al., *Dose and context dependent effects of Myc on epidermal stem cell proliferation and differentiation.* EMBO Mol Med, 2010. **2**(1): p. 16-25.
14. Beverdam, A., et al., *Yap controls stem/progenitor cell proliferation in the mouse postnatal epidermis.* J Invest Dermatol, 2013. **133**(6): p. 1497-505.
15. Mehic, D., et al., *Fos and jun proteins are specifically expressed during differentiation of human keratinocytes.* J Invest Dermatol, 2005. **124**(1): p. 212-20.

16. Eckert, R.L., et al., *AP1 transcription factors in epidermal differentiation and skin cancer.* J Skin Cancer, 2013. **2013**: p. 537028.

17. Scholl, F.A., et al., *Mek1/2 MAPK kinases are essential for Mammalian development, homeostasis, and Raf-induced hyperplasia.* Dev Cell, 2007. **12**(4): p. 615-29.

18. Dumesic, P.A., et al., *Erk1/2 MAP kinases are required for epidermal G2/M progression.* J Cell Biol, 2009. **185**(3): p. 409-22.

19. Scholl, F.A., P.A. Dumesic, and P.A. Khavari, *Mek1 alters epidermal growth and differentiation.* Cancer Res, 2004. **64**(17): p. 6035-40.

20. Tarutani, M., et al., *Inducible activation of Ras and Raf in adult epidermis.* Cancer Res, 2003. **63**(2): p. 319-23.

21. Blanpain, C., et al., *Canonical notch signaling functions as a commitment switch in the epidermal lineage.* Genes Dev, 2006. **20**(21): p. 3022-35.

22. Koster, M.I., et al., *p63 induces key target genes required for epidermal morphogenesis.* Proc Natl Acad Sci U S A, 2007. **104**(9): p. 3255-60.

23. Yang, L.C., D.C. Ng, and D.D. Bikle, *Role of protein kinase C alpha in calcium induced keratinocyte differentiation: defective regulation in squamous cell carcinoma.* J Cell Physiol, 2003. **195**(2): p. 249-59.

24. Komuves, L., et al., *Epidermal expression of the full-length extracellular calcium-sensing receptor is required for normal keratinocyte differentiation.* J Cell Physiol, 2002. **192**(1): p. 45-54.

25. Plikus, M.V., et al., *Epithelial stem cells and implications for wound repair.* Semin Cell Dev Biol, 2012. **23**(9): p. 946-53.

26. Boehnke, K., et al., *Stem cells of the human epidermis and their niche: composition and function in epidermal regeneration and carcinogenesis.* Carcinogenesis, 2012. **33**(7): p. 1247-58.

27. Kretzschmar, K. and F.M. Watt, *Markers of epidermal stem cell subpopulations in adult mammalian skin.* Cold Spring Harb Perspect Med, 2014. **4**(10).

28. Gonzales, K.A.U. and E. Fuchs, *Skin and Its Regenerative Powers: An Alliance between Stem Cells and Their Niche.* Dev Cell, 2017. **43**(4): p. 387-401.

29. Levy, V., et al., *Distinct stem cell populations regenerate the follicle and interfollicular epidermis.* Dev Cell, 2005. **9**(6): p. 855-61.

30. Ito, M., et al., *Stem cells in the hair follicle bulge contribute to wound repair but not to homeostasis of the epidermis.* Nat Med, 2005. **11**(12): p. 1351-4.

31. Schneider, M.R., R. Schmidt-Ullrich, and R. Paus, *The hair follicle as a dynamic miniorgan.* Curr Biol, 2009. **19**(3): p. R132-42.

32. Horsley, V., et al., *Blimp1 defines a progenitor population that governs cellular input to the sebaceous gland.* Cell, 2006. **126**(3): p. 597-609.

33. Nijhof, J.G., et al., *The cell-surface marker MTS24 identifies a novel population of follicular keratinocytes with characteristics of progenitor cells.* Development, 2006. **133**(15): p. 3027-37.

34. Jensen, U.B., et al., *A distinct population of clonogenic and multipotent murine follicular keratinocytes residing in the upper isthmus.* J Cell Sci, 2008. **121**(Pt 5): p. 609-17.

35. Jensen, K.B., et al., *Lrig1 expression defines a distinct multipotent stem cell population in mammalian epidermis.* Cell Stem Cell, 2009. **4**(5): p. 427-39.

36. Snippert, H.J., et al., *Lgr6 marks stem cells in the hair follicle that generate all cell lineages of the skin.* Science, 2010. **327**(5971): p. 1385-9.

37. Kloepper, J.E., et al., *Immunophenotyping of the human bulge region: the quest to define useful in situ markers for human epithelial hair follicle stem cells and their niche.* Exp Dermatol, 2008. **17**(7): p. 592-609.

38. Braun, K.M., et al., *Manipulation of stem cell proliferation and lineage commitment: visualisation of label-retaining cells in wholemounts of mouse epidermis.* Development, 2003. **130**(21): p. 5241-55.

39. Cotsarelis, G., T.T. Sun, and R.M. Lavker, *Label-retaining cells reside in the bulge area of pilosebaceous unit: implications for follicular stem cells, hair cycle, and skin carcinogenesis.* Cell, 1990. **61**(7): p. 1329-37.

40. Tumbar, T., et al., *Defining the epithelial stem cell niche in skin.* Science, 2004. **303**(5656): p. 359-63.

41. Blanpain, C., et al., *Self-renewal, multipotency, and the existence of two cell populations within an epithelial stem cell niche.* Cell, 2004. **118**(5): p. 635-48.

42. Morris, R.J., et al., *Capturing and profiling adult hair follicle stem cells.* Nat Biotechnol, 2004. **22**(4): p. 411-7.

43. Horsley, V., et al., *NFATc1 balances quiescence and proliferation of skin stem cells.* Cell, 2008. **132**(2): p. 299-310.

44. Yuhki, M., et al., *BMPR1A signaling is necessary for hair follicle cycling and hair shaft differentiation in mice.* Development, 2004. **131**(8): p. 1825-33.

45. Kobielak, K., et al., *Defining BMP functions in the hair follicle by conditional ablation of BMP receptor IA.* J Cell Biol, 2003. **163**(3): p. 609-23.

46. Jamora, C., et al., *Links between signal transduction, transcription and adhesion in epithelial bud development.* Nature, 2003. **422**(6929): p. 317-22.

47. Plikus, M.V., et al., *Cyclic dermal BMP signalling regulates stem cell activation during hair regeneration.* Nature, 2008. **451**(7176): p. 340-4.

48. Nowak, J.A., et al., *Hair follicle stem cells are specified and function in early skin morphogenesis.* Cell Stem Cell, 2008. **3**(1): p. 33-43.

49. Lowry, W.E., et al., *Defining the impact of beta-catenin/Tcf transactivation on epithelial stem cells.* Genes Dev, 2005. **19**(13): p. 1596-611.

50. Silva-Vargas, V., et al., *Beta-catenin and Hedgehog signal strength can specify number and location of hair follicles in adult epidermis without recruitment of bulge stem cells.* Dev Cell, 2005. **9**(1): p. 121-31.

51. Paladini, R.D., et al., *Modulation of hair growth with small molecule agonists of the hedgehog signaling pathway.* J Invest Dermatol, 2005. **125**(4): p. 638-46.

52. Stenn, K.S. and R. Paus, *Controls of hair follicle cycling.* Physiol Rev, 2001. **81**(1): p. 449-494.

53. Paus, R. and K. Foitzik, *In search of the "hair cycle clock": a guided tour.* Differentiation, 2004. **72**(9-10): p. 489-511.

54. Dotto, G.P. and A.K. Rustgi, *Squamous Cell Cancers: A Unified Perspective on Biology and Genetics.* Cancer Cell, 2016. **29**(5): p. 622-637.

55. Yan, W., et al., *Squamous Cell Carcinoma - Similarities and Differences among Anatomical Sites.* Am J Cancer Res, 2011. **1**(3): p. 275-300.

56. Que, S.K.T., F.O. Zwald, and C.D. Schmults, *Cutaneous squamous cell carcinoma: Incidence, risk factors, diagnosis, and staging.* J Am Acad Dermatol, 2018. **78**(2): p. 237-247.

57. Green, A.C. and C.M. Olsen, *Cutaneous squamous cell carcinoma: an epidemiological review.* Br J Dermatol, 2017. **177**(2): p. 373-381.

58. Feller, L. and J. Lemmer, *Oral Squamous Cell Carcinoma: Epidemiology, Clinical Presentation and Treatment.* Journal of Cancer Therapy, 2012. **3**: p. 263-268.

59. Marur, S. and A.A. Forastiere, *Head and Neck Squamous Cell Carcinoma: Update on Epidemiology, Diagnosis, and Treatment.* Mayo Clin Proc, 2016. **91**(3): p. 386-96.

60. Leemans, C.R., P.J.F. Snijders, and R.H. Brakenhoff, *The molecular landscape of head and neck cancer.* Nat Rev Cancer, 2018. **18**(5): p. 269-282.

61. Ng, J.H., et al., *Changing epidemiology of oral squamous cell carcinoma of the tongue: A global study.* Head Neck, 2017. **39**(2): p. 297-304.

62. Abel, E.L., et al., *Multi-stage chemical carcinogenesis in mouse skin: fundamentals and applications.* Nat Protoc, 2009. **4**(9): p. 1350-62.

63. Van Duuren, B.L., et al., *The effect of aging and interval between primary and secondary treatment in two-stage carcinogenesis on mouse skin.* Cancer Res, 1975. **35**(3): p. 502-5.

64. Morris, R.J., *Keratinocyte stem cells: targets for cutaneous carcinogens.* J Clin Invest, 2000. **106**(1): p. 3-8.

65. Sanchez-Danes, A. and C. Blanpain, *Deciphering the cells of origin of squamous cell carcinomas.* Nat Rev Cancer, 2018. **18**(9): p. 549-561.

66. Lapouge, G., et al., *Identifying the cellular origin of squamous skin tumors.* Proc Natl Acad Sci U S A, 2011. **108**(18): p. 7431-6.

67. White, A.C., et al., *Defining the origins of Ras/p53-mediated squamous cell carcinoma.* Proc Natl Acad Sci U S A, 2011. **108**(18): p. 7425-30.

68. Raimondi, A.R., A. Molinolo, and J.S. Gutkind, *Rapamycin prevents early onset of tumorigenesis in an oral-specific K-ras and p53 two-hit carcinogenesis model.* Cancer Res, 2009. **69**(10): p. 4159-66.

69. Owens, D.M. and F.M. Watt, *Contribution of stem cells and differentiated cells to epidermal tumours.* Nat Rev Cancer, 2003. **3**(6): p. 444-51.

70. Pelengaris, S., et al., *Reversible activation of c-Myc in skin: induction of a complex neoplastic phenotype by a single oncogenic lesion.* Mol Cell, 1999. **3**(5): p. 565-77.

71. Bailleul, B., et al., *Skin hyperkeratosis and papilloma formation in transgenic mice expressing a ras oncogene from a suprabasal keratin promoter.* Cell, 1990. **62**(4): p. 697-708.

72. Hoadley, K.A., et al., *Multiplatform analysis of 12 cancer types reveals molecular classification within and across tissues of origin.* Cell, 2014. **158**(4): p. 929-944.

73. Hoadley, K.A., et al., *Cell-of-Origin Patterns Dominate the Molecular Classification of 10,000 Tumors from 33 Types of Cancer.* Cell, 2018. **173**(2): p. 291-304 e6.

74. Pickering, C.R., et al., *Mutational landscape of aggressive cutaneous squamous cell carcinoma.* Clin Cancer Res, 2014. **20**(24): p. 6582-92.

75. Morris, L.G., et al., *Recurrent somatic mutation of FAT1 in multiple human cancers leads to aberrant Wnt activation.* Nat Genet, 2013. **45**(3): p. 253-61.

76. Haraguchi, K., et al., *Ajuba negatively regulates the Wnt signaling pathway by promoting GSK-3beta-mediated phosphorylation of beta-catenin.* Oncogene, 2008. **27**(3): p. 274-84.

77. Sun, G. and K.D. Irvine, *Ajuba family proteins link JNK to Hippo signaling.* Sci Signal, 2013. **6**(292): p. ra81.

78. Debaugnies, M., et al., *YAP and TAZ are essential for basal and squamous cell carcinoma initiation.* EMBO Rep, 2018. **19**(7).

79. Watanabe, H., et al., *SOX2 and p63 colocalize at genetic loci in squamous cell carcinomas.* J Clin Invest, 2014. **124**(4): p. 1636-45.

80. Schrock, A., et al., *Expression and role of the embryonic protein SOX2 in head and neck squamous cell carcinoma.* Carcinogenesis, 2014. **35**(7): p. 1636-42.

81. Bustelo, X.R., V. Sauzeau, and I.M. Berenjeno, *GTP-binding proteins of the Rho/Rac family: regulation, effectors and functions in vivo.* Bioessays, 2007. **29**(4): p. 356-70.

82. Jaffe, A.B. and A. Hall, *Rho GTPases: biochemistry and biology.* Annu Rev Cell Dev Biol, 2005. **21**: p. 247-69.

83. Bustelo, X.R., *RHO GTPases in cancer: known facts, open questions, and therapeutic challenges.* Biochem Soc Trans, 2018. **46**(3): p. 741-760.

84. Bishop, A.L. and A. Hall, *Rho GTPases and their effector proteins.* Biochem J, 2000. **348 Pt 2**: p. 241-55.

85. Cook, D.R., K.L. Rossman, and C.J. Der, *Rho guanine nucleotide exchange factors: regulators of Rho GTPase activity in development and disease.* Oncogene, 2014. **33**(31): p. 4021-35.
86. Porter, A.P., A. Papaioannou, and A. Malliri, *Deregulation of Rho GTPases in cancer.* Small GTPases, 2016. **7**(3): p. 123-38.
87. Benitah, S.A., et al., *Stem cell depletion through epidermal deletion of Rac1.* Science, 2005. **309**(5736): p. 933-5.
88. Chrostek, A., et al., *Rac1 is crucial for hair follicle integrity but is not essential for maintenance of the epidermis.* Mol Cell Biol, 2006. **26**(18): p. 6957-70.
89. Castilho, R.M., et al., *Requirement of Rac1 distinguishes follicular from interfollicular epithelial stem cells.* Oncogene, 2007. **26**(35): p. 5078-85.
90. Chai, L., et al., *Small Rho GTPase Rac1 determines human epidermal stem cell fate in vitro.* Int J Mol Med, 2010. **25**(5): p. 723-7.
91. Tscharntke, M., et al., *Impaired epidermal wound healing in vivo upon inhibition or deletion of Rac1.* J Cell Sci, 2007. **120**(Pt 8): p. 1480-90.
92. Jackson, B., et al., *RhoA is dispensable for skin development, but crucial for contraction and directed migration of keratinocytes.* Mol Biol Cell, 2011. **22**(5): p. 593-605.
93. Wang, F., et al., *RhoA promotes epidermal stem cell proliferation via PKN1-cyclin D1 signaling.* PLoS One, 2017. **12**(2): p. e0172613.
94. Zhan, R., et al., *Nitric oxide promotes epidermal stem cell migration via cGMP-Rho GTPase signalling.* Sci Rep, 2016. **6**: p. 30687.
95. Dubash, A.D., et al., *The GEF Bcr activates RhoA/MAL signaling to promote keratinocyte differentiation via desmoglein-1.* J Cell Biol, 2013. **202**(4): p. 653-66.
96. Wu, X., et al., *Cdc42 controls progenitor cell differentiation and beta-catenin turnover in skin.* Genes Dev, 2006. **20**(5): p. 571-85.
97. Menacho-Marquez, M., et al., *The Rho exchange factors Vav2 and Vav3 favor skin tumor initiation and promotion by engaging extracellular signaling loops.* PLoS Biol, 2013. **11**(7): p. e1001615.
98. Malliri, A., et al., *Mice deficient in the Rac activator Tiam1 are resistant to Ras-induced skin tumours.* Nature, 2002. **417**(6891): p. 867-71.

99. Khosravi-Far, R., et al., *Activation of Rac1, RhoA, and mitogen-activated protein kinases is required for Ras transformation.* Mol Cell Biol, 1995. **15**(11): p. 6443-53.

100. Olson, M.F., *Rho GTPases, their post-translational modifications, disease-associated mutations and pharmacological inhibitors.* Small GTPases, 2018. **9**(3): p. 203-215.

101. Chen, R., et al., *Rac1 regulates skin tumors by regulation of keratin 17 through recruitment and interaction with CD11b+Gr1+ cells.* Oncotarget, 2014. **5**(12): p. 4406-17.

102. Wang, Z., et al., *Rac1 is crucial for Ras-dependent skin tumor formation by controlling Pak1-Mek-Erk hyperactivation and hyperproliferation in vivo.* Oncogene, 2010. **29**(23): p. 3362-73.

103. Samuel, M.S., F.C. Lourenco, and M.F. Olson, *K-Ras mediated murine epidermal tumorigenesis is dependent upon and associated with elevated Rac1 activity.* PLoS One, 2011. **6**(2): p. e17143.

104. Chow, H.Y., et al., *p21-Activated kinase 1 is required for efficient tumor formation and progression in a Ras-mediated skin cancer model.* Cancer Res, 2012. **72**(22): p. 5966-75.

105. Radu, M., et al., *PAK signalling during the development and progression of cancer.* Nat Rev Cancer, 2014. **14**(1): p. 13-25.

106. Kazanietz, M.G. and M.J. Caloca, *The Rac GTPase in Cancer: From Old Concepts to New Paradigms.* Cancer Res, 2017. **77**(20): p. 5445-5451.

107. Garcia-Mariscal, A., et al., *Loss of RhoA promotes skin tumor formation and invasion by upregulation of RhoB.* Oncogene, 2018. **37**(7): p. 847-860.

108. Faried, A., et al., *Clinical and prognostic significance of RhoA and RhoC gene expression in esophageal squamous cell carcinoma.* Ann Surg Oncol, 2007. **14**(12): p. 3593-601.

109. Samuel, M.S., et al., *Actomyosin-mediated cellular tension drives increased tissue stiffness and beta-catenin activation to induce epidermal hyperplasia and tumor growth.* Cancer Cell, 2011. **19**(6): p. 776-91.

110. Liu, A.X., et al., *RhoB is dispensable for mouse development, but it modifies susceptibility to tumor formation as well as cell adhesion and growth factor signaling in transformed cells.* Mol Cell Biol, 2001. **21**(20): p. 6906-12.

111. Meyer, N., et al., *RhoB promotes cancer initiation by protecting keratinocytes from UVB-induced apoptosis but limits tumor aggressiveness.* J Invest Dermatol, 2014. **134**(1): p. 203-212.

112. Justilien, V. and A.P. Fields, *Ect2 links the PKCiota-Par6alpha complex to Rac1 activation and cellular transformation.* Oncogene, 2009. **28**(41): p. 3597-607.

113. Justilien, V., et al., *Ect2-Dependent rRNA Synthesis Is Required for KRAS-TRP53-Driven Lung Adenocarcinoma.* Cancer Cell, 2017. **31**(2): p. 256-269.

114. Fields, A.P. and V. Justilien, *The guanine nucleotide exchange factor (GEF) Ect2 is an oncogene in human cancer.* Adv Enzyme Regul, 2010. **50**(1): p. 190-200.

115. Habets, G.G., et al., *Identification of an invasion-inducing gene, Tiam-1, that encodes a protein with homology to GDP-GTP exchangers for Rho-like proteins.* Cell, 1994. **77**(4): p. 537-49.

116. Stebel, A., et al., *Progression of breast tumors is accompanied by a decrease in expression of the Rho guanine exchange factor Tiam1.* Oncol Rep, 2009. **21**(1): p. 217-22.

117. Bustelo, X.R., *Vav family exchange factors: an integrated regulatory and functional view.* Small GTPases, 2014. **5**(2): p. 9.

118. Sauzeau, V., et al., *The Rho/Rac exchange factor Vav2 controls nitric oxide-dependent responses in mouse vascular smooth muscle cells.* J Clin Invest, 2010. **120**(1): p. 315-30.

119. Sauzeau, V., et al., *Loss of Vav2 proto-oncogene causes tachycardia and cardiovascular disease in mice.* Mol Biol Cell, 2007. **18**(3): p. 943-52.

120. Menacho-Marquez, M., et al., *Chronic sympathoexcitation through loss of Vav3, a Rac1 activator, results in divergent effects on metabolic syndrome and obesity depending on diet.* Cell Metab, 2013. **18**(2): p. 199-211.

121. Sauzeau, V., et al., *Vav3 is involved in GABAergic axon guidance events important for the proper function of brainstem neurons controlling cardiovascular, respiratory, and renal parameters.* Mol Biol Cell, 2010. **21**(23): p. 4251-63.

122. Sauzeau, V., et al., *Vav3 proto-oncogene deficiency leads to sympathetic hyperactivity and cardiovascular dysfunction.* Nat Med, 2006. **12**(7): p. 841-5.

123. Bartolome, R.A., et al., *Activation of Vav/Rho GTPase signaling by CXCL12 controls membrane-type matrix metalloproteinase-dependent melanoma cell invasion.* Cancer Res, 2006. **66**(1): p. 248-58.

124. Patel, V., et al., *Persistent activation of Rac1 in squamous carcinomas of the head and neck: evidence for an EGFR/Vav2 signaling axis involved in cell invasion.* Carcinogenesis, 2007. **28**(6): p. 1145-52.

125. Kwon, A.Y., et al., *VAV3 Overexpressed in Cancer Stem Cells Is a Poor Prognostic Indicator in Ovarian Cancer Patients.* Stem Cells Dev, 2015. **24**(13): p. 1521-35.

126. Lin, K.Y., et al., *Clinical significance of increased guanine nucleotide exchange factor Vav3 expression in human gastric cancer.* Mol Cancer Res, 2012. **10**(6): p. 750-9.

127. Rao, S., et al., *A novel nuclear role for the Vav3 nucleotide exchange factor in androgen receptor coactivation in prostate cancer.* Oncogene, 2012. **31**(6): p. 716-27.

128. Citterio, C., et al., *The rho exchange factors vav2 and vav3 control a lung metastasis-specific transcriptional program in breast cancer cells.* Sci Signal, 2012. **5**(244): p. ra71.

129. Robles-Valero, J., et al., *A Paradoxical Tumor-Suppressor Role for the Rac1 Exchange Factor Vav1 in T Cell Acute Lymphoblastic Leukemia.* Cancer Cell, 2017. **32**(5): p. 608-623 e9.

130. Abate, F., et al., *Activating mutations and translocations in the guanine exchange factor VAV1 in peripheral T-cell lymphomas.* Proc Natl Acad Sci U S A, 2017. **114**(4): p. 764-769.

131. Lane, J., et al., *The expression and prognostic value of the guanine nucleotide exchange factors (GEFs) Trio, Vav1 and TIAM-1 in human breast cancer.* Int Semin Surg Oncol, 2008. **5**: p. 23.

132. Fernandez-Zapico, M.E., et al., *Ectopic expression of VAV1 reveals an unexpected role in pancreatic cancer tumorigenesis.* Cancer Cell, 2005. **7**(1): p. 39-49.

133. Hornstein, I., et al., *The haematopoietic specific signal transducer Vav1 is expressed in a subset of human neuroblastomas.* J Pathol, 2003. **199**(4): p. 526-33.

134. Fabbiano, S., et al., *Genetic dissection of the vav2-rac1 signaling axis in vascular smooth muscle cells.* Mol Cell Biol, 2014. **34**(24): p. 4404-19.
135. Doody, G.M., et al., *Signal transduction through Vav-2 participates in humoral immune responses and B cell maturation.* Nat Immunol, 2001. **2**(6): p. 542-7.
136. Salgado, G., et al., *Human reconstructed skin xenografts on mice to model skin physiology.* Differentiation, 2017. **98**: p. 14-24.
137. Pascual, G., et al., *Targeting metastasis-initiating cells through the fatty acid receptor CD36.* Nature, 2017. **541**(7635): p. 41-45.
138. Rodrigues, L., et al., *Activation of Vav by the gammaherpesvirus M2 protein contributes to the establishment of viral latency in B lymphocytes.* J Virol, 2006. **80**(12): p. 6123-35.
139. Guo, F. and Y. Zheng, *Rho family GTPases cooperate with p53 deletion to promote primary mouse embryonic fibroblast cell invasion.* Oncogene, 2004. **23**(33): p. 5577-85.
140. Schuebel, K.E., et al., *Phosphorylation-dependent and constitutive activation of Rho proteins by wild-type and oncogenic Vav-2.* EMBO J, 1998. **17**(22): p. 6608-21.
141. Barreira, M., et al., *The C-terminal SH3 domain contributes to the intramolecular inhibition of Vav family proteins.* Sci Signal, 2014. **7**(321): p. ra35.
142. Margolin, A.A., et al., *ARACNE: an algorithm for the reconstruction of gene regulatory networks in a mammalian cellular context.* BMC Bioinformatics, 2006. **7 Suppl 1**: p. S7.
143. Shannon, P., et al., *Cytoscape: a software environment for integrated models of biomolecular interaction networks.* Genome Res, 2003. **13**(11): p. 2498-504.
144. Tripathi, S., et al., *Meta- and Orthogonal Integration of Influenza "OMICs" Data Defines a Role for UBR4 in Virus Budding.* Cell Host Microbe, 2015. **18**(6): p. 723-35.
145. Janky, R., et al., *iRegulon: from a gene list to a gene regulatory network using large motif and track collections.* PLoS Comput Biol, 2014. **10**(7): p. e1003731.

146. O. Rocks, P.M.M., J. Rademacher, R. D. Bagshaw, K. M. Alp, G. Giudice, L. E. Heinrich, C. Barth, R. L .Eccles, M. Sanchez-Castro, G. Mbamalu, M. Tucholska, L. Spatt, C. Wortmann, M. T. Czajkowski, R. W. Welke, S. Zhang, V. Nguyen, L. Brandeburg, T. Rrustemi, P. Trnka, K. Freitag, B. Larsen, O. Popp, K. Colwill, P. Mertins, A. Gingras, C. Bakal, O. Pertz, F. P. Roth, T. Pawson, E. Petsalaki, *Systematic Characterization of RhoGEF/RhoGAP Regulatory Proteins Reveals Organization Principles of Rho GTPase Signaling.* bioRXiv, 2018.

147. Cardama, G.A., et al., *Preclinical development of novel Rac1-GEF signaling inhibitors using a rational design approach in highly aggressive breast cancer cell lines.* Anticancer Agents Med Chem, 2014. **14**(6): p. 840-51.

148. Gustems, M., et al., *c-Jun/c-Fos heterodimers regulate cellular genes via a newly identified class of methylated DNA sequence motifs.* Nucleic Acids Res, 2014. **42**(5): p. 3059-72.

149. Ben-Porath, I., et al., *An embryonic stem cell-like gene expression signature in poorly differentiated aggressive human tumors.* Nat Genet, 2008. **40**(5): p. 499-507.

150. Aasen, T., et al., *Efficient and rapid generation of induced pluripotent stem cells from human keratinocytes.* Nat Biotechnol, 2008. **26**(11): p. 1276-84.

151. Janich, P., et al., *The circadian molecular clock creates epidermal stem cell heterogeneity.* Nature, 2011. **480**(7376): p. 209-14.

152. Chen, J., et al., *ToppGene Suite for gene list enrichment analysis and candidate gene prioritization.* Nucleic Acids Res, 2009. **37**(Web Server issue): p. W305-11.

153. Lien, W.H., et al., *Genome-wide maps of histone modifications unwind in vivo chromatin states of the hair follicle lineage.* Cell Stem Cell, 2011. **9**(3): p. 219-32.

154. Subramanian, A., et al., *Gene set enrichment analysis: a knowledge-based approach for interpreting genome-wide expression profiles.* Proc Natl Acad Sci U S A, 2005. **102**(43): p. 15545-50.

155. Reich, M., et al., *GenePattern 2.0.* Nat Genet, 2006. **38**(5): p. 500-1.

156. Liberzon, A., et al., *The Molecular Signatures Database (MSigDB) hallmark gene set collection.* Cell Syst, 2015. **1**(6): p. 417-425.

157. Szklarczyk, D., et al., *STRING v10: protein-protein interaction networks, integrated over the tree of life.* Nucleic Acids Res, 2015. **43**(Database issue): p. D447-52.

158. Toufighi, K., et al., *Dissecting the calcium-induced differentiation of human primary keratinocytes stem cells by integrative and structural network analyses.* PLoS Comput Biol, 2015. **11**(5): p. e1004256.

159. Kumar, L. and E.F. M, *Mfuzz: a software package for soft clustering of microarray data.* Bioinformation, 2007. **2**(1): p. 5-7.

160. Langfelder, P. and S. Horvath, *WGCNA: an R package for weighted correlation network analysis.* BMC Bioinformatics, 2008. **9**: p. 559.

161. Braakhuis, B.J., R.H. Brakenhoff, and C.R. Leemans, *Second field tumors: a new opportunity for cancer prevention?* Oncologist, 2005. **10**(7): p. 493-500.

162. Nassar, D., et al., *Genomic landscape of carcinogen-induced and genetically induced mouse skin squamous cell carcinoma.* Nat Med, 2015. **21**(8): p. 946-54.

163. Saladi, S.V., et al., *ACTL6A Is Co-Amplified with p63 in Squamous Cell Carcinoma to Drive YAP Activation, Regenerative Proliferation, and Poor Prognosis.* Cancer Cell, 2017. **31**(1): p. 35-49.

164. Zanconato, F., et al., *Genome-wide association between YAP/TAZ/TEAD and AP-1 at enhancers drives oncogenic growth.* Nat Cell Biol, 2015. **17**(9): p. 1218-27.

165. Schlegelmilch, K., et al., *Yap1 acts downstream of alpha-catenin to control epidermal proliferation.* Cell, 2011. **144**(5): p. 782-95.

166. Watt, F.M., M. Frye, and S.A. Benitah, *MYC in mammalian epidermis: how can an oncogene stimulate differentiation?* Nat Rev Cancer, 2008. **8**(3): p. 234-42.

167. Fujikawa, K., et al., *VAV2 and VAV3 as candidate disease genes for spontaneous glaucoma in mice and humans.* PLoS One, 2010. **5**(2): p. e9050.

168. Coso, O.A., et al., *The small GTP-binding proteins Rac1 and Cdc42 regulate the activity of the JNK/SAPK signaling pathway.* Cell, 1995. **81**(7): p. 1137-46.

169. Hill, C.S., J. Wynne, and R. Treisman, *The Rho family GTPases RhoA, Rac1, and CDC42Hs regulate transcriptional activation by SRF.* Cell, 1995. **81**(7): p. 1159-70.

170. Rognoni, E. and F.M. Watt, *Skin Cell Heterogeneity in Development, Wound Healing, and Cancer.* Trends Cell Biol, 2018. **28**(9): p. 709-722.

171. Langton, A.K., S.E. Herrick, and D.J. Headon, *An extended epidermal response heals cutaneous wounds in the absence of a hair follicle stem cell contribution.* J Invest Dermatol, 2008. **128**(5): p. 1311-8.

172. Heath, J., et al., *Hair follicles are required for optimal growth during lateral skin expansion.* J Invest Dermatol, 2009. **129**(10): p. 2358-64.

173. Ito, M. and G. Cotsarelis, *Is the hair follicle necessary for normal wound healing?* J Invest Dermatol, 2008. **128**(5): p. 1059-61.

174. Muller-Rover, S., et al., *A comprehensive guide for the accurate classification of murine hair follicles in distinct hair cycle stages.* J Invest Dermatol, 2001. **117**(1): p. 3-15.

175. Doles, J., et al., *Age-associated inflammation inhibits epidermal stem cell function.* Genes Dev, 2012. **26**(19): p. 2144-53.

176. Lim, X. and R. Nusse, *Wnt signaling in skin development, homeostasis, and disease.* Cold Spring Harb Perspect Biol, 2013. **5**(2).

177. Watt, F.M., S. Estrach, and C.A. Ambler, *Epidermal Notch signalling: differentiation, cancer and adhesion.* Curr Opin Cell Biol, 2008. **20**(2): p. 171-9.

178. Grinberg-Bleyer, Y., et al., *Cutting edge: NF-kappaB p65 and c-Rel control epidermal development and immune homeostasis in the skin.* J Immunol, 2015. **194**(6): p. 2472-6.

179. Sur, I., M. Ulvmar, and R. Toftgard, *The two-faced NF-kappaB in the skin.* Int Rev Immunol, 2008. **27**(4): p. 205-23.

180. Howell, J.J., et al., *A growing role for mTOR in promoting anabolic metabolism.* Biochem Soc Trans, 2013. **41**(4): p. 906-12.

181. van Riggelen, J., A. Yetil, and D.W. Felsher, *MYC as a regulator of ribosome biogenesis and protein synthesis.* Nat Rev Cancer, 2010. **10**(4): p. 301-9.

182. Lin, H.Y. and L.T. Yang, *Differential response of epithelial stem cell populations in hair follicles to TGF-beta signaling.* Dev Biol, 2013. **373**(2): p. 394-406.

183. Jeong, H., et al., *Lethality and centrality in protein networks.* Nature, 2001. **411**(6833): p. 41-2.

184. Han, J.D., et al., *Evidence for dynamically organized modularity in the yeast protein-protein interaction network.* Nature, 2004. **430**(6995): p. 88-93.

185. Lopez-Pajares, V., et al., *A LncRNA-MAF:MAFB transcription factor network regulates epidermal differentiation.* Dev Cell, 2015. **32**(6): p. 693-706.

186. Werner, S., T. Krieg, and H. Smola, *Keratinocyte-fibroblast interactions in wound healing.* J Invest Dermatol, 2007. **127**(5): p. 998-1008.

187. Nguyen, L.K., B.N. Kholodenko, and A. von Kriegsheim, *Rac1 and RhoA: Networks, loops and bistability.* Small GTPases, 2018. **9**(4): p. 316-321.

188. Smith, B.A., et al., *A Human Adult Stem Cell Signature Marks Aggressive Variants across Epithelial Cancers.* Cell Rep, 2018. **24**(12): p. 3353-3366 e5.

189. Chitsazzadeh, V., et al., *Cross-species identification of genomic drivers of squamous cell carcinoma development across preneoplastic intermediates.* Nat Commun, 2016. **7**: p. 12601.

190. Jurchott, K., et al., *Identification of Y-box binding protein 1 as a core regulator of MEK/ERK pathway-dependent gene signatures in colorectal cancer cells.* PLoS Genet, 2010. **6**(12): p. e1001231.

191. Malta, T.M., et al., *Machine Learning Identifies Stemness Features Associated with Oncogenic Dedifferentiation.* Cell, 2018. **173**(2): p. 338-354 e15.

192. Park, H.W., et al., *Alternative Wnt Signaling Activates YAP/TAZ.* Cell, 2015. **162**(4): p. 780-94.

193. Skvortsov, S., et al., *Rac1 as a potential therapeutic target for chemo-radioresistant head and neck squamous cell carcinomas (HNSCC).* Br J Cancer, 2014. **110**(11): p. 2677-87.

194. Giangreco, A., et al., *Epidermal stem cells are retained in vivo throughout skin aging.* Aging Cell, 2008. **7**(2): p. 250-9.

195. Racila, D. and J.R. Bickenbach, *Are epidermal stem cells unique with respect to aging?* Aging (Albany NY), 2009. **1**(8): p. 746-50.

196. Lin, K.K., et al., *Circadian clock genes contribute to the regulation of hair follicle cycling.* PLoS Genet, 2009. **5**(7): p. e1000573.

197. Day, C.P., G. Merlino, and T. Van Dyke, *Preclinical mouse cancer models: a maze of opportunities and challenges.* Cell, 2015. **163**(1): p. 39-53.

198. Vaque, J.P., et al., *A genome-wide RNAi screen reveals a Trio-regulated Rho GTPase circuitry transducing mitogenic signals initiated by G protein-coupled receptors.* Mol Cell, 2013. **49**(1): p. 94-108.

199. Rogerson, C., D. Bergamaschi, and R.F.L. O'Shaughnessy, *Uncovering mechanisms of nuclear degradation in keratinocytes: A paradigm for nuclear degradation in other tissues.* Nucleus, 2018. **9**(1): p. 56-64.

200. Vigil, D., et al., *Ras superfamily GEFs and GAPs: validated and tractable targets for cancer therapy?* Nat Rev Cancer, 2010. **10**(12): p. 842-57.

201. Michaelson, D., et al., *Differential localization of Rho GTPases in live cells: regulation by hypervariable regions and RhoGDI binding.* J Cell Biol, 2001. **152**(1): p. 111-26.

202. Casar, B., et al., *RAS at the Golgi antagonizes malignant transformation through PTPRkappa-mediated inhibition of ERK activation.* Nat Commun, 2018. **9**(1): p. 3595.

203. Marei, H., et al., *Differential Rac1 signalling by guanine nucleotide exchange factors implicates FLII in regulating Rac1-driven cell migration.* Nat Commun, 2016. **7**: p. 10664.

204. Lorenzo-Martin, L.F., et al., *Vav proteins maintain epithelial traits in breast cancer cells using miR-200c-dependent and independent mechanisms.* Oncogene, 2019. **38**(2): p. 209-227.

205. Hunter, S.G., et al., *Essential role of Vav family guanine nucleotide exchange factors in EphA receptor-mediated angiogenesis.* Mol Cell Biol, 2006. **26**(13): p. 4830-42.

PUBLICATIONS

The findings presented in this Ph.D. thesis have been submitted for publication. In addition, further work performed during my thesis has contributed to the following publications:

1. Robles-Valero J., **Lorenzo-Martín L.F.**, Menacho-Márquez M., Fernández-Pisonero I., Abad A., Camós M., Toribio M.L., Espinosa L., Bigas A., Bustelo X.R. A paradoxical tumor-suppressor role for the Rac1 exchange factor Vav1 in T cell acute lymphoblastic leukemia. *Cancer Cell* 2017 Nov 13;32(5): 608-623.

2. Robles-Valero J., **Lorenzo-Martín L.F.**, Fernández-Pisonero I., Bustelo X.R. Rho guanosine nucleotide exchange factors are not such bad guys after all in cancer. *Small GTPases* 2018 Jan 24: 1-7.

3. Bustelo X.R., **Lorenzo-Martín L.F.**, Cuadrado M., Fernández-Pisonero I., Robles-Valero J. An unexpected tumor supressor role for VAV1. *Mol Cell Oncol* 2018 Feb 23;5(3): e1432257.

4. Liceras-Boillos P., Jimeno D., García-Navas R., **Lorenzo-Martín L.F.**, Menacho-Márquez M., Segrelles C., Gómez C., Calzada N., Fuentes-Mateos R., Paramio J.M., Bustelo X.R., Baltanás F.C., Santos E. Differential Role Of The RasGEFs Sos1 And Sos2 In Mouse Skin Homeostasis And Carcinogenesis. *Mol Cell Biol* 2018 Jul 30;38(16): e00049-18.

5. Cortazar A., Torrano V., Martín-Martín N., Caro-Maldonado A., Camacho L., Hermanova I., Guruceaga E., **Lorenzo-Martín L.F.**, Caloto R., Gomis R., Apaolaza I., Quesada V., Trka J., Gomez-Muñoz A., Vicent S., Bustelo X.R., Planes F., Aransay A., Carracedo A. CANCERTOOL, a visualization and representation interface to exploit cancer datasets. *Cancer Res* 2018 Nov 1;78(21): 6320-6328.

6. Casar B., Badrock A., Jiménez I., Arozarena I., Colón-Bolea P., **Lorenzo-Martín L.F.**, Barinaga-Rementeria Ramirez I., Barriuso J., Cappitelli V., Donoghue D., Bustelo X.R., Hurlstone A., Crespo P. RAS at the Golgi antagonizes malignant transformation through PTPRκ-mediated inhibition of ERK activation. *Nat Commun* 2018 Sep 5;9 (1): 3595.

7. **Lorenzo-Martín L.F.**, Citterio C., Menacho-Márquez M., Conde J., Larive R.M., Rodríguez-Fdez S., García-Escudero R., Robles-Valero J., Cuadrado M., Fernández-Pisonero I., Dosil M., Sevilla M.A., Montero M.J., Fernández-Salguero P.M., Paramio J.M., Bustelo X.R. Vav proteins maintain epithelial traits in breast cancer cells using miR-200c-dependent and independent mechanisms. *Oncogene* 2019 Jan;38(2): 209-227.

8. **Lorenzo-Martín L.F.**, Menacho-Márquez M., Fabianno S., Al-Massai O., Abad A., Rodríguez-Fdez S., Sevilla M.A., Montero M.J., Diéguez C., Nogueiras R., Bustelo X.R. Vagal afferents contribute to sympathoexcitation-driven metabolic dysfunctions. *J Endocrinol* 2019 Mar 1;240(3): 483 - 496.

ACKNOWLEDGEMENTS

Data, figures and research achievements are thoroughly described in the pages that compose this thesis with a double intention: the proper conveyance of such findings to the scientific and academic communities, and the preservation in time and memory of the essence of my doctorate. Although hopefully proficient at the former, this dissertation will inevitably fail at the latter, as a doctorate is a long journey of both profesional and personal metamorphosis that cannot be captured by merely displaying the goals eventually attained. A journey is not the finishing line, it is the journey itself, and that is not only a story of data, it is also a story of people. These last pages are for them.

I will not begin by saying thank you, but I am sorry, for I am aware that many people whose name is not included here should receive a more explicit recognition. Be sure that this is not lack of consideration or gratefulness, both of which I have, but are just flaws of this Ph.D. student who, thorough in his acknowledgements as he has tried to be, will surely not be able to bring up all those people who were of invaluable assistance, in one way or another, along these years. Let me assure you that what is written here is also for you.

English is undoubtedly the language of science, which is the reason why I chose it to transmit all the scientific matters contained in this thesis. And although it would also be a perfectly valid tool to convey my akcnowledgements, parece que es la lengua materna la que más se acerca al corazón o al alma, cualquiera que sea el ente encargado de estos asuntos, y la que de manera más fiel y sentida puede transmitir lo que en él habita. Emito, por lo tanto y por segunda vez, disculpas antes que agradecimientos por aquellas personas que queriendo leer estas páginas encuentren problema en el repentino cambio de idioma.

Sin lugar a dudas, cuando se aborda la delicada tarea de encontrar las palabras que arraiguen en un capítulo titulado “agradecimientos”, el estudiante de doctorado se encuentra en un momento de turbación. Y es que la escritura de la tesis doctoral está siempre embebida en una suerte de frenesí y de etérea, y a veces no tan etérea, tensión. La redacción de cientos de páginas, la consulta de incontables publicaciones científicas, el diseño de docenas de figuras, el cuidado del formato del documento final y toda una serie de tareas adicionales bajo el peso de una losa cada vez más pesada: el menguante tiempo restante hasta la fecha del depósito. Esto hace que generalmente el doctorando esté flaco de fuerzas y falto de tiempo a la hora de

escribir estas líneas finales. Como consecuencia, muchas veces estas hojas languidecen y adquieren un aspecto tísico, lo cual parece no corresponderse con la extensión de los capítulos precedentes. Y es que si es posible escribir cientos de páginas sobre los hallazgos científicos obtenidos durante el doctorado, no menos podrían escribirse aquí, que son de hecho las que sustentan a las anteriores. Por ello, sin que sea mi intención alargarme más de la cuenta, me he propuesto tratar de impedir que mi determinación desfallezca en la redacción de estas últimas páginas, para así agradecer sin prisas ni apuros todo lo que es necesario que agradezca, que no es poco.

A mi familia

A mis padres, José Luis y Mariana; a mi hermano, Andrés; a mis abuelos, Eutimio, Úrsula, Ludgerico y Teresa. Lo que soy, lo soy por vosotros. Desde el día en que nací, vosotros me habéis sujetado en cada uno de mis pasos, enseñado qué ser y cómo serlo, y apoyado de manera tan incondicional como incansable. Soy consciente de que probablemente esta será la única parte de la tesis que leeréis, si es que la leéis, pues todo lo anterior os parecerá un galimatías incomprensible y, por qué no decirlo, soberanamente aburrido. No obstante, quiero que sepáis que por extraños y distantes que parezcan los contenidos de este libro, vosotros estáis en ellos, y que lo único que necesito para considerar este trabajo *summa cum laude* es que os sintáis orgullosos.

A mis tíos, Marisol, Tomi, Valentín, Carlina, Román y Gertru; a mis primos, Luis y Cristina. Poco más se puede pedir cuando uno está arropado por una familia como vosotros. Muchas gracias por los pequeños y los grandes detalles que siempre habéis tenido conmigo, que han hecho todo mucho más fácil, dentro y fuera del laboratorio.

Sabed que podría escribir un sinfín de cosas por las que os estoy agradecido a cada uno de todos vosotros, y que si no lo hago no es por dejadez o pereza, sino porque estoy convencido de que no puedo deciros nada que no sepáis. Prefiero simplemente plasmar, de manera breve pero clara, que siempre habéis sido y seréis lo más importante para mí.

A mi laboratorio

Agradecer a los compañeros, y además amigos, del laboratorio todo lo que han hecho por mí no es tarea fácil. Personas con las que he compartido tanto tiempo día tras día y que un impacto tan directo han tenido tanto en mi desarrollo profesional como personal. De hecho, hasta la simple elección del orden de citación es un tema ya delicado de por sí, pues parece la interpretación generalizada que cuanto antes se habla de alguien, más agradecido se le está a esa persona, lo cual desde luego no es tal cosa. Así pues, yo optaré por un criterio quizás más ordenado que me librará de la asignación de posiciones: el cronológico con respecto a cuándo fui conociendo a cada uno.

A Xosé. Tenía 22 años y estaba cursando el penúltimo curso de carrera cuando fui a entrevistarme contigo para entrar en tu laboratorio. En aquel entonces sabía mucho (o eso pensaba) de que dicen los libros, pero mi conocimiento acerca del mundo de la investigación era más bien nulo. Hoy han pasado 7 años, una tesina, un máster y un doctorado, y desde luego ya no soy ese muchacho de la entrevista. Eso es gracias a ti. Siempre había escuchado que en la carrera profesional del investigador, la persona que más influye en su carácter y personalidad científica es el director de su tesis doctoral. Ahora veo lo bien cierto que puede ser eso. Sin duda me quedan infinidad de cosas por aprender, tanto técnicas como científicas, pero el cómo las aprenderé y cómo las aplicaré ya lo sé: como tú me has enseñado. Sean cuales sean los pasos que han de venir en mi futuro, siempre llevaré la escuela del Doctor Bustelo conmigo, de la cual me siento especialmente orgulloso. Gracias también por darme los recursos necesarios para embarcarme en proyectos tan enriquecedores, por fomentar mi crecimiento como científico más allá de una sucesión de experimentos y por hacer que todo mi doctorado haya sido tan cómodo para mí, tanto profesional como personalmente. Creo que con todo lo que me llevo estoy preparado para pasar a la siguiente etapa, y si esta tiene éxito, quiero que sepas que en gran parte será gracias a ti. Muchas gracias, Xosé.

A Mauricio. El primer año de un estudiante predoctoral es típicamente una época en la que el doctorando lucha por no ahogarse en ese océano que es un laboratorio de investigación. Para mí no fue así, gracias a ti. Tu generosidad no tuvo límites conmigo, y tú y tus enseñanzas fuisteis los cimientos sobre los que se sustentan toda esta tesis doctoral, cosa que nunca podré agradecerte lo suficiente.

Fuiste una figura que no he vuelto a encontrar, ni siquiera en mí mismo: ahora soy yo el que recibe estudiantes a su cargo, y aunque por supuesto que los trato con lo mejor que hay en mí, sé que ni se acerca a cómo te portaste tú conmigo. Por eso ahora más que nunca soy consciente de todo lo que tengo que agradecerte. Fuiste y eres un modelo a seguir, en todos los aspectos, algo que sabemos todos los que tuvimos la suerte de coincidir contigo. Muchas gracias, Mauri.

A Mercedes. Si bien es cierto que el hecho de trabajar en laboratorios y proyectos distintos ha limitado nuestro contacto profesional, siempre que ha ocurrido lo he valorado mucho. Tu pensamiento meticuloso y concienzudo es una auténtica inspiración para cualquiera que busque convertirse en un buen científico. Presentarte el desarrollo de mi trabajo para recibir tus preguntas y comentarios siempre ha sido una manera infalible de encontrar cómo podía mejorar. Además, quiero agradecerte de manera especial la ayuda que me has prestado para fomentar mi crecimiento al margen del ámbito experimental, sobre todo de cara a mi formación como docente. Ha sido una suerte contar contigo como tutora. Muchas gracias, Mercedes.

A Salvatore. Cuando un joven estudiante de carrera empieza en un laboratorio con *Principal Investigators* y *Senior Postdocs*, sin duda es de gran ayuda contar con la figura menos intimidatoria de un, por aquel entonces, *predoc* con el que poder aprender de manera cercana. Tú fuiste esa figura para mí, muchas gracias por ser mi hermano mayor en la poyata y además todo un ejemplo de cómo forjar una carrera profesional exitosa. Gracias, además, por ser tan buen amigo fuera del laboratorio y por la inauguración del ciclismo salmantino, una tradición que ha seguido muchos años después de tu marcha. Muchas gracias, Salva.

A Virginia. Para ser estrictos, sin desmerecer a Mauri ni a Salva, tú fuiste quien me enseñó a dar los primeros pasos en el laboratorio, cuando iba al salir de la facultad. Si bien nuestros proyectos no tenían ni tienen nada que ver, a día de hoy sigo haciendo los *Western blots* como tú me enseñaste. Tú me diste los rudimentos con los que después realicé mi propia andadura en el laboratorio. Por tu paciencia y tu dedicación en esos siempre complicados momentos iniciales, muchas gracias, Vir.

A Maite. Siendo tú de La Nava y yo teniendo sangre de Tordillos, no había buenos augurios sobre cómo nos íbamos a llevar durante tantos años. Sin embargo, esos augurios estaban muy equivocados: estar contigo en el laboratorio, preocupándote día a día de que las cosas funcionen como es debido, ha sido algo que no puedo dejar de agradecer. Nuestro sitio, calculadora y codazos compartidos es solo una breve muestra de lo mucho que me llevo en mi memoria de ti y de lo mucho que me alegro de haber coincidido contigo. Muchas gracias, Maite.

A Antonio. ¡Doctor! Tras tanto debatir sobre el tema, al fin ha llegado el esperado momento. Trabajar contigo, además de un placer, ha sido fundamental para mucho de lo que hay aquí escrito. Tu predisposición, profesionalidad y ganas de aprender han hecho de las “matanzas” y carcinogénesis a las que nos hemos enfrentado, que han sido muchas a lo largo de estos años, experiencias por las que tengo mucho que agradecer. Tú has hecho que todo sea mucho más cómodo y fácil. Muchas gracias, Antonio.

A Javier Robles. A pesar de la flaqueza de piernas que hemos tenido este último año, muchos kilómetros hemos recorrido juntos, fuera pero también dentro del laboratorio. Siempre has sabido combinar ser un gran profesional con la mayor de las humildades y el mejor de los humores, lo que ha hecho un placer compartir y aprender cosas contigo, que no han sido pocas. Muchas gracias, Javi.

A Maribel. Echando la vista atrás me doy cuenta de la cantidad de buenos recuerdos que guardo contigo, incluyendo juegos de mesa y viajes en ascensor. Pero además de esos buenos ratos, compartir laboratorio contigo ha sido una suerte. Durante todo este tiempo contigo he disfrutado de una amabilidad y una disposición a ayudar por la que te estoy profundamente agradecido. Muchas gracias, Maribel.

A Sonia "2". Mi compañera de viaje, si bien en proyectos diferentes y siguiendo caminos paralelos, hemos descubierto qué es un doctorado, hemos sido transformados por él y ahora estamos a punto de acabarlo juntos. Me alegro de haber contado contigo y valoro mucho todo lo que hemos aprendido el uno del otro. Muchas tracias, Sonia

A Giulia. Puedo afirmar sin temor a equivocarme que eres de las personas más dulces que he conocido nunca. Coincidir contigo en el laboratorio y disfrutar de tu visión del mundo era motivo suficiente para sentir mas llevadera cualquiera que fuese la tarea entre manos. Muchas gracias, Giulia.

A Blanca. ¿Cómo decidimos llamarla? ¿”La Ruta de Los Lamentos”? Nuestras marcadas personalidades no siempre nos han permitido tener el mas fácil de los tratos, pero tampoco me han impedido ver el buen corazón que tienes debajo de tanto carácter, ni disfrutar de tu compañía. Prometo ir contigo a *crossfit*... algún día. Muchas gracias, Blanca

A Mamen. Pocas personas hay con una actitud tan positiva y con ese afán por hacer sentir bien a todo el que le rodea. Has hecho del centro de investigación, incluido nuestro laboratorio, un lugar mejor y más humano. Muchas gracias, Mamen.

A Sonia "3". Me debes tu apellido (“3”), pero yo te debo cosas a ti también. Cosas como las amables charlas en cultivos y, sobre todo, como el "Por Naza", pero supongo que este no es el contexto para explayarse en eso. Muchas gracias, Sonia.

A Rodrigo. Creo que no me equivoco si digo que eres la persona mas diametralmente opuesta a mí que ha pasado por el laboratorio. Quizás por eso aprendí de ti a contemplar muchas cosas de manera distinta, creciendo tanto profesional como personalmente. Los ocho pétalos de Salamanca son sin duda el hito deportivo de esta tesis. Muchas gracias, Rodri.

A Javier Conde. Sin dejar de ser el profesional que eres, tú has sido el protagonista de muchas de las risas ocurridas dentro y fuera del laboratorio durante estos años. Coincidir contigo ha sido una gran suerte; y tu valor y determinación para conseguir tus objetivos, todo un ejemplo. Muchas gracias, Javi.

A Jesús. Me alegro mucho de haber contado contigo, tanto dentro del laboratorio para aprender lo mucho que tienes que enseñar, pues siempre he creído que eres un excelente orientador profesional, como fuera de él, ya sea jugando a videojuegos, corriendo una media maratón o haciendo una “Farinato Race”. Tú estás en muchos de los buenos recuerdos que me llevo de la tesis. Muchas gracias, Jesús.

A Rubén. Recuerdo el día que llegaste al laboratorio, con la intención de empezar a formarte en Bioinformática. Poco sabía yo en aquel entonces que no solo te convertirías en mi único compañero de teclado, sino también en el mejor de los amigos. Siempre he podido contar contigo, para todo, independientemente de lo que se tratase: escribir algoritmos bioinformáticos, batir nuestras marcas personales en *bench press*, descubrir los mejores *whiskies* (o güisquis, como debe escribirse) o asar los más suculentos chuletones. Un amigo todoterreno en el que se puede confiar ciegamente, de esos que son muy difíciles de encontrar y, sobre todo, de esos que merece la pena conservar toda la vida. Muchas gracias, Rubén.

A Laura. Me temo que no pronunciar el sonido /s/ es una mancha de la que nunca te librarás, pero creo que eso es lo único malo que puedo decir de ti (porque sí, eso es malo). Y si empiezo diciendo esto es porque si, en lugar de las malas, dijera todas las cosas buenas que tienes, este libro bastante abultado ya de por sí adquiriría unas dimensiones grotescas. Nunca había conocido a nadie con un alma tan cándida. Tu amabilidad, ilusión, disposición y generosidad revolucionaron completamente mi vida dentro y fuera del laboratorio desde que llegaste. Hay uno de los grandes hitos de mi tesis que no está recogido ni en resultados, ni en discusión, ni en conclusiones, que es el haberte conocido. Muchas gracias, Laura.

A Ariana. Has sido todo un ejemplo de cómo el tener que enfrentarse a una plétora de dificultades no está reñido con la mayor simpatía, bondad y generosidad. Tu compañía a lo largo de esta tesis no solo la ha hecho mucho más llevadera, sino que me ha permitido aprender de tu visión del mundo. Muchas gracias, Ariana.

A Natalia. Tuviste la buena o la mala suerte de aterrizar en el laboratorio bajo mi tutela, pues se me encomendó la tarea de guiarte en tus primeros pasos y de enseñarte. Pasado el tiempo, creo que así ha sido, y estoy orgulloso de en lo que te estás convirtiendo poco a poco. Lo que no sabía cuando llegaste es que yo también aprendería mucho de ti. Gracias por obligarme a ofrecer la mejor versión de mí mismo y por estar a mi lado. Muchas gracias, Natalia.

A Lucía. Aunque has sido la última en llegar, no te ha faltado tiempo para demostrar lo excelente compañera y amiga que vas a ser en el laboratorio, y fuera de él. Coincidir contigo siempre ha hecho todo mucho más entretenido, por tediosa que fuese la tarea entre manos. Muchas gracias, Lucía.

A todos los demás. No se me escapa que muchos más nombres deberían estar aquí. Gente que está o ha pasado por el laboratorio: Elsa, Naza, Myriam, Ana, Regina, Alba, Luis, Sergio, Facundo. Gente que compone los servicios de apoyo a la investigación del Centro de Investigación del Cáncer: Patología Molecular Comparada, Microscopía, Citometría, Genómica, Informática, Mantenimiento, Administración. Gente ajena al CIC que ha contribuido a mi formación como Doctor, incluyendo al Dr. Salvador Aznar y su laboratorio, y al CIBERONC. A todos vosotros, muchas gracias, os aseguro que os tengo muy presentes y que valoro mucho lo que me habéis aportado, cada uno en su momento.

A muchos más

Si bien creo que no es oportuno ni práctico acometer la titánica labor de citar a todos aquellos que, sin ser de mi familia ni de mi laboratorio, han contribuido desde el punto de vista personal a que llegue a donde hoy me encuentro, tampoco quiero eludir el deber que creo que tengo de mencionar explícitamente a algunos de ellos. A Raquel, por acompañarme hasta el umbral de este viaje. A Ángela, por la fidelidad de tu amistad. A Muler, Pablo, Tanque, Lauri y Varo, por entender, o no entender pero aceptar, las ausencias y la falta crónica de tiempo libre que ha sufrido este joven investigador. Aquí queda uno de los motivos de la misma, *ut placeat Deo et hominibus*.

APPENDIX: RESUMEN EN CASTELLANO

FACTORES DE INTERCAMBIO DE NUCLEÓTIDO DE GUANINA DE LA FAMILIA RHO EN LA REGULACIÓN DE LAS CÉLULAS MADRE Y LAS CÉLULAS TUMORALES DEL EPITELIO ESCAMOSO

TABLA DE CONTENIDOS

LISTA DE FIGURAS 13

LISTA DE ABREVIATURAS 15

INTRODUCCIÓN 17

1. FISIOLOGÍA DEL EPITELIO ESCAMOSO ESTRATIFICADO 19
1.1. Estructura y función 19
1.2. Regulación molecular 21

2. CÉLULAS MADRE EPIDÉRMICAS 24
2.1. Nichos y poblaciones 24
2.2. Regulación molecular de la célula madre del *bulge* 26

3. EL CARCINOMA DE CÉLULAS ESCAMOSAS 29
3.1. Epidemiología 29
3.2. Célula de origen 30
3.3. Rasgos moleculares 31

4. SEÑALIZACIÓN DE LAS GTPASAS RHO EN EPITELIOS ESCAMOSOS 35
4.1. Las GTPasas Rho como interruptores moleculares 35
4.2. Las GTPasas Rho en la homeostasis de las células madre epidérmicas 37
4.3. Las GTPasas Rho en el carcinoma de células escamosas 38
4.4. Los GEF de la familia Rho en el carcinoma de células escamosas 41
4.5. ¿Albergan los Rho GEF valor terapéutico? 43

OBJETIVOS 45

MÉTODOS 49

MODELOS EXPERIMENTALES 51

DETALLES DE MÉTODOS 54

CUANTIFICACIONES Y ANÁLISIS ESTADÍSTICOS 69

RESULTADOS 73

1. VAV2 INDUCE LA PROLIFERACIÓN REGENERATIVA Y EL MAL PRONÓSTICO DEL CARCINOMA DE CÉLULAS ESCAMOSAS 75
1.1. El incremento de la abundancia de VAV2 está asociado con mal pronóstico en SCC 75
1.2. El aumento de la señalización de Vav2 en epidermis crea un nicho protumorigénico 80
1.3. El fenotipo de Vav2 es autónomo de queratinocitos y dependiente de catálisis 83

1.4. Vav2 controla un programa protumorigénico propio de células madre 88
1.5. El transcriptoma Vav2^{Onc} está regulado por los factores c–Myc, Yap, E2F y AP1 93
1.6. La hiperplasia epitelial inducida por Vav2 es dependiente de c-MYC y YAP 98
1.7. El mantenimiento del oSCC requiere altos niveles de VAV2 endógeno 100

2. VALIDACIÓN PRECLÍNICA DEL VALOR TERAPÉUTICO DE LA ACTIVIDAD CATALÍTICA DE Vav2 107
2.1. La mutación L332A modela el bloqueo parcial de la actividad catalítica de Vav2 107
2.2. Existen ventanas terapéuticas para la inhibición catalítica de Vav2 109

3. Vav2 REGULA LA ACTIVIDAD DE LAS CÉLULAS MADRE EPIDÉRMICAS EN EL FOLÍCULO PILOSO 115
3.1. La señalización de Vav2 induce una expansión de las células madre epidérmicas 115
3.2. Vav2 favorece la capacidad de respuesta de las células madre epidérmicas 118
3.3. El fenotipo de Vav2 en las EpSC es autónomo de queratinocitos 123
3.4. Vav2 gobierna programas transcripcionales clave para la homeostasis de las EpSC 127
3.5. Vav2 controla el transcriptoma de las EpSC a lo largo del tiempo 129
3.6. Vav2 afecta a la regulación temporal de rutas esenciales para las EpSC 134
3.7. Vav2 favorece la coordinación transcripcional en células madre epidérmicas 138
3.8. Vav2 gobierna el transcriptoma de las EpSC a través de *hubs* transcripcionales 140

4. MAS ALLÁ DE VAV2: INTERCAMBIADORES DE NUCLEÓTIDO DE LAS GTPASAS RHO EN LA CARCINOGÉNESIS DEL EPITELIO ESCAMOSO 145
4.1. Dos grupos de RHO GEFs se encuentran transcripcionalmente alterados en SCC 145
4.2. La alteración transcripcional de los RHO GEFs ocurre de manera coordinada 148
4.3. ECT2, FARP1, FGD6, TRIO y VAV2 tienen función protumorigénica *in vitro* 152
4.4. ECT2, TRIO y VAV2 desempeñan papeles protumorigénicos clave *in vivo* 155
4.5. La represión de VAV3 induce proliferación en contextos transformantes *in vitro* 157
4.6. ITSN2, KALRN y VAV3 desempeñan papeles antitumorigénicos *in vivo* 160
4.7. Vav3 inhibe el desarrollo y la agresividad de los tumores de SCC 161

DISCUSIÓN 165

La sobreexpresión de VAV2 es funcionalmente relevante en la carcinogénesis del SCC 167
Vav2 es un mediador clave de *stemness* en células escamosas cutáneas y orales 169
VAV2 es una potencial diana terapéutica para el carcinoma de células escamosas 170
Vav2 regula a las células madre del folículo piloso 171
La señalización de Vav2 en la piel: dos conceptos de célula madre 174
VAV2 pertenece a un grupo de RHO GEFs con papeles clave en el SCC 175
Los mecanismos subyacentes a la idiosincrasia de los RHO GEF: un enigma que abordar 179
Vav2 y Vav3: amigos y enemigos 182

CONCLUSIONES 185

REFERENCIAS 189

PUBLICACIONES 209

AGRADECIMIENTOS 215

APÉNDICE: RESUMEN EN CASTELLANO 227

RESUMEN DE LA INTRODUCCIÓN

El epitelio escamoso es uno de los más abundantes del cuerpo humano, el cual cubre multitud de órganos y tejidos. La epidermis, en la piel, y las mucosas masticatoria y especializada, en la cavidad oral, son dos claros representantes del mismo. Estos epitelios están compuestos por un conjunto de células apiladas, denominadas queratinocitos, que se organizan en una serie de capas o estratos. Dichas estructuras se encuentran sometidas a un proceso de renovación constante, en el que los queratinocitos más maduros, situados en el estrato más externo, se desprenden continuamente y son reemplazados por células provenientes de las capas más internas. Esta renovación está sustentada por las células madre del epitelio, las cuales se dividen y autoperpetúan para responder a esta demanda y mantener la homeostasis tisular. Tales células madre se clasifican en diferentes tipos que se localizan en regiones muy concretas del epitelio, bien en su parte más basal o, en el caso de la epidermis, alojadas en el folículo piloso. De entre todas ellas, la célula madre epidérmica (EpSC) por excelencia es aquella que reside en la protuberancia (o *bulge*) del folículo piloso, una célula de división infrecuente que es capaz de regenerar todos los linajes epiteliales de la epidermis.

La acumulación de eventos oncogénicos en el epitelio escamoso conduce a su transformación tumoral y al desarrollo del carcinoma de células escamosas (SCC). El SCC cutáneo (cSCC) es el segundo cáncer epitelial más frecuente de la piel y está generalmente asociado a la exposición a la radiación UV. Por otro lado, el SCC que surge a partir del epitelio oral se engloba dentro de los cánceres de cabeza y cuello (hnSCC), y suponen sexto tipo tumoral más frecuente. Estos tumores están asociados al consumo de tabaco, alcohol y a infecciones por el virus del papiloma humano. La incidencia de ambos cánceres se encuentra actualmente en aumento, y si bien la tasa de supervivencia a 5 años del cSCC supera el 95%, este porcentaje se sitúa en el 50–60% en el caso del hnSCC. La reciente caracterización molecular de estos tumores ha desvelado que los distintos factores oncogénicos que contribuyen a su origen convergen en una serie de alteraciones genómicas y transcriptómicas. Dichas alteraciones afectan a genes vinculados a al control del ciclo celular, la transducción de señales, la diferenciación celular, la regulación epigenética y la señalización a través de las GTPasas de la familia RHO. Puesto que aún se conoce muy poco acerca de cómo la señalización a través de dichas GTPasas participa en la carcinogénesis del epitelio escamoso y, sobre todo, de si su modulación puede emplearse como una nueva herramienta terapéutica, hemos decidido enfocar el presente trabajo doctoral en tales cuestiones.

Las GTPasas de la familia RHO son pequeñas proteínas que controlan una serie de procesos fundamentales para la biología celular, incluyendo el control del citoesqueleto, la migración, la proliferación, la diferenciación y la supervivencia. Estas proteínas funcionan como interruptores moleculares, alternando entre una conformación activa y una inactiva como respuesta a un amplio grupo de señales moleculares. Los agentes encargados de catalizar la activación de estas GTPasas en presencia de señales activadoras reciben el nombre de factores de intercambio de nucleótido de guanina (GEFs), mientras que aquellos que desempeñan la acción opuesta son denominados proteínas activadoras de GTPasas (GAPs). RAC1, RHOA y CDC42 son las GTPasas mejor caracterizadas dentro de la familia RHO, las cuales desempeñan papeles fundamentales en la homeostasis de las células madre del epitelio escamoso, en especial RAC1. Evidencias derivadas de muestras de pacientes y de distintos modelos animales han demostrado que dicha GTPasa cuenta con un rol inequívocamente protumorigénico en la carcinogénesis del SCC, mientras que la función de RHOA y CDC42 parece ser mucho más dependiente del contexto tumoral particular.

A pesar de la implicación de las GTPasas de la familia RHO en el desarrollo tumoral, sus propiedades bioquímicas las convierten en proteínas difícilmente abordables desde el punto de vista farmacológico, lo cual dificulta su explotación con fines terapéuticos. No obstante, puesto que su activación es dependiente de la actividad GEF, el trabajo expuesto en esta tesis doctoral se ha centrado en los factores de intercambio de nucleótido de guanina como mediadores clave de la señalización por las GTPasas RHO cuya actividad sí puede ser modulada farmacológicamente. Si bien existen más de 70 GEFs en la célula, estudios previos en líneas celulares y modelos animales sugieren que Vav2 representa un candidato ideal para realizar estos estudios.

Por lo anteriormente expuesto, esta tesis se ha dirigido a:

1. La caracterización de la implicación del GEF Vav2 en la carcinogénesis del carcinoma de células escamosas cutáneo y de cabeza y cuello.

2. La evaluación del valor terapéutico de la inhibición catalítica de Vav2 para el tratamiento del carcinoma de células escamosas.

3. El descubrimiento de las funciones fisiológicas de Vav2 asociadas al mantenimiento fisiológico del epitelio escamoso.

4. La identificación y validación de otros GEFs con funciones relevantes en la formación y progresión del carcinoma de células escamosas.

RESUMEN DE LOS RESULTADOS

VAV2 induce la proliferación regenerativa y el mal pronóstico del carcinoma de células escamosas

El análisis de muestras de cSCC y hnSCC derivadas de pacientes ha revelado que VAV2 se encuentra frecuentemente sobreexpresado en estos tipos tumorales y que sus niveles de expresión están asociados con la supervivencia de los pacientes. Con objeto de evaluar cuál es el impacto fisiopatológico de tal ganancia de función de VAV2, hemos empleado un modelo murino *knockin* que expresa una versión hiperactiva de este GEF (denominada $Vav2^{Onc}$). Estos ratones desarrollan hiperplasia en distintos epitelios escamosos, incluyendo al epidermis, el paladar y la lengua, caracterizada por la expansión de células progenitoras inmaduras con altas tasas de proliferación. La presencia de lesiones genéticas adicionales conduce a estos ratones al desarrollo de tumores de manera temprana, que además son más abundantes y de mayor tamaño y malignidad, con una mayor frecuencia de SCCs infiltrantes en estadio avanzado. Tales hallazgos indican que VAV2 induce un estadio protumorigénico en el epitelio escamoso que favorece la transformación tumoral del mismo.

Puesto que VAV2 se expresa de manera prácticamente ubicua en el organismo, hemos implementado cultivos tridimensionales *in vitro* de queratinocitos, humanos y murinos, con objeto de confirmar que el fenotipo inducido por este GEF en el epitelio escamoso radica en los tales células. Estos modelos experimentales han permitido además establecer que VAV2 gobierna dicho programa protumorigénico de manera catalítica a través de la activación de las GTPasas RAC1 y RHOA.

La caracterización del transcriptoma epidérmico de los ratones *Vav2*^{Onc} ha desvelado que este GEF dirige un amplio programa transcripcional implicado en el control de la proliferación, diferenciación y procesos asociados a la respuesta inmune y a la regulación metabólica. El análisis de las proteínas que median dicho programa transcripcional ha conducido a los reguladores c-Myc, Yap, AP1 y E2F, cuya actividad es inducida por Vav2. De entre ellos, la señalización a través de c-Myc y YAP es fundamental para la activación de los procesos de proliferación e indiferenciación controlados por dicho GEF. Todo ello hace que la ganancia de función de Vav2 en queratinocitos favorezca un perfil transcripcional semejante al presente en progenitores y células madre epidérmicas. Tal perfil transcripcional se encuentra también altamente conservado en tumores humanos de cSCC y hnSCC, y funciona como elemento predictor de la supervivencia del paciente. La aplicación de una serie de algoritmos bioinformáticos ha permitido destilar esta asociación entre el programa molecular gobernado por Vav2 y la supervivencia del paciente en una firma transcripcional de alto valor pronóstico compuesta por 41 genes.

Validación preclínica del valor terapéutico de la actividad catalítica de Vav2

Con objeto de evaluar la relevancia de la actividad de VAV2 en las propiedades tumorales del SCC, hemos reprimido los niveles de expresión de este GEF en líneas celulares derivadas de pacientes. Tanto en cultivos tridimensionales *in vitro*, como en modelos de xenotrasplante ortotópico en ratones inmunodeficientes, la pérdida de función de VAV2 conduce a una represión de la capacidad proliferativa y a una inducción de la diferenciación en células tumorales. Este hallazgo se ha trasladado a un contexto terapéutico mediante la generación de una serie de modelos murinos que presentan distintos niveles de actividad catalítica de Vav2. De esta manera se mimetiza el tratamiento con fármacos, los cuales rara vez consiguen bloquear la actividad de sus dianas en su totalidad. Así, hemos encontrado que reducir la actividad catalítica de Vav2 al ~20% confiere protección frente al desarrollo y la progresión del SCC. Sin embargo, esa actividad catalítica residual es suficiente para prevenir la aparición de efectos secundarios asociados a las funciones fisiológicas de Vav2 en el sistema cardiovascular. Este hallazgo demuestra que existen ventanas terapéuticas de inhibición de Vav2 que permiten obstaculizar el desarrollo tumoral sin afectar a la homeostasis de los tejidos sanos.

Vav2 regula la actividad de las células madre epidérmicas en el folículo piloso

Análisis adicionales de los ratones $Vav2^{Onc}$ han demostrado que al margen de su rol en carcinogénesis, Vav2 desempeña funciones fundamentales en el contexto fisiológico de la epidermis. Tanto la regeneración de la piel ante heridas como la regeneración del pelo ante la depilación ocurren de manera acelerada en ratones dotados de la versión hiperactiva de Vav2. Este fenotipo está asociado a una mayor abundancia de células madre epidérmicas en la protuberancia del folículo piloso (EpSC), que además presentan una mayor capacidad de respuesta frente a estímulos activadores. La realización de trasplantes de células epidérmicas provenientes de ratones $Vav2^{Onc}$ a ratones desnudos inmunodeficientes ha permitido verificar que este fenotipo es autónomo de este tipo celular.

Todas estas observaciones se revierten en el caso de los ratones $Vav2^{-/-};Vav3^{-/-}$, que presentan una regeneración más lenta de piel y pelo y un menor número y capacidad de respuesta de las EpSC. La contraposición entre los fenotipos de las EpSC dotadas de Vav2 hiperactivo y aquellas carentes de Vav2 y Vav3 ha sido caracterizada transcriptómicamente con el fin de elucidar el programa molecular gobernado por Vav2 en este contexto. Dichos análisis han desvelado que este GEF controla la expresión de un amplio número de genes implicados en pluripotencia a la par que establece un perfil transcripcional asociado a quiescencia. Este hecho, unido a que el fenotipo inducido por $Vav2^{Onc}$ se mantiene en el tiempo, ha conducido a la ampliación del análisis transcriptómico para abarcar EpSC comprendidas entre 18 días y 1 año de edad. El tratamiento de estos datos con diversos algoritmos bioinformáticos ha permitido evaluar cómo varía el transcriptoma de las EpSC con el paso del tiempo, así como la influencia de Vav2 en dicho fenómeno. Esto ha revelado que el 31.9% de los mRNA de las EpSC presentan un comportamiento dinámico en el tiempo, puesto que su expresión varía con la edad. La hiperactivación de Vav2 se traduce en un marcado incremento de dicho dinamismo transcripcional, tanto por la remodelación de los patrones transcripcionales de genes que son dinámicos en condiciones nativas, como por la inducción de nuevos genes dinámicos. Esta remodelación transcripcional dirigida por Vav2 altera, de manera específica en función de la edad, el enriquecimiento funcional de procesos biológicos y rutas de señalización esenciales para la homeostasis de las células madre epidérmicas. En particular, hemos encontrado que la actividad de Vav2 coordina una serie de genes y procesos asociados a proliferación, diferenciación y metabolismo anabólico que permite enriquecer y perpetuar la población de células madre sin obstaculizar su activación en presencia de estímulos.

Con objeto de investigar cuáles son los agentes mediadores de esta remodelación transcriptómica inducida por Vav2, hemos identificado computacionalmente aquellos genes que se encuentran en el núcleo transcripcional de los patrones de expresión gobernados por Vav2^{Onc}. Estos análisis, unidos a la evaluación de sitios de unión de factores de transcripción, han permitido descubrir que Vav2 favorece la activación de un grupo de factores de transcripción específicamente asociados al mantenimiento de la quiescencia en las células madre epidérmicas.

Más allá de VAV2: la familia de intercambiadores de nucleótido de las GTPasas RHO en la carcinogénesis del epitelio escamoso

La caracterización de los roles fisiopatológicos desempeñados por VAV2 en la homeostasis y la carcinogénesis del epitelio escamoso nos ha conducido a evaluar si tales funciones son exclusivas de este GEF o, por el contrario, existen otros miembros de la familia de factores de intercambio de nucleótido que desempeñan papeles similares. El análisis de datos transcriptómicos de muestras de hnSCC derivadas de pacientes ha demostrado que, además de VAV2, ECT2, FARP1, FGD6 y TRIO se encuentran frecuentemente sobreexpresados en el tejido tumoral. Inesperadamente, también hemos hallado que un número similar de GEFs, incluyendo a ARHGEF10L, ITSN2, KALRN, TIAM1 y VAV3, se encuentra transcripcionalmente reprimido. Esta expresión diferencial correlaciona en muchos casos con el pronóstico del paciente: mientras que los GEFs sobreexpresados están asociados a un peor pronóstico, lo contrario ocurre en el caso de los reprimidos.

Diversos análisis bioinformáticos nos han permitido descubrir que los cambios en la expresión de este grupo de GEFs ocurren de manera coordinada, tanto en el contexto tumoral como durante la diferenciación de queratinocitos sanos. Este fenómeno es relevante desde el punto de vista pronóstico, pues la regulación conjunta de estos GEFs se asocia fuertemente con la supervivencia del paciente. Esta coordinación transcripcional se encuentra enmarcada dentro de grandes redes de coexpresión que aglutinan genes involucrados en la regulación de procesos fundamentales para la tumorigénesis del epitelio escamoso, tales como la interacción con la matriz extracelular, el potencial morfogénico, la proliferación y la diferenciación.

Con objeto de validar biológicamente el potencial protumorigénico de los GEFs que se encuentran sobreexpresados en hnSCC, hemos recurrido a nuestra colección de células tumorales derivadas de pacientes. La represión de los niveles de expresión de dichos GEFs obstaculiza la proliferación e induce la diferenciación de estas células en cultivos tridimensionales *in vitro*. La implantación de las mismas en la cavidad oral de ratones inmunodeficientes ha permitido demostrar que, además de VAV2, ECT2 y TRIO desempeñan una función protumorigénica a la cual las células tumorales presentan un alto grado de dependencia *in vivo*. Dichas funciones están mediadas por mecanismos no redundantes dirigidos por cada GEF.

La elucidación del potencial papel antitumorigénico de los GEFs que se encuentran transcripcionalmente reprimidos en SCC se ha llevado a cabo en modelos celulares dotados de diferentes cargas mutacionales. Esta estrategia experimental ha permitido desvelar que, en presencia de lesiones oncogénicas adicionales, la represión de VAV3 favorece el crecimiento hiperplásico de las células escamosas *in vitro*. Asimismo, hemos descubierto que la represión de tanto VAV3 como ITSN2 y KALRN fomenta el crecimiento tumoral *in vivo*. De acuerdo con esto, la aplicación de protocolos de carcinogénesis química a ratones carentes de Vav3 ha demostrado que la pérdida de función de este GEF conduce al desarrollo de un número exacerbado de tumores, los cuales presentan un gran tamaño y un alto grado de malignidad.

En conjunto, estos descubrimientos demuestran que los factores de intercambio de nucleótido de guanina de las GTPasas de la familia RHO desempeñan papeles clave tanto en al inducción como en la represión del carcinoma de células escamosas. La modulación de su actividad, por tanto, constituye un recurso potencial para el desarrollo de nuevas estrategias terapéuticas frente a este tipo tumoral.

CONCLUSIONES

1. VAV2 dirige un programa molecular autónomo implicado en el mantenimiento de un estado proliferativo e indiferenciado en los epitelios escamosos cutáneo y oral. La activación de dicho programa ocurre de manera catalítica mediante la activación de las GTPasas RAC1 y RHOA.

2. El programa molecular dirigido por VAV2 está frecuentemente activado en células malignas y premalignas del epitelio escamoso, favoreciendo la progresión tumoral y conduciendo a un mal pronóstico. El potencial tumorigénico del carcinoma de células escamosas está fuertemente condicionado por la actividad de VAV2.

3. La inhibición de la actividad catalítica de Vav2 previene el desarrollo tumoral del carcinoma de células escamosas. Existen ventanas terapéuticas en las que dicho efecto se puede inducir sin ocasionar los efectos secundarios asociados a las funciones fisiológicas de este GEF.

4. Vav2 regula la abundancia, actividad y capacidad de respuesta de las células madre epidérmicas alojadas en la protuberancia del folículo piloso. Esta función está parcialmente coordinada con Vav3.

5. Vav2 controla circuitos transcriptómicos de las EpSC y su reconfiguración dinámica a lo largo del tiempo. Dicho programa transcripcional regula la homeostasis y la quiescencia de las células madre epidérmicas.

6. Junto a VAV2, los RHO GEF ECT2, FARP1, FGD6 y TRIO contribuyen al potencial tumorigénico del carcinoma de células escamosas. Dicha función protumorigénica está mediada por mecanismos no redundantes.

7. Los RHO GEF ITSN2, KALRN y VAV3 desempeñan funciones antitumorigénicas en el desarrollo del carcinoma de células escamosas.